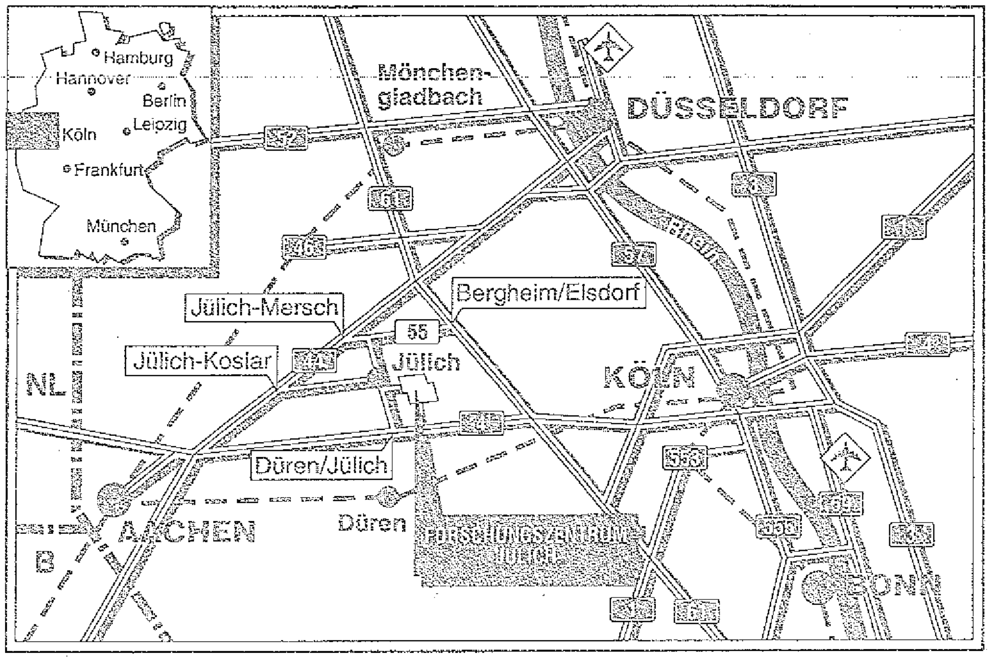

Berichte des Forschungszentrums Jülich ; 2500
ISSN 0366-0885
Institut für Kernphysik Jül-2500

Zu beziehen durch: Forschungszentrum Jülich GmbH · Zentralbibliothek
Postfach 1913 · D-5170 Jülich · Bundesrepublik Deutschland
Telefon: 02461/61-6102 · Telefax: 02461/61-6103 · Telex: 833556-70 kfa d

Low-Lying States of Pionic Atoms

First Collaboration Meeting COSY Experiment 10
Forschungszentrum Jülich, Jülich, 26 June 1991

Edited by

H. Machner, H.S. Plendl

INTRODUCTION

COSY Experiment 10 is the experimental study of low–lying states of pionic atoms through the nuclear reaction

$$p + A \rightarrow (A-1)^{\pi^-} + 2p,$$

i.e. through the elementary process

$$p + n \rightarrow \pi^- + 2p$$

under recoil–free kinematics conditions and with a 4π detector geometry.
The formation of pionic atoms and the energy and width of their low–lying states is to be determined. Such an investigation is feasible only with a beam that has the spatial and energy definition of the new COSY facility.

The transparencies that were shown by the speakers at a recent collaboration meeting are presented here. Transcripts of the discussions that followed each talk are also included. Some of the key papers and preprints that the speakers referred to have been included to provide a better understanding of the transparencies. Abstracts of each talk were added by the editors for the same purpose.
The theoretical background and motivation for the experiment and the major components of the detector system and of the data handling system were treated in some detail. Also discussed was a proposal for an experiment that is to test the separate components of the detector and data handling systems, a study of the reaction

$$\vec{p} + {}^2H \rightarrow {}^3He + \eta$$

with a 4π detector from threshold up to 1.9 GeV/c. The study of that reaction is of interest by itself, since it will allow one to distinguish between one– and two–step processes.

The editors wish to thank all collaborators and other interested persons who participated in the meeting, in particular the speakers. Thanks are also due to Professor Dr. J. Treusch and the other members of the Vorstand, Forschungszentrum Jülich for supporting this collaboration meeting and to Frau E. Wittig, IKP, for her assistance in conducting the meeting and in compiling the proceedings.

J. Konijn

NIKHEF, Amsterdam

The Pion–Nucleus Interaction

A summary of the sources of experimental information on the pion–nucleus interaction is given, with emphasis on pionic atom formation and on the problems associated with conventional pionic atom experiments. The specific information that can be obtained by forming pionic atoms as proposed here, i.e. by an elementary interaction in the nucleus, is also discussed.

NIKHEF

Pion - nucleus interaction

Main sources of information:

pion-nucleus scattering

photo pion production

pionic atoms

Low-energy pion scattering ($T_\pi \approx 20$ MeV):
central s-wave and the more peripheral p-wave
to change relative importance $\Rightarrow$ increase T_π

Pionic atoms:
pion capture in a highly excited atomic state with n,l

$\Downarrow$

cascade through circular orbits
with well defined angular momentum ($l=n-1$)

$\Downarrow$

pion reaches orbits that feel the short-range π-nucleus interaction

$\Downarrow$

π^- is finally absorbed by the nucleus

NIKHEF

Pionic Atoms

Any long-lived negatively charged particle can be captured by the static Coulomb field of a nucleus in a bound atomic orbit and can form a

⇓

Hydrogen - like exotic atom

Such a system has pecular and unique properties regarding ist *spatial dimensions* and its dynamical *time structure*

⇓

Tool to explore the nucleus

The Bohr-model of an atom tells us that the radius of such an exotic atom will be

$$R_n = \frac{\hbar c}{m_\pi c^2} \frac{n^2}{(\alpha Z)}$$

and the orbital binding energy

$$B_n = -\frac{(\alpha Z)^2 m_\pi c^2}{2 n^2}$$

from these formulae it is easy to see that the following relation is valid

$$\frac{n_\pi}{n_{e^-}} = \sqrt{\frac{m_\pi}{m_{e^-}}}$$

This implies that at a distance of the atomic K shell electron where the main quantum number $n_e = 1$ the quantum number of the π^- at the same distance from the nucleus will be approximately $n_\pi \approx 17$.

$\Downarrow$

NIKHEF

As the pion is a boson with spin-parity $J^{\pi}=0^{-}$, the pion–nucleus system is, therefore, described by the Klein-Gordon equation:

$$[\nabla^2 - \mu^2 + (E - V_C(r))]\Psi(r) = 2\mu V_S(r)\Psi(r)$$

where $2\mu V_s(r)$ expresses the π-nucleus optical potential used for low-energy pion scattering and for pionic atoms.

The pion interacts with the nucleus by

elctromagnetic interaction

and

strong interaction

$\Downarrow$

In the case of electromagnetic interaction only, thus neglecting the strong interaction and assuming a point-like charge distribution, $V_c=Z\alpha/r$, the exact solution to the Klein-Gordon equation for the total energy of the *point nucleus* is

$$E_{n,l} = \frac{\mu c^2}{\sqrt{1 + \left\{ \frac{Z\alpha}{n - (l + \frac{1}{2}) + \sqrt{(l + \frac{1}{2})^2 - (Z\alpha)^2}} \right\}^2}}$$

where μ is the reduced pion-nucleus mass.

A negatively charged muon will in the same way form an exotic atom, although as the muon is a lepton with spin 1/2, we have to use the Dirac-equation to describe muonic atoms. Because of its smaller mass, the main quantum number of the muon at the position of the atomic K-shell electron will be $n_\mu \approx 14$.

NIKHEF

Examples of quantities that can be investigated by measuring pionic and muonic X-ray spectra are:

i. finite nuclear sizes
ii. nuclear charge distributions
iii. nuclear quadrupole moments
iv. BE(2)-values of excited nuclear states
v. nuclear polarization
vi. Lamb shift and vacuum polarization
vii. magnetic dipole moments of the nucleus
viii. strong interaction
ix. mass determination of the exotic particle
x. induce nuclear fission
xi. induce nuclear fusion
xii. Q.E.D. tests
xiii. probing neutron distributions
xiv. chemical binding effects
xv. weak interaction
xvi. transfer rates of the muon (pion) in exotic hydrogen
xvii. solid state research using μSR as a probe
xviii. chemical trace studies

NIKHEF

The strong interaction *shifts* the energy of the pionic level with respect to the electromagnetic Coulomb value and - due to the absorption of the pion - leads to an increased *width* of the level.

⇓

Observable effects produced by nuclear size and strong interaction

⇓

shift ε_0
and
width Γ_0
of pionic orbits

⇓

Due to the strong interaction the pion will already be absorbed during the cascade. The lowest orbit reached so far in various nuclei:

1s - orbit observed in nuclei with $Z \leq 14$ (Si)
2p - orbit observed in nuclei with $Z \leq 44$ (Ru)
3d - orbit observed in nuclei with $Z \leq 83$ (Bi)
4f - orbit observed in nuclei with $Z \leq 94$ (Pu)

Therefore, only the more peripheral levels - e. g. the 5g and 4f levels in heavier targets - are observable.

NIKHEF

N.B.: In low-energy pion scattering about 50% of the reaction cross section is absorption. Therefore, is *pion absorption* important to study in the π-nucleus interaction. The cleanest way to study this is in pionic atoms as the absorption is almost the only open channel.

The optical potential

The optical potential used to describe pionic atoms and low-energy pion-nucleus scattering has two components:

i. one part is derived from multiple scattering theory, (Ericson & Ericson)

ii. the other is purely phenomenological and accounts for higher order effects such as π-absorption.

$$V_S(\mathbf{r}) = -\frac{2\pi}{\mu}\left[q(\mathbf{r}) - \nabla \bullet \frac{\alpha(\mathbf{r})}{1 + \frac{4}{3}\pi\,\xi\alpha(\mathbf{r})}\nabla\right] \quad (1)$$

$\Uparrow$ s-wave $\qquad$ $\Uparrow$ p-wave with:

$$q(r) = \left(1 + \frac{m_\pi}{m_N}\right)\{b_0\,\rho(r) + b_1\,\delta\rho(r)\},$$

$$\alpha(r) = \left(1 + \frac{m_\pi}{m_N}\right)^{-1}\{c_0\,\rho(r) + c_1\,\delta\rho(r)\},$$

where we have defined the densities as:

$\rho(r) = \rho(r)_n + \rho(r)_p$, and $\delta(r) = \rho(r)_n - \rho(r)_p$,

and where $\rho(r)_n$ and $\rho(r)_p$ are the neutron and proton densities, normalized to N and Z, respectively.

b_0 and b_1 represent the in-medium isoscalar and isovector s-wave scattering lengths, respectively.

c_0 and c_1, analogously the p-waves scattering volumes.

The parameter ξ depends crucially on the assumed range of the πN interaction, $r_{\pi N}$, and of the nucleon-nucleon correlation length, r_C. Assuming both to be of zero range, as was done in the original derivation of this non linear term, yields ξ=1. However, choosing $r_C \approx r_{\pi N} \approx 0.5$ fm yields ξ=0.05. Nevertheless, in most fits the value ξ=1 has been used.

NIKHEF

Pion absorption

The optical potential discussed so far is real and an important dynamical aspect still has to be discussed:

π-absorption

To include pion absorption into the optical potential, phenomenological terms are added in both the s-wave and p-wave term.

The following points have to be considered when dealing with the pion-nucleus interaction:

i. The pion is a spinless particle
ii. The process $N + \pi \Leftrightarrow N$ is *only* possible if the energy momentum balance is furnished. The required momentum for a π^- at rest is ≈500 MeV/c and as the Fermi momentum of a nucleon is about 250 MeV/c

$$\Downarrow$$

absorption on a single nucleon is highly suppressed and, therefore, occurs mainly on at least two nucleons and one includes a phenomenological term that is proportional to the square of the nuclear density to account for absorption processes such as:

$$\pi^- + (pp) \rightarrow pn, \text{ and } \pi^- + (pn) \rightarrow nn.$$

NIKHEF

The conventional optical potential

$$q(r) = \left(1 + \frac{m_\pi}{m_N}\right)\{b_0\rho(r) + b_1\,\delta\rho(r)\} + \left(1 + \frac{m_\pi}{2m_N}\right)B_0\rho^2(r)$$

$$\alpha(r) = \left(1 + \frac{m_\pi}{m_N}\right)^{-1}\{c_0\rho(r) + c_1\,\delta\rho(r)\} + \left(1 + \frac{m_\pi}{2m_N}\right)^{-1}C_0\rho^2(r)$$

This parametrization assumes:

i. the absorption mechanism has zero range

ii. the two nucleons involved are *uncorrelated.*

iii. the imaginary part of these "absorption" terms is associated with pion absorption.

iv. including the p-wave absorption term in denominator of p-wave term.

v. we do not include factors ZN/A^2 as an estimate of *np* pairs on which absorption can occur as is done in some earlier fits.

NIKHEF

The extended parametrization of the optical potential

⇓

Only two overall strength parameters B_0 and C_0 used until now.

⇓

Base the absorption of the optical potential on a more general quadratic dependence on the nucleon densities

⇓

$$q(\mathbf{r}) = \left(1 + \frac{m_\pi}{m_N}\right)\{b_0\,\rho(\mathbf{r}) + b_1\,\delta\rho(\mathbf{r})\} + \left(1 + \frac{m_\pi}{2m_N}\right)$$

$$\times\left\{B_0\,\rho^2(\mathbf{r}) + B_1\,\rho(\mathbf{r})\delta\rho(\mathbf{r}) + B_2[\delta\rho(\mathbf{r})]^2\right\}$$

$$\alpha(\mathbf{r}) = \left(1 + \frac{m_\pi}{m_N}\right)^{-1}\{c_0\,\rho(\mathbf{r}) + c_1\,\delta\rho(\mathbf{r})\} + \left(1 + \frac{m_\pi}{2m_N}\right)^{-1}$$

$$\times\left\{C_0\,\rho^2(\mathbf{r}) + C_1\,\rho(\mathbf{r})\delta\rho(\mathbf{r}) + C_2[\delta\rho(\mathbf{r})]^2\right\}$$

where $\delta r(\mathbf{r})$ has been defined earlier.

⇓

The parameters B_0 and C_0 are here responsible for absorption in the case $\delta r(\mathbf{r})=0$, thus nuclei with N=Z. The remaining parameters play a role when N>Z.

⇓

If π^- absorption was a zero-range process with two uncorrelated nucleons

⇓

new parameters could be used for identifying the absorption strength for *np* and *pp* pairs

⇓

The fits do show that such a simple explanation is not possible

⇓

Carr et al.(1982) used an extended potential to test low-energy pion-nucleus scattering.

De Laat et al.(1988) showed that an improved fit of the "anomalous" 3d shifts and widths in heavy pionic atoms could be achieved by using B_1 and C_1 absorption terms.

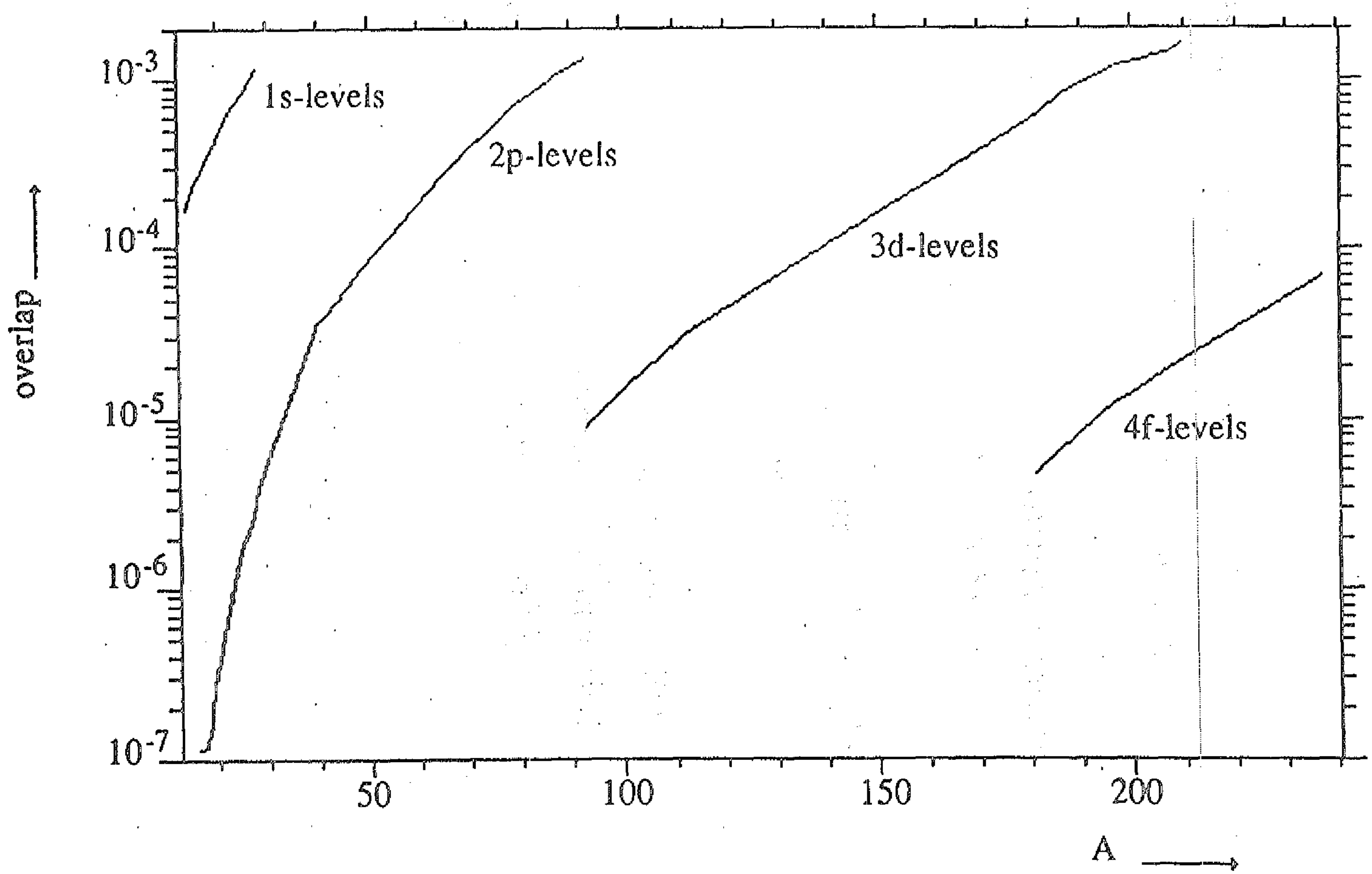
1s-levels
2p-levels
3d-levels
4f-levels
overlap
A
10^-3
10^-4
10^-5
10^-6
10^-7
50
100
150
200

Old parameter sets for the optical potential

	Tauscher	Tauscher	Batty	Seki
$\xi=$	0	1	1	1
b_0	−0.0296	−0.0293	−0.023	0.003
b_1	−0.077	−0.078	−0.085	−0.143
c_0	0.172	0.227	0.21	0.21
c_1	0.22	0.18	0.089	0.18
ReB_0	0	0	−0.021	−0.15
ImB_0	0.0436	0.0428	0.049	0.046
ReC_0	0	0	0.118	0.11
ImC_0	0.036	0.076	0.058	0.09

$\chi^2-\varepsilon_{1s}$	5.21	4.50	3.35	11.25
$\chi^2-\Gamma_{1s}$	5.61	6.51	3.20	6.58
$\chi^2-\varepsilon_{2p}$	37.23	19.53	8.44	12.23
$\chi^2-\Gamma_{2p}$	22.40	13.60	11.47	7.08
$\chi^2-\varepsilon_{3d}$	12.35	3.00	1.71	32.51
$\chi^2-\Gamma_{3d}$	35.28	20.95	22.16	3.22
$\chi^2-\varepsilon_{4f}$	1.71	2.69	6.60	22.06
$\chi^2-\Gamma_{4f}$	3.13	1.12	1.17	5.90

New parameters for the standard optical potential

$\xi=$	0	1
b_0	0.024	0.025
b_1	−0.090	−0.094
c_0	0.272	0.273
c_1	0.107	0.184
ReB_0	−0.261	−0.265
ImB_0	0.0552	0.0546
ReC_0	−0.26	−0.14
ImC_0	0.0640	0.105

$\chi^2-\varepsilon_{1s}$	2.62	2.59
$\chi^2-\Gamma_{1s}$	2.10	2.08
$\chi^2-\varepsilon_{2p}$	1.88	1.76
$\chi^2-\Gamma_{2p}$	2.84	2.35
$\chi^2-\varepsilon_{3d}$	3.24	3.19
$\chi^2-\Gamma_{3d}$	8.03	6.26
$\chi^2-\varepsilon_{4f}$	3.88	3.64
$\chi^2-\Gamma_{4f}$	0.97	1.09

Parameters expressed in nn, np and pp pairs

$\xi =$	0	1	3.6
b_0	-0.001 (6)	-0.001	-0.006
b_1	-0.077(20)	-0.068	-0.071
c_0	0.278(23)	0.29	0.33
c_1	0.35 (9)	0.39	0.76
ReB_{nn}	0.4(4)	0.3	-2.19
ImB_{nn}	-1.05(27)	-0.97	-0.64
ReB_{np}	-1.4(1.1)	-1.4	-0.40
ImB_{np}	2.2(7)	2.0	1.23
ReB_{pp}	0.5(8)	0.6	-2.19
ImB_{pp}	-0.9(4)	-0.8	-0.37
ReC_{nn}	-1.5(9)	-1.7	0
ImC_{nn}	1.2(5)	1.5	0
ReC_{np}	-0.7(2.1)	-0.4	-12.5
ImC_{np}	-1.7(1.3)	-1.9	5.3
ReC_{pp}	1.3(1.5)	1.6	16.5
ImC_{pp}	0.8(8)	0.9	2.4
χ^2 $\varepsilon(1s)$	1.42	1.33	1.59
$\Gamma(1s)$	1.35	1.31	1.06
χ^2 $\varepsilon(2p)$	1.32	1.23	1.19
$\Gamma(2p)$	1.84	1.77	1.28
χ^2 $\varepsilon(3d)$	1.34	1.22	1.01
$\Gamma(3d)$	1.12	1.10	0.96
χ^2 $\varepsilon(4f)$	0.64	0.62	0.60
$\Gamma(4f)$	1.29	1.34	1.44
χ^2 per data point	1.36	1.30	1.16

$$\Sigma(\mathrm{Im}\,B_{nn} + \mathrm{Im}\,B_{np} + \mathrm{Im}\,B_{pp}) = 0.224 \pm 0.003$$

Parameters for the extended optical potential

$\xi=$	0	1	3.4
b_0	−0.002	−0.001	−0.007
b_1	−0.071	−0.073	−0.061
c_0	0.280	0.290	0.34
c_1	0.33	0.38	0.66
ReB_0	−0.13	−0.14	−0.10
ImB_0	0.0566	0.0570	0.0561
ReB_1	−0.18	−0.14	−0.19
ImB_1	−0.06	−0.08	−0.09
ReB_2	0.95	058	0.64
ImB_2	−1.0741	−0.9463	−0.7580
ReC_0	−0.25	−0.14	0.8
ImC_0	0.062	0.100	0.63
ReC_1	−1.2	−1.6	−5.1
ImC_1	0.18	0.31	1.2
ReC_2	−0.55	0.08	−1.3
ImC_2	0.950	0.695	−1.46
$\chi^2-\varepsilon_{1s}$	1.32	1.24	1.38
$\chi^2-\Gamma_{1s}$	1.32	1.28	1.07
$\chi^2-\varepsilon_{2p}$	1.36	1.23	1.19
$\chi^2-\Gamma_{2p}$	1.83	1.79	1.24
$\chi^2-\varepsilon_{3d}$	1.36	1.23	1.04
$\chi^2-\Gamma_{3d}$	1.10	1.12	0.93
$\chi^2-\varepsilon_{4f}$	0.67	0.65	0.61
$\chi^2-\Gamma_{4f}$	1.29	1.35	1.44

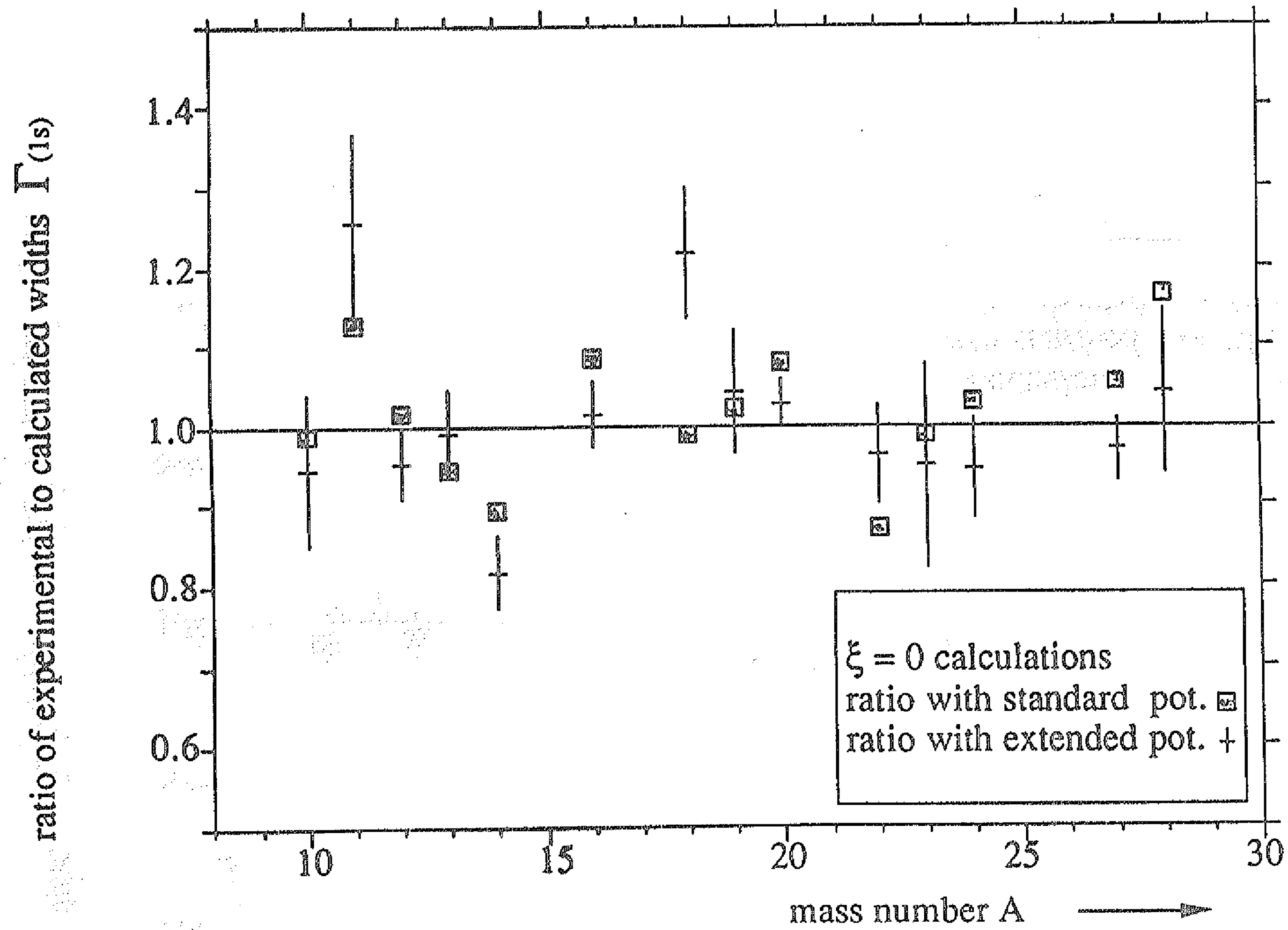
ratio of experimental to calculated widths Γ(1s)
1.4
1.2
1.0
0.8
0.6
10
15
20
25
30
mass number A
ξ = 0 calculations
ratio with standard pot.
ratio with extended pot.

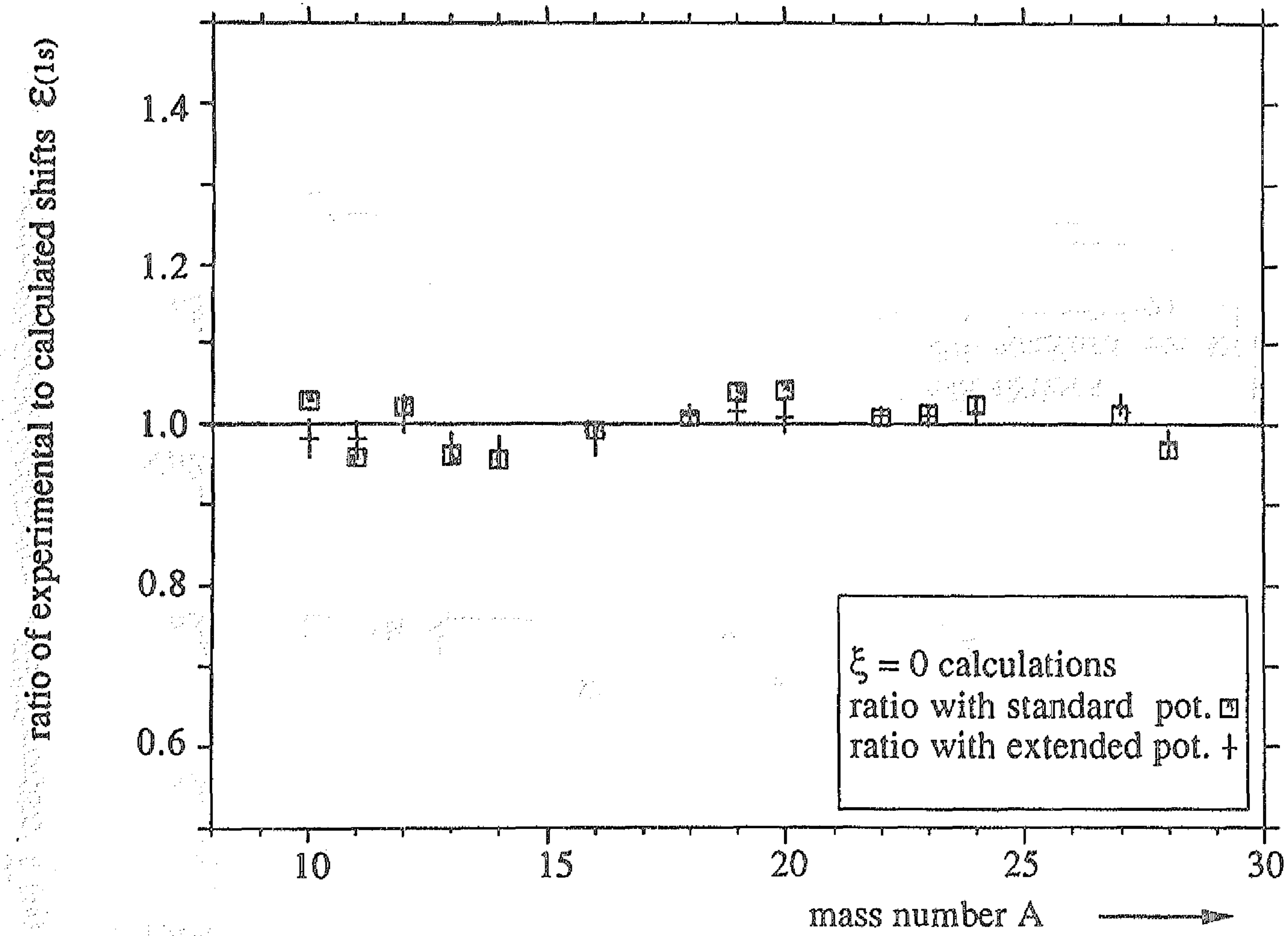
ratio of experimental to calculated shifts ε(1s)
1.4
1.2
1.0
0.8
0.6
10
15
20
25
30
mass number A
ξ = 0 calculations
ratio with standard pot.
ratio with extended pot.

Strong Interaction shifts and widths in pionic 1s orbits

	standard keV	extended pot. keV	Toki et al. keV
^{40}Ca			
ε_{1s}:	−434	−430	−416
Γ_{1s}:	82	94	105
B(1s):	−1093	−1097	−1108
^{48}Ca			
ε_{1s}:	−512	−501	
Γ_{1s}:	58	32	
B(1s):	−1015	−1027	
^{208}Pb			
Γ_{1s}:	475	63	632
B(1s):	−6785	−6924	−6959

Table 3. Strong interaction shifts and widths as well as pionic orbit binding energies calculated with the new parameter sets obtained in the fits to old and new type of optical potentials. The * sign in the ε-column indicates that the Klein-Gordon equation with the point Coulomb potential does not provide solutions for s-states.

type of potential	ξ	Binding energy pionic level [keV]	width [keV]	shift with respect to pointnuclear value [keV]	Binding pionic level [keV]	width [keV]	shift with respect to pointnuclear value [keV]
^{40}Ca		$B_\pi(1s)$	$\Gamma(1s)$	$\varepsilon(1s)$	$B_\pi(2p)$	$\Gamma(2p)$	$\varepsilon(2p)$
old	0	-1093.2	81.9	-433.8	-372.7	1.51	1.75
old	1	-1093.9	82.0	-433.1	-372.0	1.53	1.72
new	0	-1097.4	93.8	-429.6	-373.0	1.65	1.74
new	1	-1097.0	93.4	-430.1	-373.0	1.65	1.74
new	3.4	-1097.9	95.3	-429.2	-373.0	1.60	1.73
Toki et al. [34]	1	-1108	105	-416	-373	1.7	1
^{48}Ca		$B_\pi(1s)$	$\Gamma(1s)$	$\varepsilon(1s)$	$B_\pi(2p)$	$\Gamma(2p)$	$\varepsilon(2p)$
old	0	-1015.0	58.2	-512.3	-372.5	1.51	1.06
old	1	-1014.2	57.2	-513.1	-372.6	1.50	1.07
new	0	-1026.5	32.0	-500.7	-372.6	1.29	1.14
new	1	-1026.5	32.3	-501.8	-372.6	1.29	1.15
new	3.4	-1026.7	34.9	-500.6	-372.6	1.26	1.08
^{208}Pb		$B_\pi(1s)$	$\Gamma(1s)$		$B_\pi(2p)$	$\Gamma(2p)$	$\varepsilon(2p)$
old	0	-6784.8	474.5	*	-5082.2	321.8	-1537.2
old	1	-6776.7	457.5	*	-5079.3	311.7	-1540.1
new	0	-6923.9	63.4	*	-5138.0	153.9	-1481.6
new	1	-6896.7	88.9	*	-5132.6	156.3	-1486.9
new	3.4	-6932.3	118.0	*	-5143.3	158.6	-1476.1
Toki et al. [34]	1	-6959	632	*	-5162	410	-1441
		$B_\pi(2s)$	$\Gamma(2s)$		$B_\pi(3p)$	$\Gamma(3p)$	$\varepsilon(3p)$
old	0	-2891.3	137.9	*	-2383.2	108.2	-548.4
old	1	-2889.0	133.6	*	-2382.2	104.8	-549.4
new	0	-2954.1	12.5	*	-2407.6	51.7	-524.0
new	1	-2941.6	18.8	*	-2405.5	52.0	-526.2
new	3.4	-2960.0	37.2	*	-2411.6	54.2	-520.0
Toki et al. [34]	1	-2962	183	*	-2418	410	-509
		$B_\pi(3s)$	$\Gamma(3s)$		$B_\pi(4p)$	$\Gamma(4p)$	$\varepsilon(4p)$
old	0	-1602.6	58.7	*	-1381.6	49.2	-248.0
old	1	-1602.6	56.9	*	-1381.1	47.7	-248.4
new	0	-1633.3	5.4	*	-1393.7	23.7	-235.8
new	1	-1627.1	7.5	*	-1392.7	23.7	-236.9
new	3.4	-1636.3	17.8	*	-1395.9	25.0	-233.6
Toki et al. [34]	1	1642	78	*	-1408	71	-226

Table 4. Calculated transition energies and strong interaction widths for pionic X-rays populating deeply bound pionic orbits.

nucleus	type of potential	ξ	X-ray transition	transition energy [keV]	estimated line width [keV]
^{40}Ca					
	old	0	2p→1s	720.5	83.4
	old	1	2p→1s	721.9	83.6
	new	0	2p→1s	724.4	95.4
	new	1	2p→1s	724.0	95.1
	new	3.4	2p→1s	724.9	96.9
	Toki et al. [34])	1	2p→1s	735	106.7
^{48}Ca					
	old	0	2p→1s	642.4	59.7
	old	1	2p→1s	641.6	58.7
	new	0	2p→1s	653.9	33.3
	new	1	2p→1s	652.8	33.6
	new	3.4	2p→1s	654.1	36.2
^{208}Pb					
	old	0	2p→1s	1702.6	796
	old	1	2p→1s	1697.4	771
	new	0	2p→1s	1785.9	218
	new	1	2p→1s	1764.2	245
	new	3.4	2p→1s	1789.0	277
	Toki et al. [34])	1	2p→1s	1797	1042
	old	0	3p→2s	508.1	246
	old	1	3p→2s	506.8	238
	new	0	3p→2s	546.5	64
	new	1	3p→2s	536.2	71
	new	3.4	3p→2s	548.4	91
	Toki et al. [34])	1	3p→2s	544	593
	old	0	4p→3s	221.0	108
	old	1	4p→3s	221.5	105
	new	0	4p→3s	239.6	29
	new	1	4p→3s	234.4	31
	new	3.4	4p→3s	240.4	43
	Toki et al. [34])	1	4p→3s	234	149

Nuclear Physics A519 (1990) 773–804
North-Holland
[Title Page only]

AN IMPROVED PARAMETRIZATION OF THE OPTICAL POTENTIAL FOR PIONIC ATOMS

J. KONIJN, C.T.A.M. DE LAAT[1] and A. TAAL[1]
NIKHEF-K, P.O. Box 4395, 1009 AJ Amsterdam, The Netherlands

J.H. KOCH
NIKHEF-K, P.O. Box 4395, 1009 AJ Amsterdam, The Netherlands
and
Institute for Theoretical Physics, University of Amsterdam, The Netherlands

Received 2 July 1990

Abstract: We try to find an improved phenomenological optical potential for pionic atoms in two steps. First, we perform a new fit of the parameters in the standard optical potentials by using a large data base of 140 pionic atom data. A χ^2 is obtained that is substantially lower than with any previous parameter set. In a second step, we extend the number of parameters by using a more general form for the terms quadratic in the nuclear density. This extended version yields a reduction of the χ^2 by about a factor of two. The new fit includes a good description of shifts and widths of the deeply bound 3d orbits in heavy nuclei such as ^{181}Ta, ^{nat}Re, ^{nat}Pt, ^{197}Au, ^{208}Pb and ^{209}Bi. The value of the additional parameters in the extended version are difficult to interpret in the context of the chosen form of the optical potential and indicate that higher-order effects play a role.

1. Introduction

There are two main sources of information on the pion–nucleus interaction at low energies: pion–nucleus scattering and pionic atoms. In pion scattering, only a few angular momentum states of the π–nucleus system contribute to the scattering wave function. For light targets and at the lowest energies one presently can measure ($T_\pi \approx 20$ MeV), usually only the central s-wave and the more peripheral p-wave contribute significantly. To change the relative importance of these partial waves or to bring in higher l-states one can increase the scattering energy.

The situation is different in pionic atoms. After its capture, the pion finally cascades through circular orbits, each having a well defined angular momentum state $l = n - 1$. As the orbits come close enough to the nucleus, the pion feels the strong interaction. This interaction shifts the energy of the pionic level with respect to the electromagnetic Coulomb value and – due to the possibility of pion absorption – leads to an increased width of the level. By measuring the position and width of pionic atom states, we can, therefore, get information on the π–nucleus interaction for a fixed, discrete angular momentum state at essentially constant energy (on the scale relevant for the π–nucleus interaction). In practice, the absorption process becomes so strong

[1] Present address: University of Utrecht, Buys Ballot Laboratorium, Princetonplein 5, 3584 CC Utrecht.

0375-9474/90/$03.50

DISCUSSION

H. MACHNER pointed out that a pion captured into an atomic s–state experiences repulsion and one captured into a p–state attraction due to the strong interaction for light nuclei.

J. KOONIJN, in reply to a question, stated that nuclear deformation is taken into account in his calculations.

J. KOONIJN stated that a valuable experiment complementary to COSY 10 would be the attempt to observe low–lying pionic atom states in ^{40}Ca directly by detecting the X–rays. Such an experiment, although difficult, could be done by the COSY 10 collaboration at PSI with available high–resolution X–ray detectors and with appropriate background suppression.
H. MACHNER, after some discussion, suggested that this possibility be further discussed in more detail at a separate occasion.

K. Kilian

IKP, KFA Jülich

Two–Step Processes

The elementary interaction $p+n \rightarrow \pi^{-} + 2p$ embedded in a nuclear medium and similar reactions are treated as two–step processes. The importance of choosing kinematic conditions under which the residual particle (or nucleus) has essentially zero recoil energy so that the produced particle has close to zero energy and linear momentum is demonstrated.

26.7.91 K.

Two step reactions (+ kinemat. tricks)

- π^- atoms + recoil free kinematics (RFK
- other mesons (e.g. η) and energy (e.g. Δ excit.) in nuclei + RFK
- pionic molecules + RFK : $\{p\pi^- p\} \triangleq H_2^+$
- 33 Velocity matching (VM) of outgoing baryons in two step reactions ⟹ special case of RFK ⟹ find effects in Dalitz plot, do 3 body reactions

---

Two step: (1st) Meson production (2nd) Meson nucleus FSI (RFK)

Or: (1st) Meson production (2nd) Rescattering + Baryon FSI (VM)

RFK: K.K. New possibilities with recoilless kinematics using high quality proton beams Proc. Conf. on Nuclear Physics with stored cooled beams, Indiana 1984, P. Schwand H.O. Meyer Editor, AIP Conf. Proc. # 128 p. 319

V.M: K.K. and H. Nann: Meson Production and Velocity Matching Proc. Conf. on: Particle Production near Threshold Nashville 1990 H. Nann + E. Stephenson Editor, AIP Conf. Proc. # 2..

Meson-Kern W.W. in FS I

#10 Rückstoßfreie Produktion von π^--Atomen: $pn \to 2p\pi^-$

π^- ersetzt n ohne Rückstoß → π Kern W.W. in Ruhe
$2p = {}^2He$ im Magnetspektrometer (und Ge Zähler...)
Signaturen: 2p Koinzidenz; 2p Impuls = Strahlimpuls
(π^--Atom Zerfall)
Messung der Protonenrichtungen dicht nach Target

Kleine Relativenergie $\{\pi^-/\text{Rumpfkern}\}$ ⟹ hohe Bildungsrate für Atom

$$P \propto \exp\left(-\left(\frac{q^2}{2m_\pi}\right)/E_{Bind}\right)$$

COSY ✱ p (R/n) → (R/π^-)* $2p$ RFK! bei 830 MeV/c $q_\pi \approx 0$

IUCF $p\ {}^{13}C \to \{{}^{14}B + \pi^-\} \to p\ {}^{13}C$ $q_\pi > 200$ MeV/c

Saturne $d\ A_Z \to \{\pi^- A_{Z+1}\} + 2p$ $q_\pi > 200$ MeV/c ⟹ $T_\pi > 100$ MeV

N.B.: p (R) → (R)* d RFK bei 3,04 GeV/c {η-Kerne}

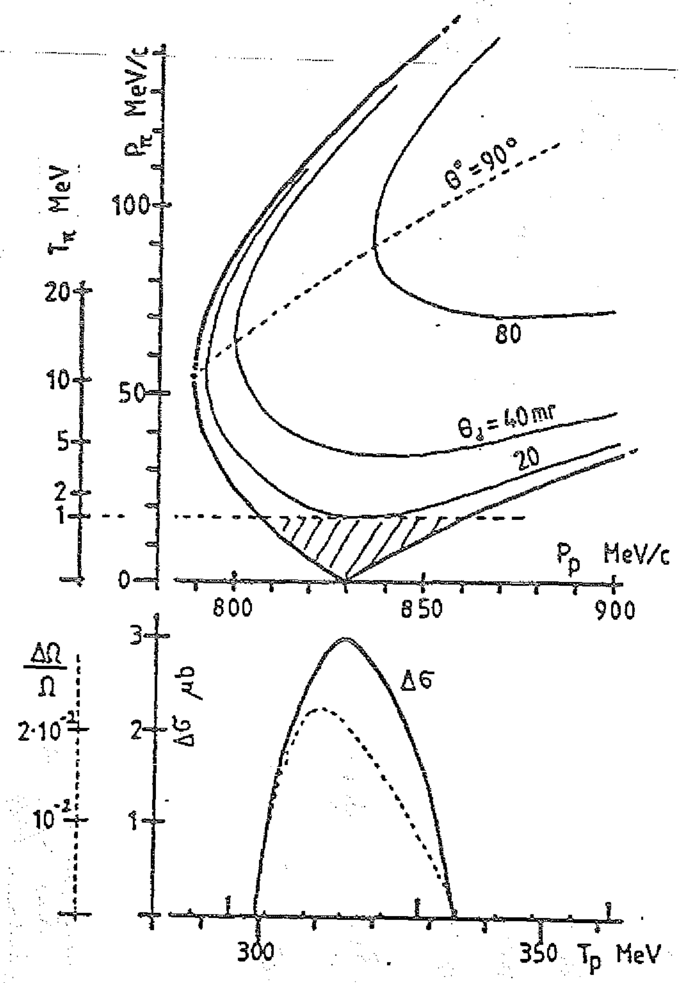

Fig. 2: Upper part: Pion laboratory momentum p_π as a function of proton beam momentum p_p in $pp \to d\pi^+$. The solid lower curve is the minimal pion momentum (180° emission in cm). The "magic" momentum is at p_p=829 MeV/c.

Lower part: Partial cross section $\Delta\sigma$ for production of pions with <1 MeV lab energy ($\Delta\sigma=(d\sigma/d\Omega)\Delta\Omega$). The relevant $\Delta\Omega$ is shown as dashed curve.

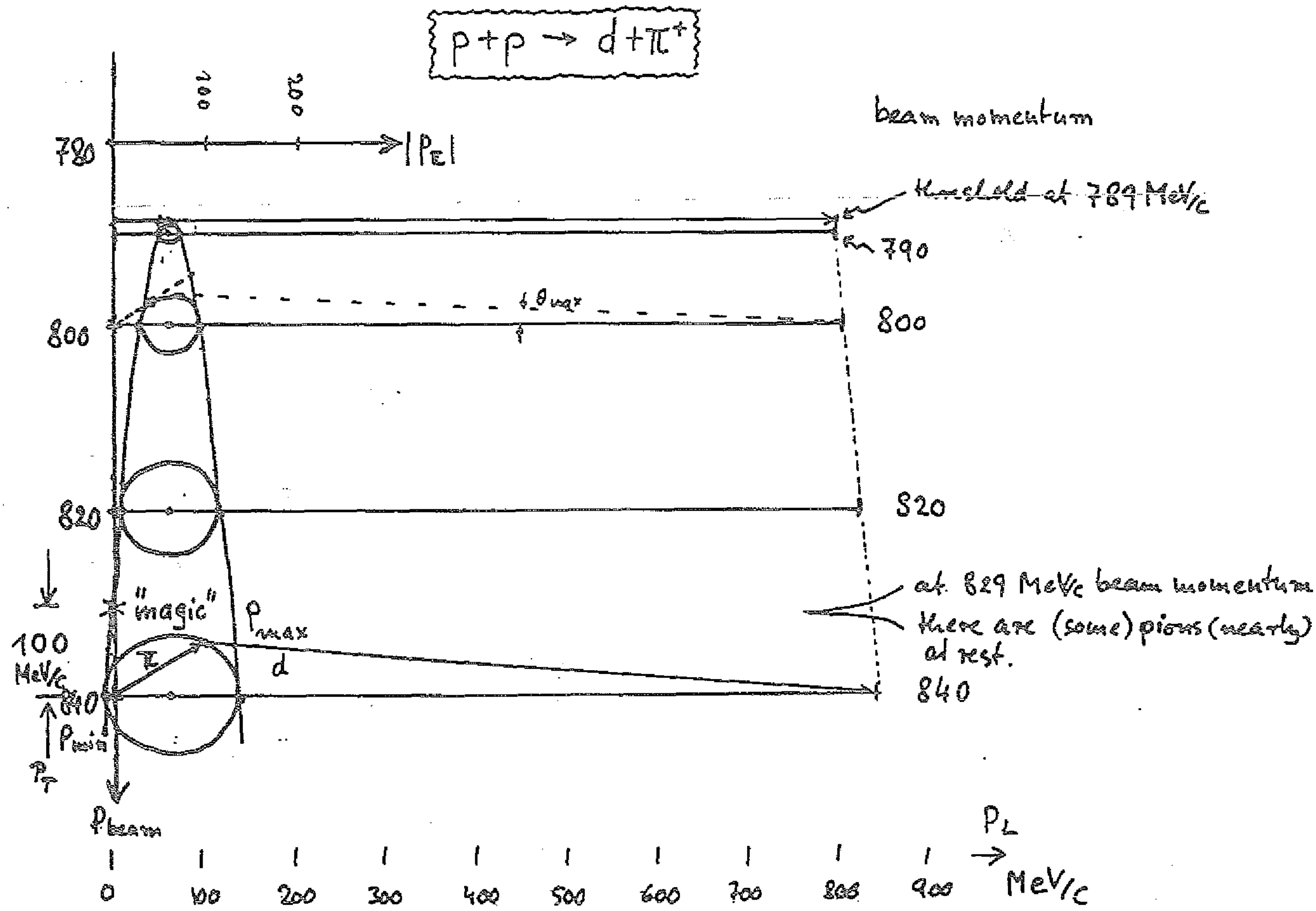
p+p → d+π⁺
beam momentum
|p_E|
100
200
780
threshold at 789 MeV/c
790
θ_max
800
800
820
820
at 829 MeV/c beam momentum there are (some) pions (nearly) at rest.
"magic"
p_max
π
d
100 MeV/c
840
840
p_min
p_T
p_beam
p_L
0
100
200
300
400
500
600
700
800
900
MeV/c

$$\boxed{E_n + E_R = M_A}$$

$$E_n = \sqrt{m_n^{*2} + q_F^2}$$

$$E_R = \sqrt{m_R^{*2} + q_F}$$

↑

festes Wert

⟹ m^* sinkt wenn q_F steigt

Für die quasifreie Kinematik hat das bewegte, gebundene Nukleon notwendigerweise ⟹ **variable Masse** p.107 $M_A = \sqrt{m_n^2 + q_n^2} + \sqrt{m_R^2 + q^2}$ $\boxed{\vec{q}_R = -\vec{q}_n}$

Calculated probability for pionic atom production in RFK: $P \propto \exp(-E_{recoil}/E_0)$
→ Fermi momentum in entrance gives smearing
(→ binding in exit would reduce smearing)

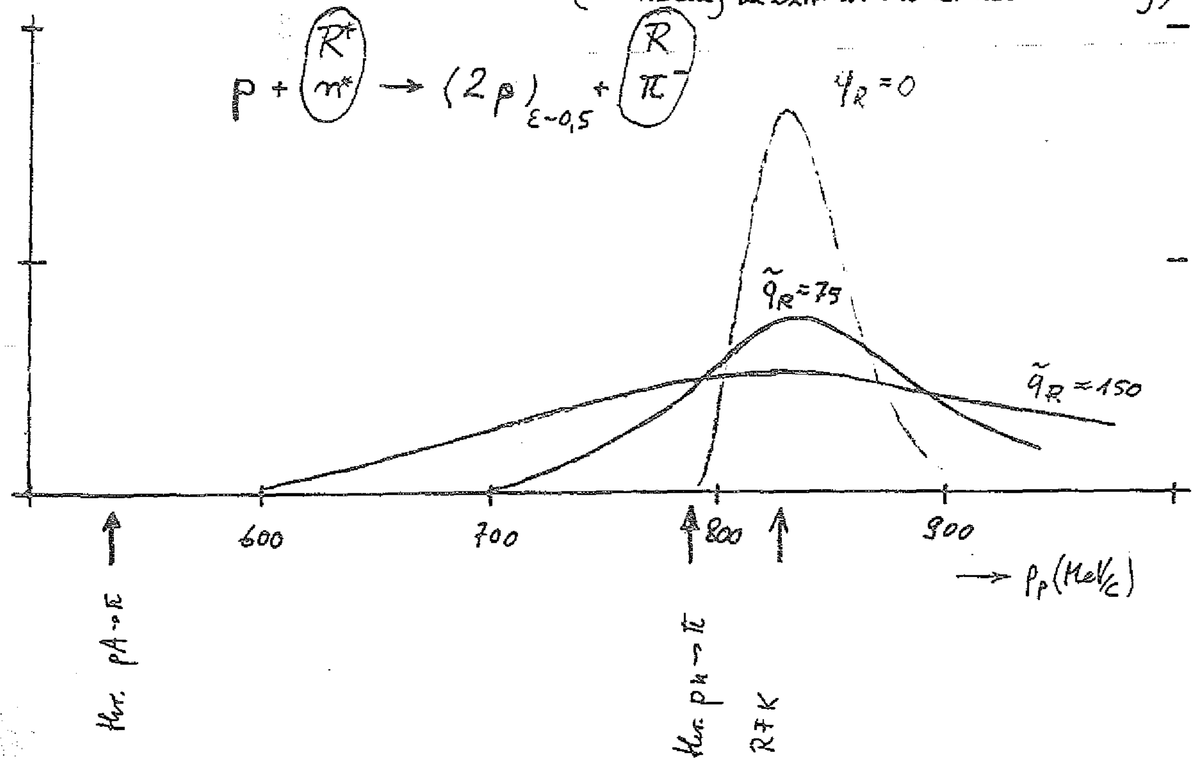

Rückstoßfreie Kinematik

Reaktion $1 + \left(\begin{smallmatrix}R\\2\end{smallmatrix}\right) \rightarrow 3 + \left(\begin{smallmatrix}R\\4\end{smallmatrix}\right)$

Magischer Impuls für $p_1 = p_3 \Leftrightarrow p_2 = p_4 \equiv 0$

$$p_1 = p_{mag} = \frac{1}{2}\sqrt{\frac{\left[(m_1^2 + m_3^2) - (m_2 - m_4)^2\right]^2 - 4m_1^2 m_3^2}{(m_2 - m_4)^2}}$$

m_2 und m_4 erscheinen als Differenz

Man kann zu beiden eine Masse R addieren ohne daß sich die „Rückstoßfreiheit" ändert

38

z.B.

$$\left.\begin{array}{l} K^- + n \rightarrow \pi^- + \Lambda \\ K^- + \left(\begin{smallmatrix}^{11}C\\ n\end{smallmatrix}\right) \rightarrow \pi^- + \left(\begin{smallmatrix}^{11}C\\ \Lambda\end{smallmatrix}\right) \end{array}\right\} p_{mag} = 531\ MeV/c$$

Table 1: Kinematic quantities for "magic" conditions in proton-nucleon interactions. When "particle 3" is a two-nucleon system then 10 MeV/c^2 have been added to take into account the relative NN energy. Recoilless hyperon production is shown for comparison.

Elementary reaction				threshold momentum	"magic" quantities momentum	energy	mass
beam 1 +	target 2 →	scatt 3 +	recoilless 4	p_1^{th} MeV/c	p_1^{mag} MeV/c	T_1^m MeV	$\sqrt{s}$ MeV/c^2
p	n	d	"50 MeV"	436,8	443.3	99.5	1927
p	p	d	π^+	788.8	828.65	287.5	2027
p	p	(pp)	π^0	809.8	849.4	327.4	2034
p	n	(pp)	π^-	820.3	862.1	335.9	2039
p	p	d	$\pi^+\pi^0$	1202.7	1363.4	716.7	2206
p	p	(NN)	"300 MeV"	1308	1512	841	2258
p	n	d	η^0	1978.4	3037.9	2241.2	2782
p	p	(pp)	η^0	2014.5	3105.5	2305.8	2802
p	N	(NN)	ω	2699	8463	7576	4212
K^-	n	π^-	Λ^0	–	530.9	231.3	1.578
K^-	n	π^-	Σ^0	–	284.5	76.1	1.482

p d ^3He η 1573 1740

O.k. for "Big Karl"

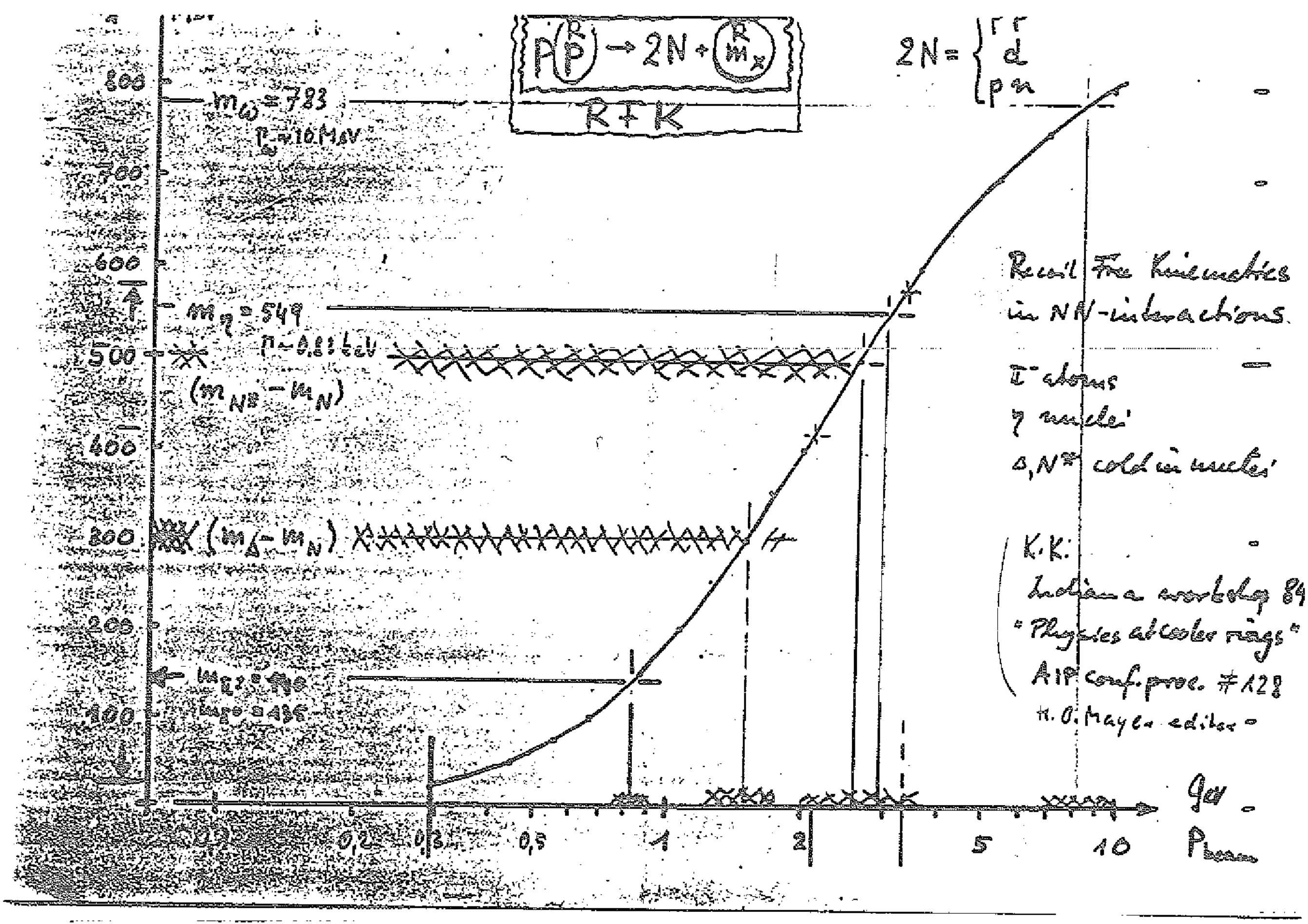

$$\{ p + n \to d + \eta^0 \}$$

$p_{mag} = 3038$ MeV/c ($p_{thr} = 1978.4$ MeV/c)

$\Delta\sqrt{s}_{mag} = (\sqrt{s}_{mag} - m_d - m_\eta) = 357$ MeV

$\theta_d^{max} = 17°$

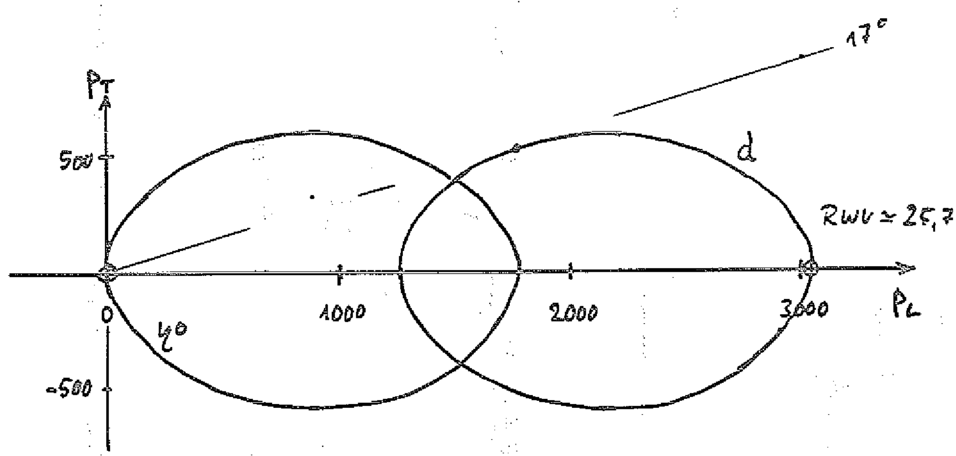

ToF. Spectrometer Tagging

K. Kilian + H. Nann

"Sub-threshold" production

Two step reactions

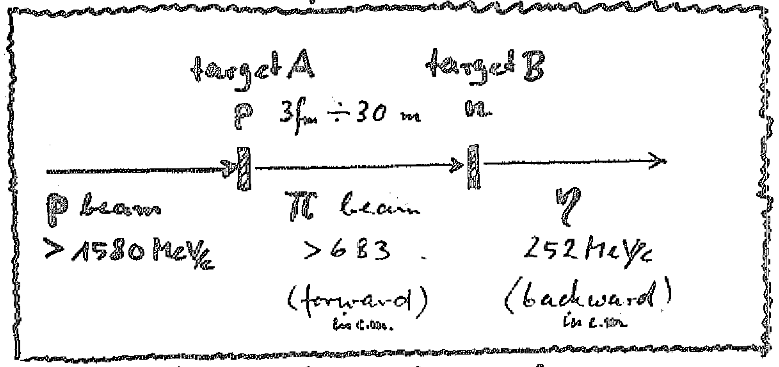

$q_1 \gtrsim 300$ $q_2 \gtrsim 400$

$\hat{=}$ 0,66 fm $\hat{=}$ 0,5 fm $< R_{deuteron}$

Ⓐ $p + p \to \pi^+ + d$ Ⓑ $\pi^+ + n \to \eta + p$

goal: $pd \to \eta\,{}^3He$

40

In a two step ~~reaction~~ we get

η mesons ~~with 1.58 GeV/c protons~~

⇒ "SUBTHRESHOLD"

⁂ Single step ~~pp → ppη threshold at 1.99 GeV/c~~

⁎ This "subthreshold" production selects the two step reaction (even on deuteron targets)

⁎ There is no high momentum component in the two target nucleons needed.

Table I: Threshold momenta in GeV/c for proton induced meson (M) production in a two-step process with different intermediate particles (m) and in a single step process. The brackets around the baryonic systems indicate zero relative energy ε. This assumption allows us to compare the thresholds for the different reactions. The values shown in the table are calculated for the cases of A: $p+n \to m^* + (n+p)_{\varepsilon=0}$ B: $m^* + p \to M^* + p$

final heavy meson M	intermediate particle m	two step threshold $N+N \to m+(2N)$ $m+N \to M+N$	single step threshold on a (2N) target $N+(2N) \to M+(3N)$	Beam momentum for which velocity matching occurs in the 2N-N exit system at 0°
π	γ	676.9	657.2	800
	π	776.5		940
η	γ	1584.6	1584.5	1590
	π	1584.7		1590
	η	1985.9		2120
ω	γ	2083	2072	2120
	π	2080		2120
	η	2124		2190
	ω	2669		2680
φ	γ	2621	2579	2700
	π	2617		2700
	η	2579		2580
	ω	2707		2780
	φ	3405		

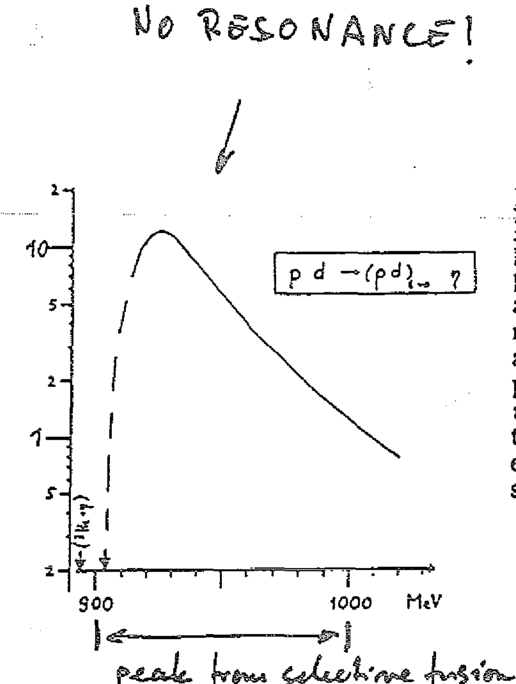

Figure 2: Probability for ^3He fusion in a two step process A: $pp \to d\pi^+$ B: $\pi^+ n \to p\eta$ overall: $pd \to (pd)\eta$ (assumptions see text) as function of energy. Note the rather narrow energy band. The arrows indicate the thresholds for pd reactions to $^3He\ \eta$ and to pd η. The (off shell) ^3He fusion leads to a shift of the calculated excitation function, so that it starts at the $^3He\ \eta$ threshold.

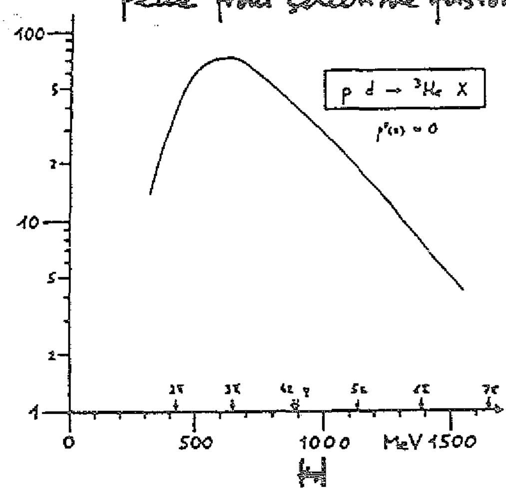

Figure 3: Excitation function for ^3He fusion calculated in a two step process (A: $pp \to d\pi^+$ B: $\pi^+ n \to pX$) for the overall reaction $pd \to {}^3HeX$ (see text). The ^3He acceptance is tuned such that it always corresponds closely to the maximally possible mass X like in the Saclay experiment [7]. The broad enhancement found in ref. [7] can be qualitatively reproduced by a two step process.

In a Dalitz–plot e.g. of the (squared masses of) subsystems, $M^2(p+d) = (V(p) + V(d))^2$ against $M^2(X+p) = (V(X) + V(p))^2$ there can be very distinct density modulations due to the two step process. They will not extend across the Dalitz plot like a resonance would do. In order to find out the relative importance of two step processes one should therefore study besides the two body channels also the three body reactions ($pd \to X^0pd$, $pd \to X^+nd$, $pd \to K^+\Lambda^0d$, $pd \to K^0\Sigma^+d$ etc.) in kinematically complete experiments over the full phasespace.

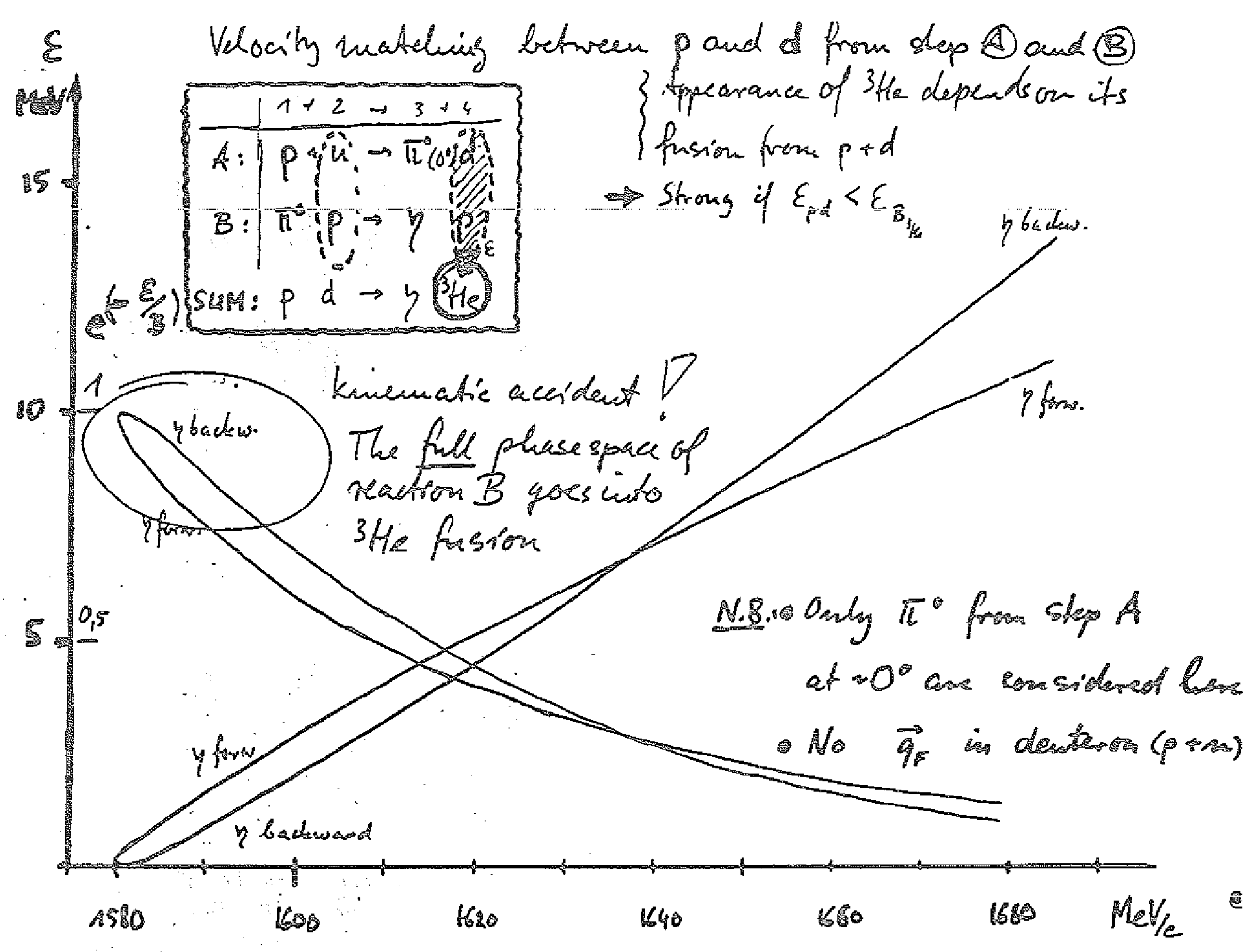
Velocity matching between p and d from step A and B
Appearance of 3He depends on its fusion from p+d
⇒ Strong if ε_pd < ε_B3He
1 + 2 → 3 + 4
A: p + n → π°(0°) d
B: π° p → η p
SUM: p d → η 3He
ε
MeV
15
10
5
exp(−ε/B)
1
0,5
kinematic accident !
The full phase space of reaction B goes into 3He fusion
η backw.
η forw.
η backward
N.B. • Only π° from step A at ~0° are considered here
• No q_F in deuteron (p+n)
1580
1600
1620
1640
1660
1680
MeV/c

MESON PRODUCTION AND VELOCITY MATCHING

K. Kilian and H. Nann*
Institut für Kernphysik, Forschungszentrum Jülich, D–5170 Jülich, FRG
*Indiana University, Cyclotron Facility, Bloomington, Indiana 74705, USA

Abstract
A sequential mechanism of meson production in proton–nucleus collisions leads to meson production at beam energies below the nucleon–nucleon–meson–threshold. In a cascade–like sequence, a light intermediate particle is created in a first nucleon nucleon collision. In a second step, this intermediate particle produces a heavier outgoing meson by interacting with a second nucleon of the same target nucleus. If besides the light intermediate particle there is a deuteron produced in the first step, this can fuse with the nucleon N from the second step to form a bound final (3N) baryonic system. If the velocities of the baryons produced in the two steps are matched then their relative energy is close to zero. Then the 3N fusion to one nucleus will be enhanced and the meson production cross section for a two body channel should show a bump in the excitation function which has nothing to do with a resonance. Results of Monte–Carlo simulations of this sequential reaction mechanism are shown.

Kinematical considerations

The new storage rings with phasespace cooling like the IUCF cooler in Bloomington, CELSIUS in Uppsala and COSY in Jülich will open possibilities to study meson production close to thresholds. They will provide the high resoultion which is needed here [1]. In elementary proton proton interactions thresholds are interesting since only a few partial waves are contributing so that the complex hadronic process can be more easily interpreted. Meson production on nuclei in p–A (or even in A–A) interactions is more complicated and the above argument for thresholds becomes even more important. Thus in a first step, we will concentrate on the simplest nuclear target, the deuterium.

For two step processes on the two nucleons of the deuterium target we make two simple but important statements concerning the kinematics:

1. There is a reduction of the threshold for particle production already without the necessity of Fermi momentum [2] or cooperative nuclear effects [3].

Take for example η production. Its threshold in p+p interaction lies at 1985.9 MeV/c. If we however first produce a pion in a p+p reaction (step A) and use this pion in a pion–neutron reaction (step B) to make the η, then the threshold is only at 1584.7 MeV/c.

The momentum transfer in both reaction steps is about 900 MeV/c and so high that even in the case when the pion goes only the distance of a few fm inside the deuteron range, we can assume that the reaction partners have still particle properties. Thus normal on–shell particle interaction is still an allowed approximation.

Topical Conference: Particle production near threshold, 30.9.-3.10.1990, Nashville, Indiana, USA

One should expect that two step processes are relatively strong in the "sub-threshold" region (at momenta below the elementary threshold) where quasi-free one step meson production is kinematically suppressed. Examples of threshold momenta for proton induced meson production in one– and two–step processes on a two–nucleon system are given in Table 1. The thresholds for heavy meson production in two–step processes shown in Table 1 lie close to the lowest possible kinematical threshold which is given by the p + (2N) → M + (3N) single–step reaction.

Table 1: Threshold momenta in MeV/c for proton induced meson (M) production in a two–step process with intermediate particles (m) and in a single step process. Brackets around the baryonic systems indicate zero relative energy ϵ. This assumption allows to compare the one and two step thresholds. The values are calculated for

step A: $p+n \rightarrow m^o + (n+p)_{\epsilon=0}$ step B: $m^o + p \rightarrow M^o + p$

final heavy meson M	intermed. meson m	two step threshold $N+N \rightarrow m+(2N)$ $m+n \rightarrow M+N$	single step threshold on $(2N)$ target $N+(2N) \rightarrow M+(3N)$	momentum where velocity matching occurs in the $(2N)+N$ exit system
π	γ	676. 9	657. 2	800
	π	776. 5		940
η	γ	1584. 6	1584. 5	1590
	π	1587. 7		1590
	η	1985. 9		2120
ω	γ	2083.	2072.	2120
	π	2080.		2120
	η	2124.		2190
	ω	2669.		2680
ϕ	γ	2621.	2579.	2700
	π	2617.		2700
	η	2579.		2580
	ω	2707.		2780
	ϕ	3405.		

2. The experimentally interesting two body channels with ^{3}He or ^{3}H as final nuclei,

p + d → (3 nucleons bound) + X

are strongly enhanced in certain energy and angular regions by the kinematics of two step processes when "velocity matching" between the three nucleons of the three–baryon system occurs.

It is evident that those channels are strongly favoured only when already in the first step a deuteron is formed. In the following we therefore consider as model cases reactions of the type

Step A	$p + p \to \pi^+ + d$	
Step B	$\pi^+ + n \to X + p$	(or X^++n)
Total	$\overline{p + d \to X^o + {}^3He}$	(or $X^+ + {}^3H$)

We can calculate the relative energy ϵ between the deuteron from step A and the proton from step B. ϵ is minimal if the velocities of the two partners match. The invariant mass squared $S(d+p) = (V(d) + V(p))^2$ depends on the four–vectors V of d and p. The excess energy in the d+n exit system, $\epsilon = \sqrt{S} - M(d) - M(p)$ can be used to get an estimate for the fusion probability P into ^{3}He. The fusion becomes the more probable the smaller the excess energy ϵ is in comparison with the binding energy E_b of the three body system (5.49 MeV for p+d binding in ^{3}He).

$$P = \exp(-\epsilon/E_b)$$

Exactly the same effects of an enhanced final state interaction in corners of the phase space where relative energies of reaction partners are small, also happen in "recoilless" kinematics. Here a particle is produced at rest in the laboratory system so that it can favourably interact with the residual target nucleus [4].

Examples of velocity matching

This "velocity matching" in sequential meson production is shown in Fig. 1 for the case of the nd $\to$ (3N) + π reaction in which the intermediate particle $m(=\pi)$ is produced at forward angles and then backscattered or undergoes charge exchange in step B. Figures 1a and b show the relative energy ϵ as a function of incident neutron momentum and the probability P for the formation of the final bound (3N) baryonic system, respectively. One sees that the forward going intermediate pions can give rise to small values of ϵ. Folding in the pp $\to$ dπ cross section for step A and restricting the emission of the final pion to very backward angles, the excitation function, depicted in Fig. 1c, is obtained. We predict a cross section enhancement around (1025 $\pm$ 100)MeV/c. Data of Rössle et al. [5] for backward produced pions in the nd $\to$ ^{3}He π^- reaction show indeed this behavior (see Fig. 1c). We want to stress that this type of "velocity matching" effect might be misinterpreted as a (3N) resonance in the direct channel. Moreover, also in the p+d $\to$ t+π^+ reaction an enhanced backward emission of pions was observed at T_p = 470 MeV (p_p = 1050 MeV/c) incident energy, which so far no theoretical calculation was able to reproduce (for details see Ref. [6]). The present model of sequential meson production accounts for this enhanced backward emission.

A more realistic description of the two step process has to take into account the full angular– and energy range of reaction partners in both steps. Also one has to consider that the proton and neutron are bound in the deuteron. They have Fermi momenta $\vec{q}(p) = -\vec{q}(n)$ with a continuous distribution and consequently they have off shell masses m^*. The deuteron mass $m(d) = m(p) + m(n) - 2.22$ MeV has to be reproduced by the total p and n energies

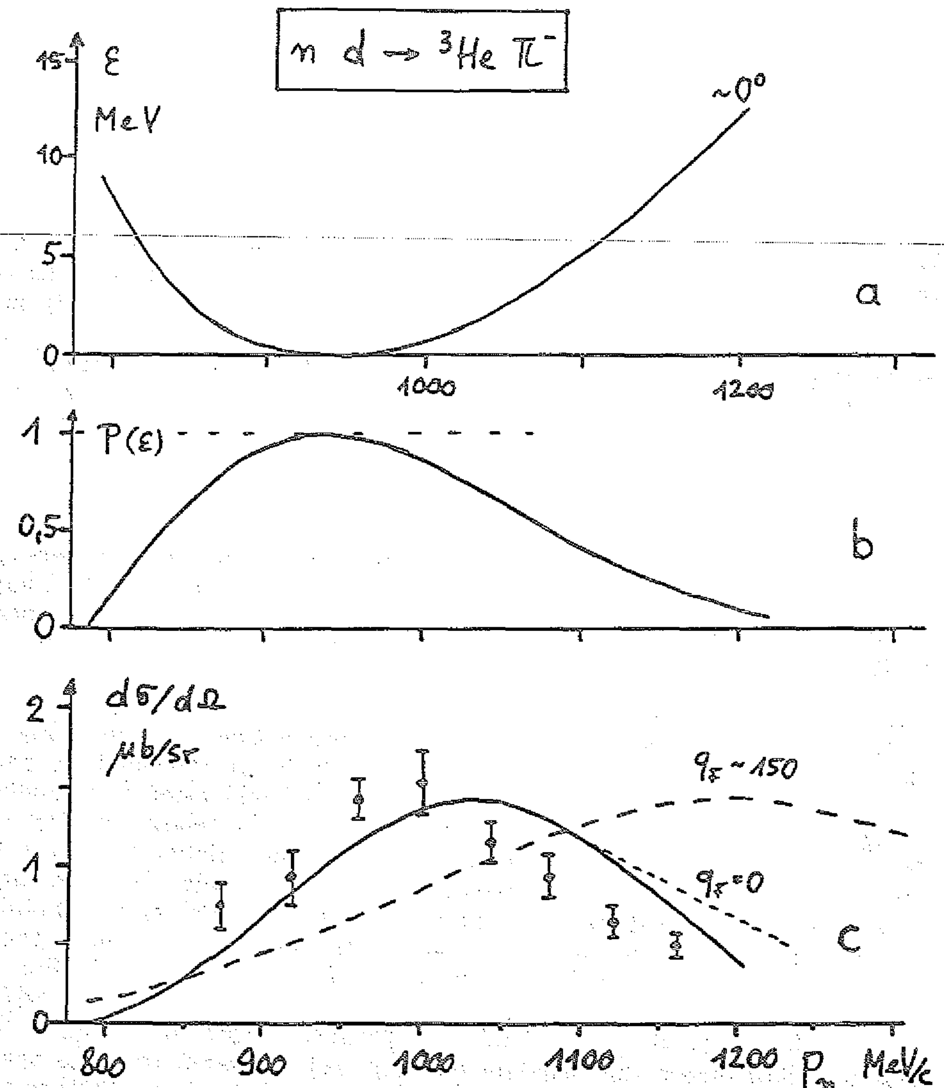

Figure 1: a) Relative energy ϵ of the outgoing p and d in a two step π rescattering process with step A: n+n → π^-d and step B: π^-p→π^-p in quasifree kinematics without Fermi momentum. Forward 0° angles of the outgoing π^- in step A are considered. π^- scattering angles in step B are backward. b) Shows the corresponding fusion probability $P = \exp(-\epsilon/E_b)$ for (p+d)↔^{3}He. c) Comparison of measured n+p→π^- ^{3}He data [5] with a prediction using the fusion probability in Fig. 1b multiplied with the total np→π^-d cross section (solid line) and a prediction with a Monte Carlo Simulation (dashed line) on bound nucleons with Fermi momenta $\langle\vec{q}\rangle$ - 150 MeV/c and energy dependent differential cross sections in step A. In step B a constant cross section is used.

$$m(d) = \sqrt{m^*(p)^2 + q^2} + \sqrt{m^*(n)^2 + q^2}\ .$$

If we assume that the off–shell masses of p and n have the same ratio as the on–shell masses, then we can calculate for each q the kinematically relevant fourvectors V of the bound and moving reaction partners in the deuteron target.

$$V(m^*) = (E^*, \vec{q}) = (\sqrt{m^{*2} + q^2}, \vec{q}) = ((m - 1.11\ \text{MeV}), \vec{q})$$

We have done Monte Carlo simulations of several reactions where the result of the first step was used as input for the second step. Fermi momenta with an average of $<|\vec{q}|> = 150$ MeV/c were used. The energy dependent differential cross section for $p+p \to \pi^+ + d$ was included in step A. For step B we assumed an energy independent isotropic (s–wave) differential cross section. The probability for three baryon fusion in the final state was caltulated for each event. The same was done for effects of acceptances in solid angle $\Delta\Omega$ and momentum Δp. The effect of the averaging over all kinematical variables is shown in Fig. 1c for $nd \to \pi^-\ {}^3He$. There is a shift of the maximum towards higher energies. It is worth noting that without Fermi momentum the averaging leads to a prediction very close to the simple 0^o approximation in fig. 1c.
A famous example of a reaction with spectacular threshold behaviour is $p^+d \to \eta\ {}^3He$ [7]. A spike appears in the 0^o ${}^3He$ production close to the η threshold in $p+d \to {}^3He + \eta$.
This spike has stimulated interest. Two step processes [8] and coupled channel effects [9] have been used to describe properties of this reaction. Its very narrow shape is caused by the narrow momentum acceptance of the used magnetic spectrometer [7]. Independent of this narrowness we find, that there should be a strong enhancement of the total $pd \to {}^3He\ \eta$ two body cross section due to velocity matching just close to threshold. Fig. 2 shows our prediction for a large acceptance measurement of $pd \to {}^3He\ \eta$.

In Fig. 3 we compare a two step simulation and data of the reaction $pd \to X^3He$. We simulated the experimental situation described in ref. 7. Here the momentum acceptance of the ${}^3He$ spectrometer sitting at 0^o was always tuned such that it accepted ${}^3He$ corresponding to threshold production of the actual maximal possible mass X. As one can see the assumption of a two step process explains the appearance of a wide enhancement of the forward ${}^3He+X$ cross section. The opening of several inelastic channels in step B with rising energy (and rising mass X) should give an increasing total cross section in step B. There should be therefore a slower decrease of the high energy cross section.

Conclusion

The concept of two step interactions with final state fusion of particles which have matched velocities helps to understand experimental results in few body interactions, especially in two body meson production with protons on deuterium close to thresholds.
Another manifestation and a further proof of the two step processes should show up in the three body exit channels

$$p + d \to X^0 + p + d \qquad (\text{or } X^+ + n + d).$$

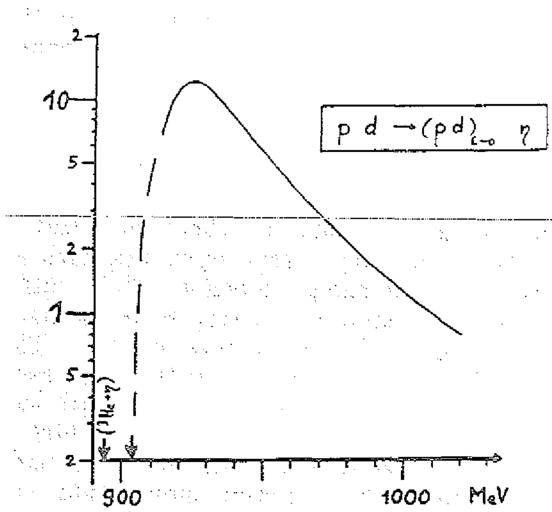

Figure 2: Probability for ³He fusion in a two step process A: pp→dπ⁺ B: π⁺n→pη overall: pd→(pd)η (assumptions see text) as function of energy. Note the rather narrow energy band. The arrows indicate the thresholds for pd reactions to ³He η and to pd η. The (off shell) ³He fusion leads to a shift of the calculated excitation function, so that it starts at the ³He η threshold.

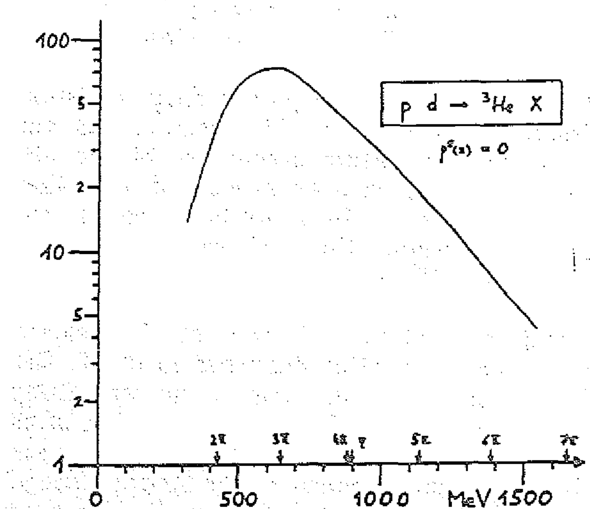

Figure 3: Excitation function for ³He fusion calculated in a two step process (A: pp→dπ⁺ B: π⁺n→pη) for the overall reaction pd→³HeX (see text). The ³He acceptance is tuned such that it always corresponds closely to the maximally possible mass X like in the Saclay experiment [7]. The broad enhancement found in ref. [7] can be qualitatively reproduced by a two step process.

In a Dalitz–plot e.g. of the (squared masses of) subsystems, $M^2(p+d) = (V(p) + V(d))^2$ against $M^2(X+p) = (V(X) + V(p))^2$ there can be very distinct density modulations due to the two step process. They will not extend across the Dalitz plot like a resonance would do. In order to find out the relative importance of two step processes one should therefore study besides the two body channels also the three body reactions (pd → X^0pd, pd → X^+nd, pd → $K^+\Lambda^0$d, pd → $K^0\Sigma^+$d etc.) in kinematically complete experiments over the full phasespace.

References

1. K. Kilian et al., Proc. Workshop on Physics at LEAR with Low Energy Cooled Antiprotons, Erice, May 1982, Plenum Press 1984, Ettore Majorana International Science Series Nr. 17, p. 843, edited by U. Gastaldi and R. Klapisch
2. G.F. Bertsch, Phys. Rev. C15 (1977) 713
3. R. Shyam and J. Knoll, Nucl. Phys. A426 (1984) 606
4. K. Kilian, Nuclear Physics with Stored, Cooled Beams, edited by P. Schwandt and O. Meyer, AIP Conf. Proc. Nr. 128 (1985) 319
5. E. Rössle et al., Pion Production and Absorption in Nuclei, edited by R.D. Bent, AIP Conf. Proc. Nr. 79 (1982) 171
6. H.W. Fearing, Phys. Rev. C11 (1975) 1210
7. F. Plouin, Proc. Workshop on Production and Decay of Light Mesons, Paris 1988, p. 114, edited by P. Fleury, World Scientific, Singapore
8. J.M. Laget et al., Phys. Rev. Lett. 61 (1988) 2069
9. C. Wilkin, same proceedings as ref. 7, p. 187

DISCUSSION

H. MACHNER wrote down the cross section equation for the $(p,{}^2He)$ reaction that is of interest in COSY 10,

$$\frac{d\sigma}{d\Omega} = \frac{d\sigma}{d\Omega}_{p+n\rightarrow {}^2He+\pi^-} \times \left| \int \Phi^*_{n,l}(\mathrm{r}) \exp[-i(\mathrm{k}_{{}^2He} - \mathrm{k}_n)\mathrm{r}] \phi_\alpha(\mathrm{r}) d^3r \right|^2$$

where the bound neutron on which the reaction takes place is assumed to be in a quantum state ϕ_α with quantum numbers α and where $\phi_{n,l}$ is the pionic wave function. He noted that it is evident from this equation that σ is largest when the momentum transfer $q = k_{{}^2He} - k_n = 0$, i.e. when the reaction is recoil–free.

K. KILIAN noted that particle production at the magic momentum is a two–step process and not a resonance.

G. Riepe

IKP, KFA Jülich

The Germanium Wall

A position–sensitive 4π detector for charged particles with high energy and space resolution is under construction. Its main features are described.

"Germanium Wall"

Ge detector system

total thickness: 23 mm → range of protons with 443 MeV/c
→ 99.3 MeV;

acceptance: 400 mrad - required angular resolution: 2 mrad
energy resolution: 10^{-3} (fwhm);
opening of 56 mrad - for the primary beam and for a fraction of the reaction protons to enter the magnetic spectrometer (corresp. to its acceptance);

system made up of 3 transmission type HPGe detectors
(thin dead layers on both contact faces - doping by ion implantation),
mounted in a stack arrangement,
geometry determined by the largest achievable detector diameter (available material) for position three
and by requirement to have 4π solid angle in C.o.M. system for detection of the two protons from the reaction.

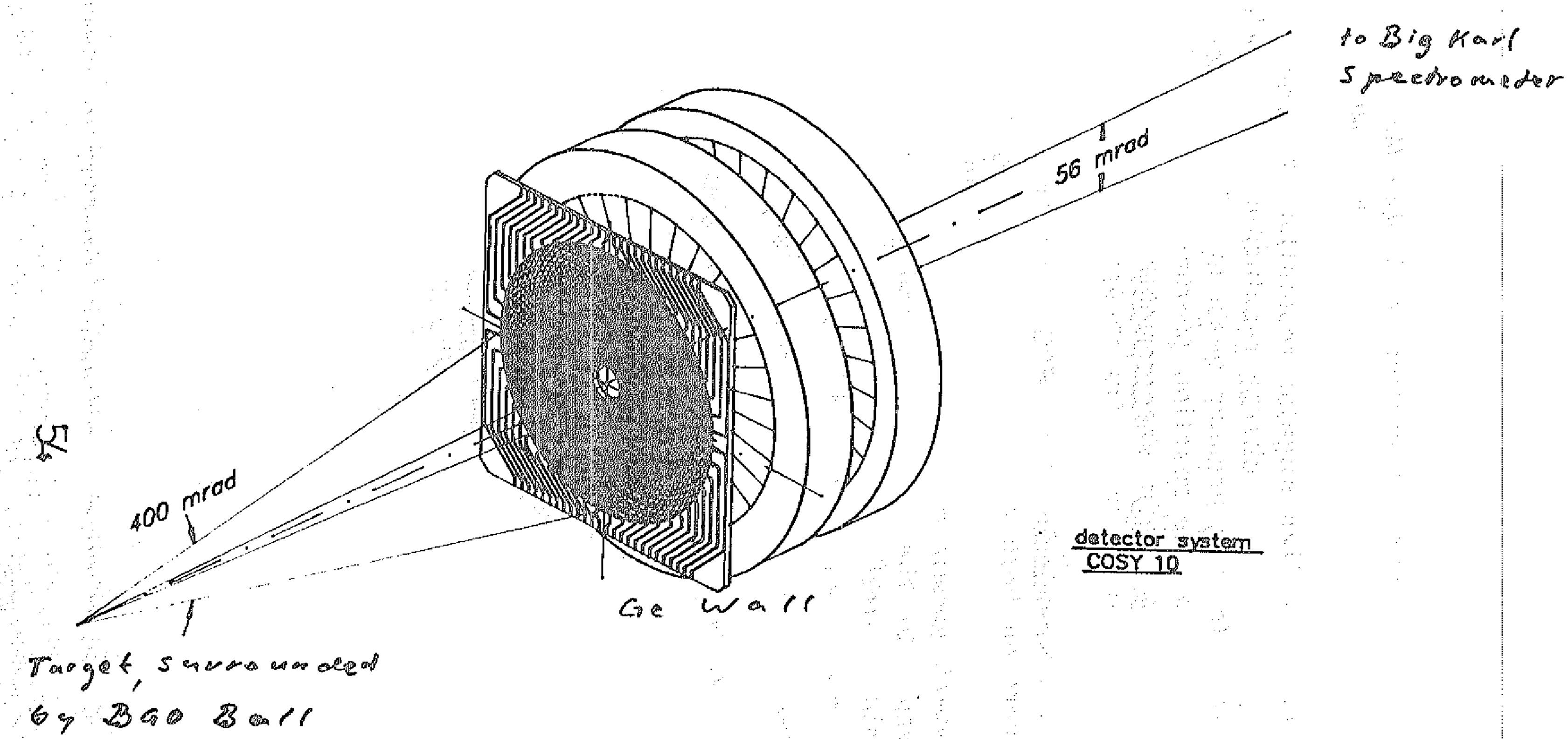
to Big Karl
Spectrometer
56 mrad
400 mrad
Ge Wall
Target, surrounded
by BGO Ball
detector system
COSY 10

Ge Wall components:

1. detector 1 mm thick - diameter of sensitive area 53,5 mm
   position structure consisting of 200 elements on both sides
   system of Archimedes spirals on front and rear side in opposite directions

2. detector 11 mm thick - diameter of sensitive area 61 mm (rear) with radial position structures consisting of 32 segments on one side

3. detector 11 mm thick - diameter of sensitive area 70 mm (rear) similar structure as no. 2 - total diameter 82 mm

   in addition to the position-sensitive pattern in the center of the detector a structure at its circumference is foreseen to facilitate connections from the detector to printed circuit boards (epoxy) by ultrasonic bonding (aluminium wire of 25 µm)

   space at the edges needed for mounting
   - clamping with indium wire
   - Al_2O_3 used for electrical insulation

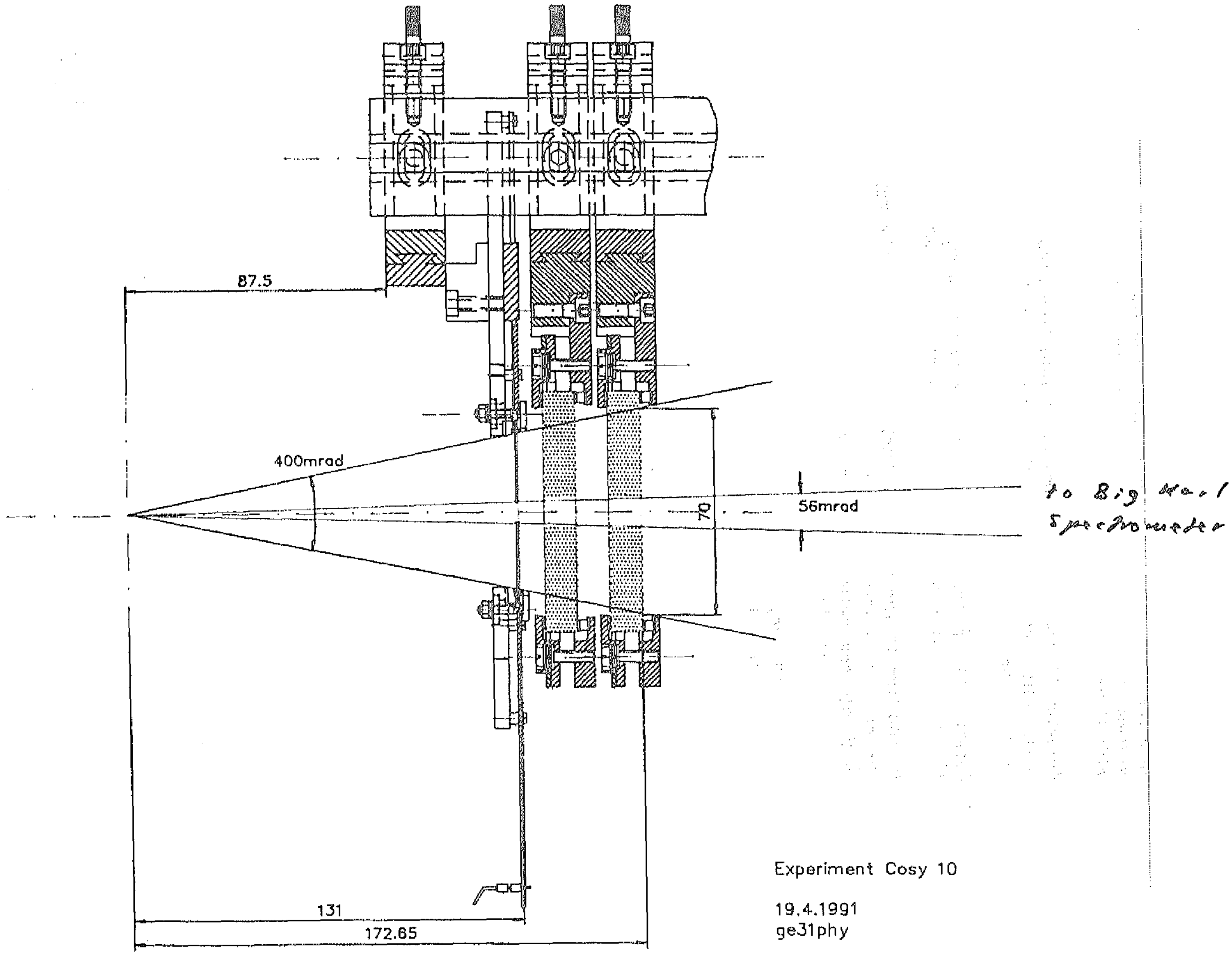

Experiment Cosy 10

19.4.1991
ge31phy

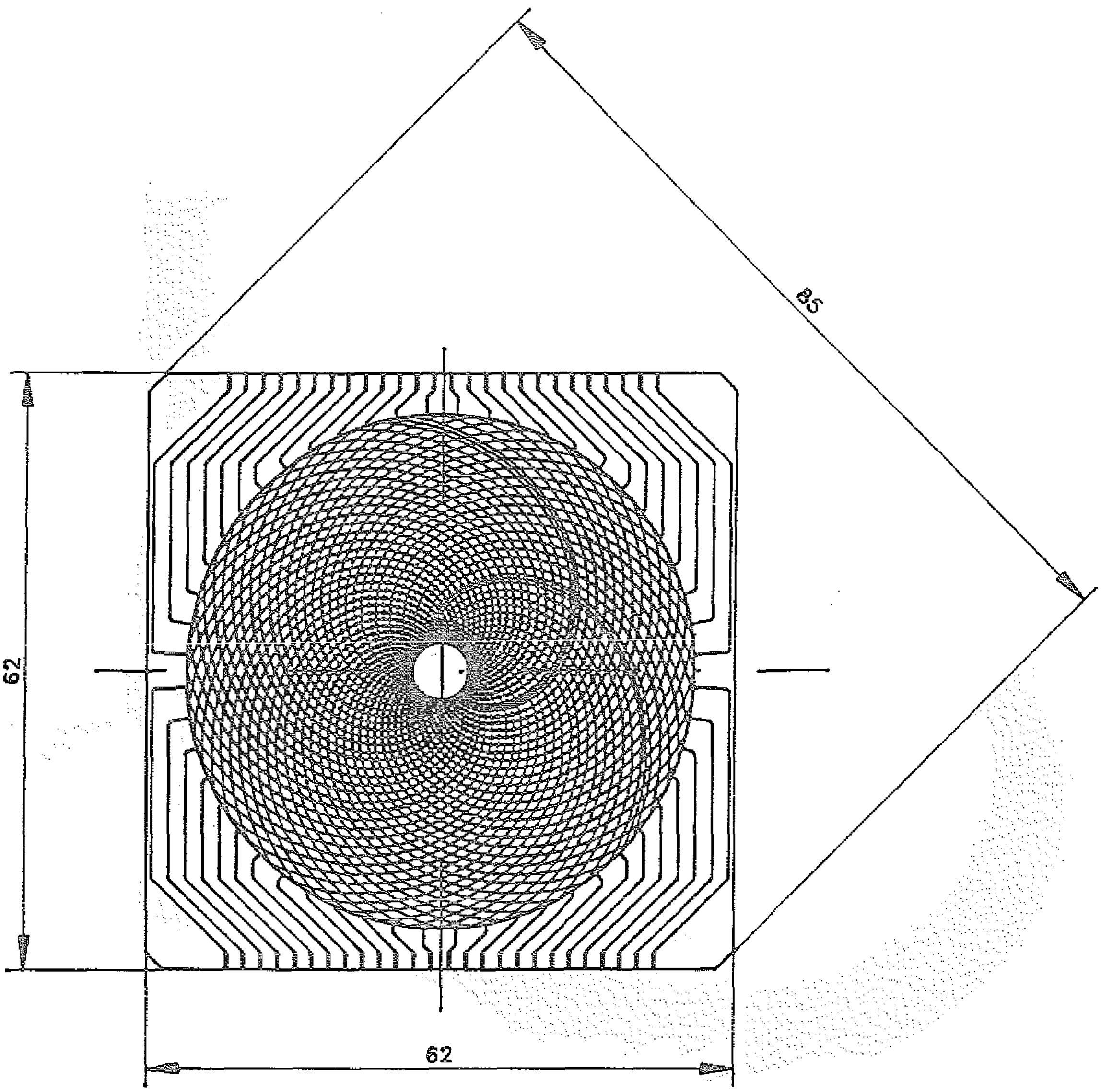

position structure of detector 1
only 52 elements (instead of 200) are shown

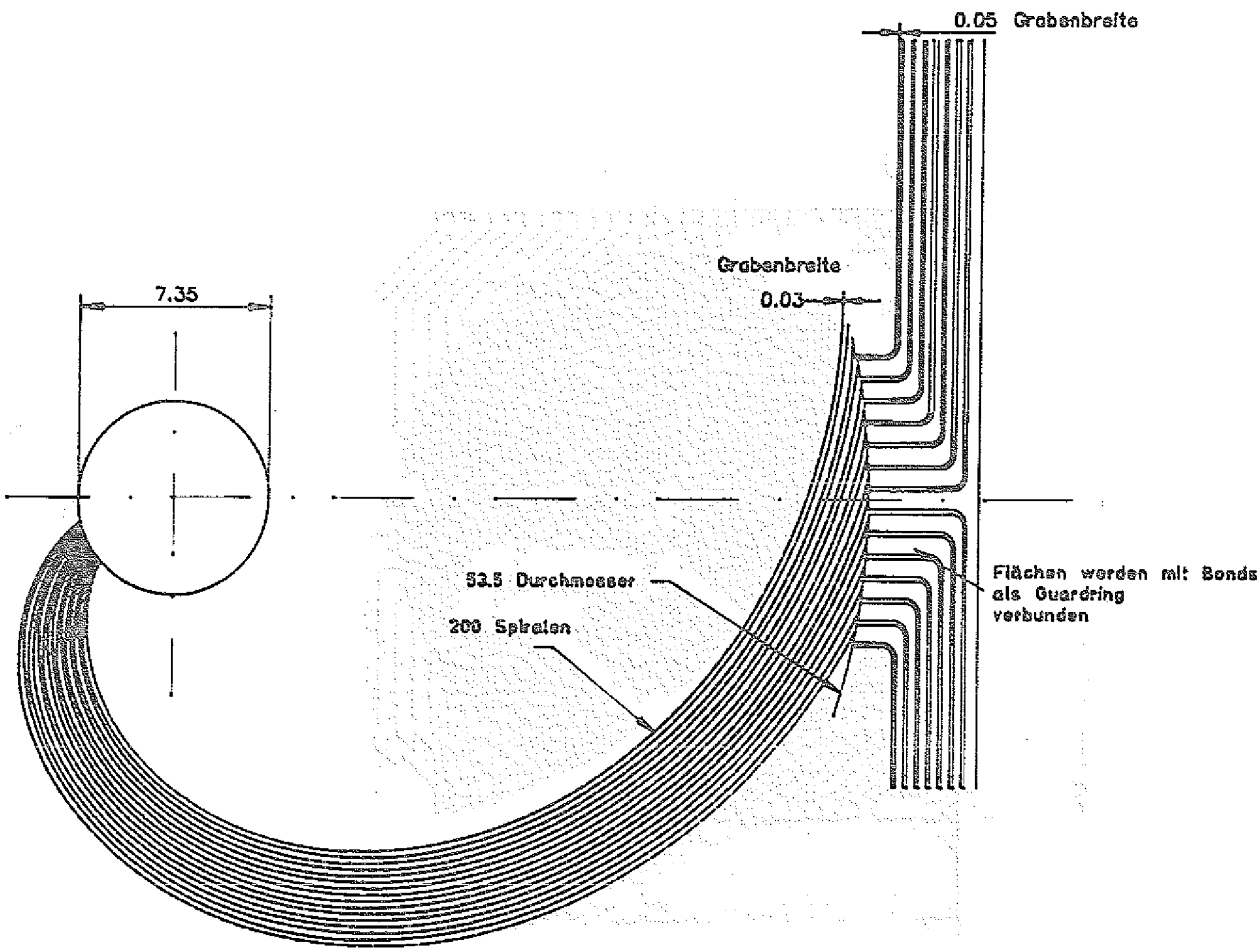

Details der Detektorstruktur (Detektor 1, COSY 10)

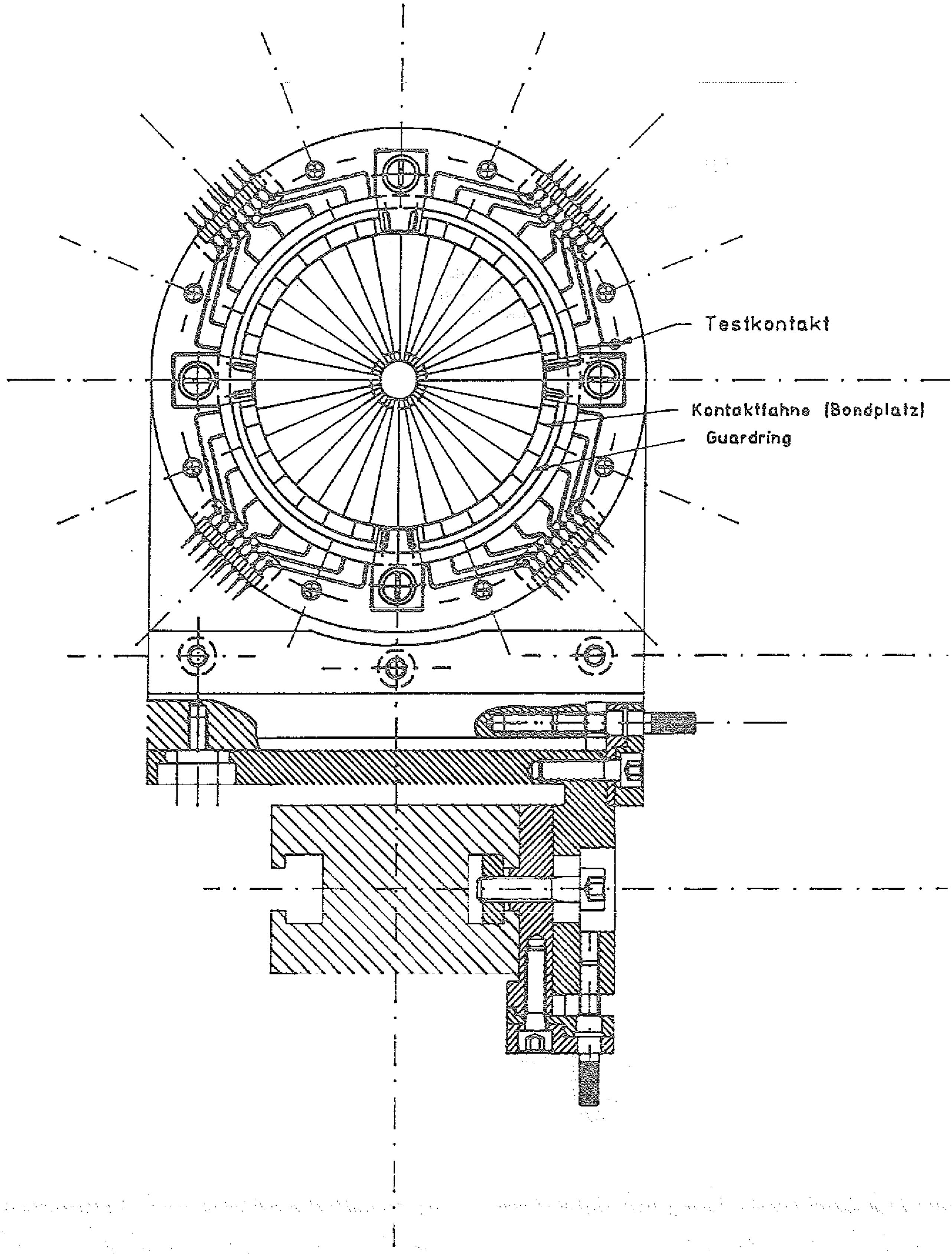
Testkontakt
Kontaktfahne (Bondplatz)
Guardring

cryostat

temperature: liquid N_2, vacuum: < 10^{-6} mbar,
mounts for the 3 detectors adjustable in x- and y-direction
(centering the holes)
leads from the epoxy boards to the feedthroughs
temperature drop (stainless steel),
stray capacitance (resolution, cross-talk)
400 for the first dE detector
33 for each of the 2 following detectors

electronics

single read-out
box with 50 preamplifiers (SMD technology)
mounted on the feedthroughs
cables to NIM crates (linear amplifiers etc.)

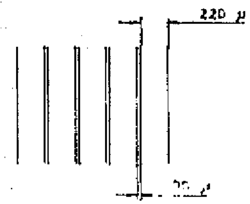

Zähler

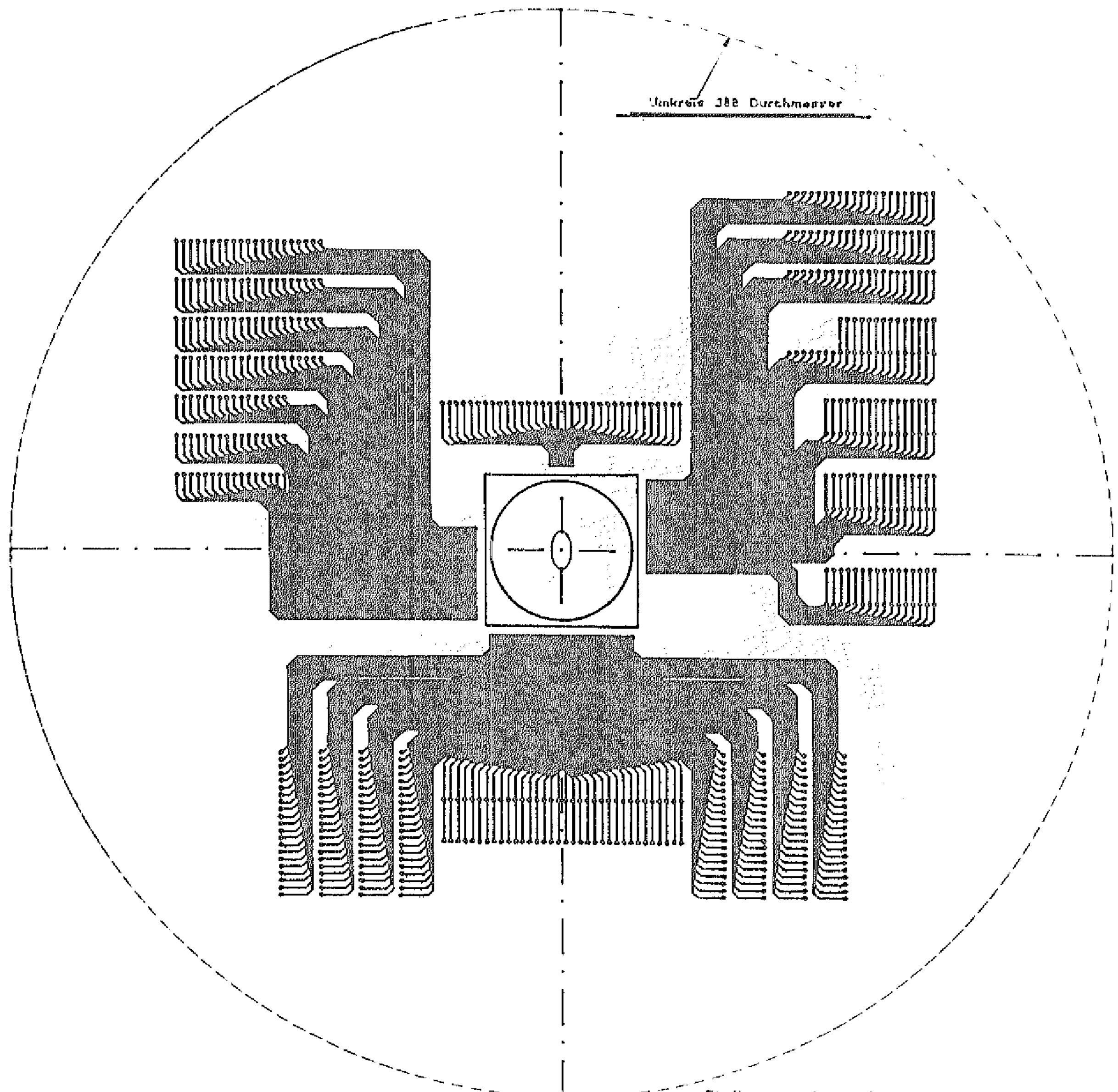

Platinenanordnung für ΔE-Zähler.
COSY-Detektor
KFA-IKP

prototypes

8 x 8 strips (see Annual Report '90)
- 2 mm thick, strips of 1,7 mm width
- SMD type preamps, linear amps, discriminators (MPI)
- bit pattern circuits, 2-parameter display
- tested with gamma-rays
- cross-talk studied

50 x 50 strips (hole in the center: 6 mm diameter)
- 2 mm thick, strips of 0,57 mm width
- 2 diodes of the needed dimensions tested
- prepared: mask, detector mount, cryostat, preamp boxes linear amps etc.

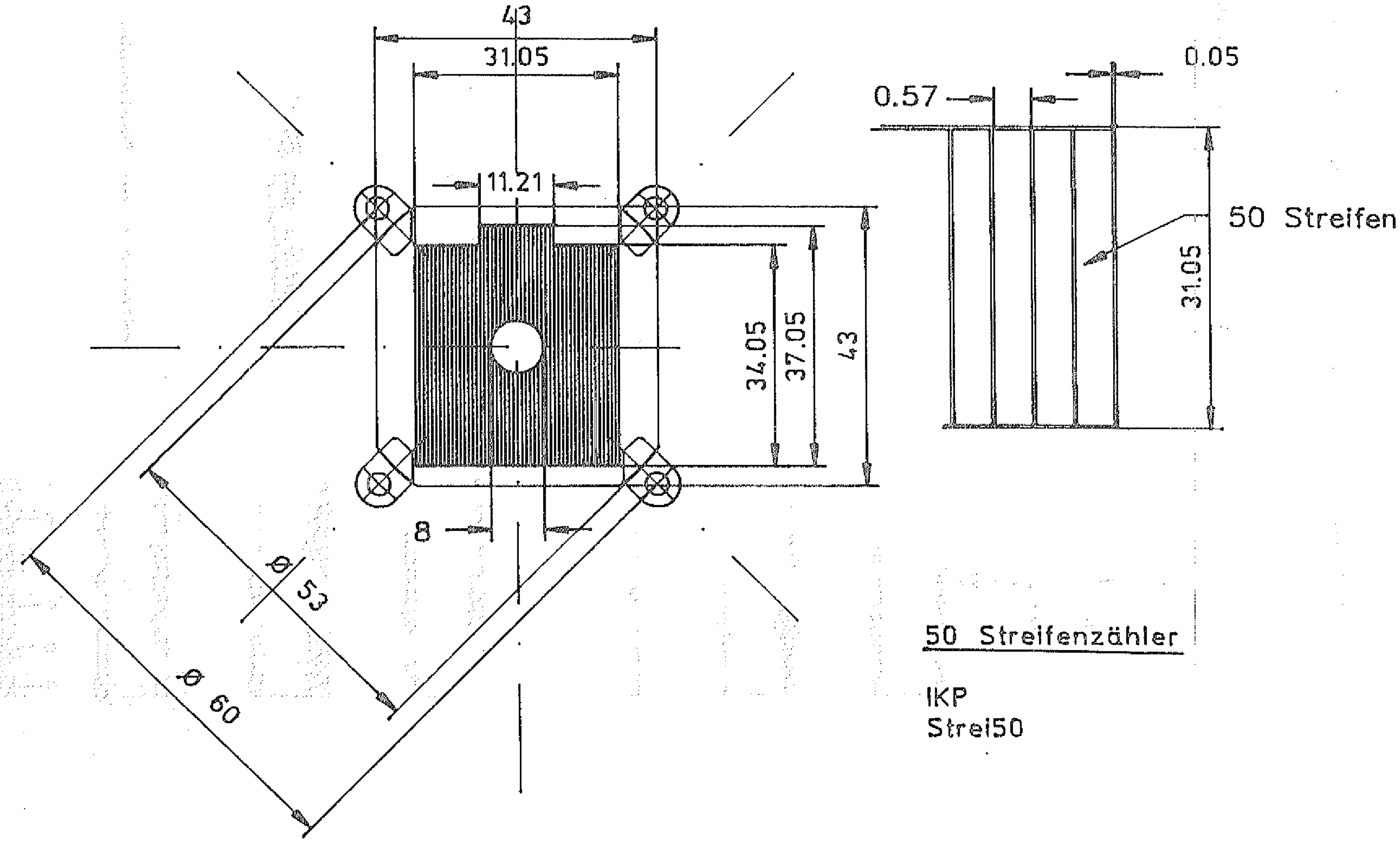

50 Streifenzähler

IKP
Strei50

Herstellung von ortsempfindlichen Detektoren

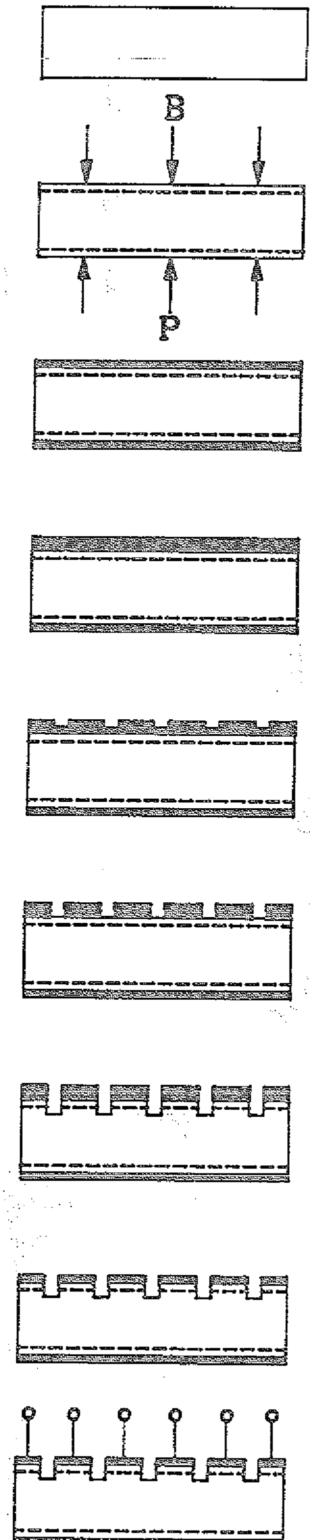

Halbleiterkristall, chemisch poliert

Dotierung durch Implantation

Al-Bedampfung

Beschichtung mit Photolack

Belichten durch eine Maske und Entwickeln

Oeffnen der Al-Schicht

Einaetzen der Struktur in das Halbleitermaterial

Entfernen des Photolacks

Kontaktieren durch Ultraschall-Bonden

DISCUSSION

K. KILIAN noted that there remain problems in the structure of the Germanium Wall that have to be overcome. In particular, any conflict with the Hadron Ball structure that is to surround the target has to be avoided, and as much as possible of the material of the Wall structure has to be moved into the geometrical shadow of the detector itself.
H. MACHNER replied that conflicts with Hadron Ball and Ge Wall structures are being avoided by discussions between the persons responsible for these structures.

J. SMYRSKI asked about possible radiation damage to the Ge detectors, in particular by the neutron background.
H. MACHNER replied that experience from previous experiments showed a sufficient radiation hardness.

J. KOONIJN asked about the possible number of pixels in the detector spiral design of the first Ge detector.
H. MACHNER replied that this number is 20 000 and that it is essentially determined by the cost of the electronics needed for each pixel element.

A. BUDZANOWSKI expressed an interest in the details of the production of the position–sensitive detectors.
G. RIEPE thereupon showed the last of the transparencies and explained some of the steps in the production summarized there.

P. v. Rossen

IKP, KFA Jülich

Modification of the BIG KARL Spectrometer

The modifications of the BIG KARL magnetic spectrometer that will be required by the demands of the COSY 10 experiment are outlined.

MODIFICATION OF BIG KARL

— Presentation of the Spectrometer

Tasks Under Way

— Moving to a new Location
— Adaption and Upgrading
  — New Control System
  — Zero-Degree Beam Exit
  — New Entrance Region
  — New Detector System

The COSY accelerator facility

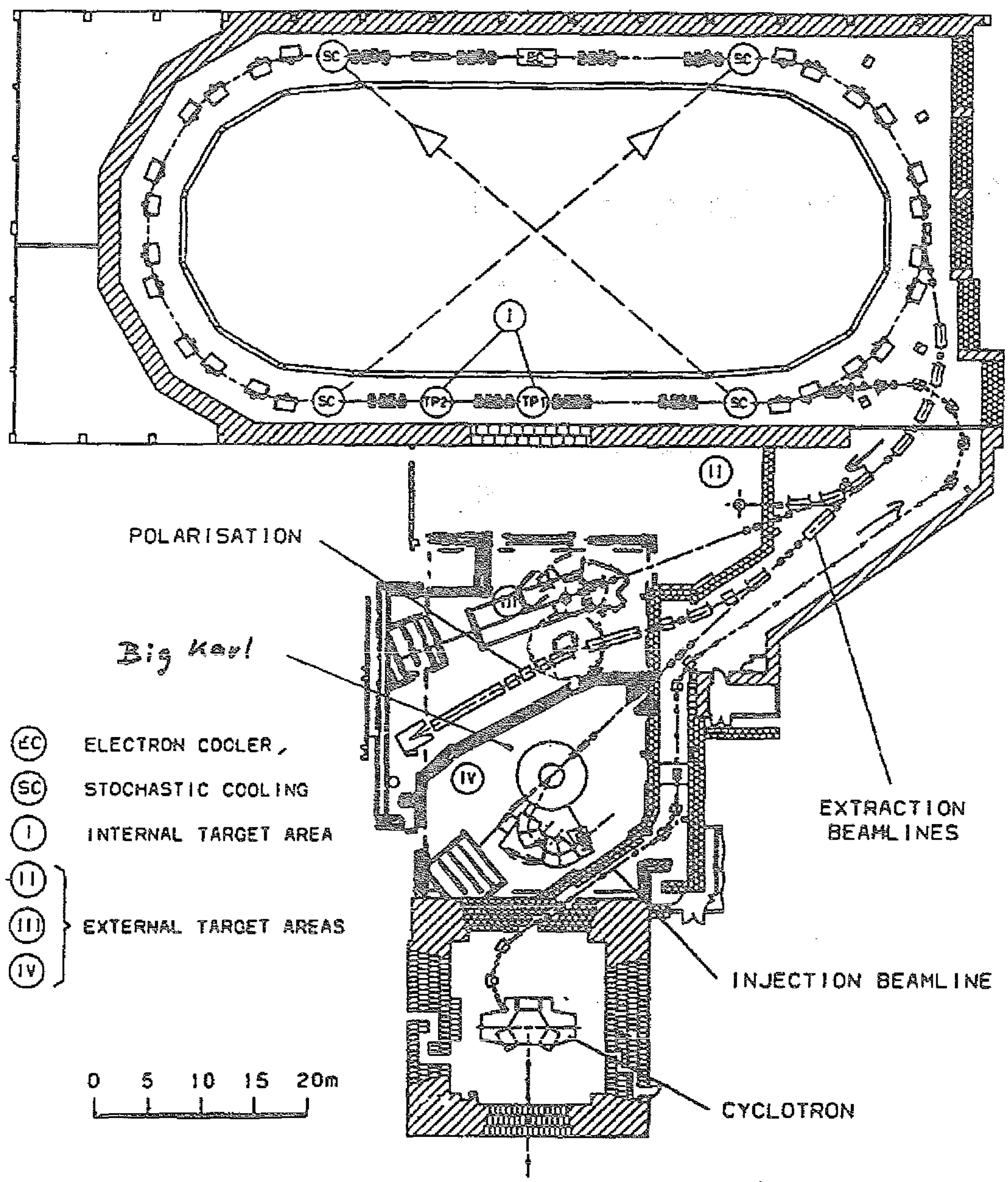

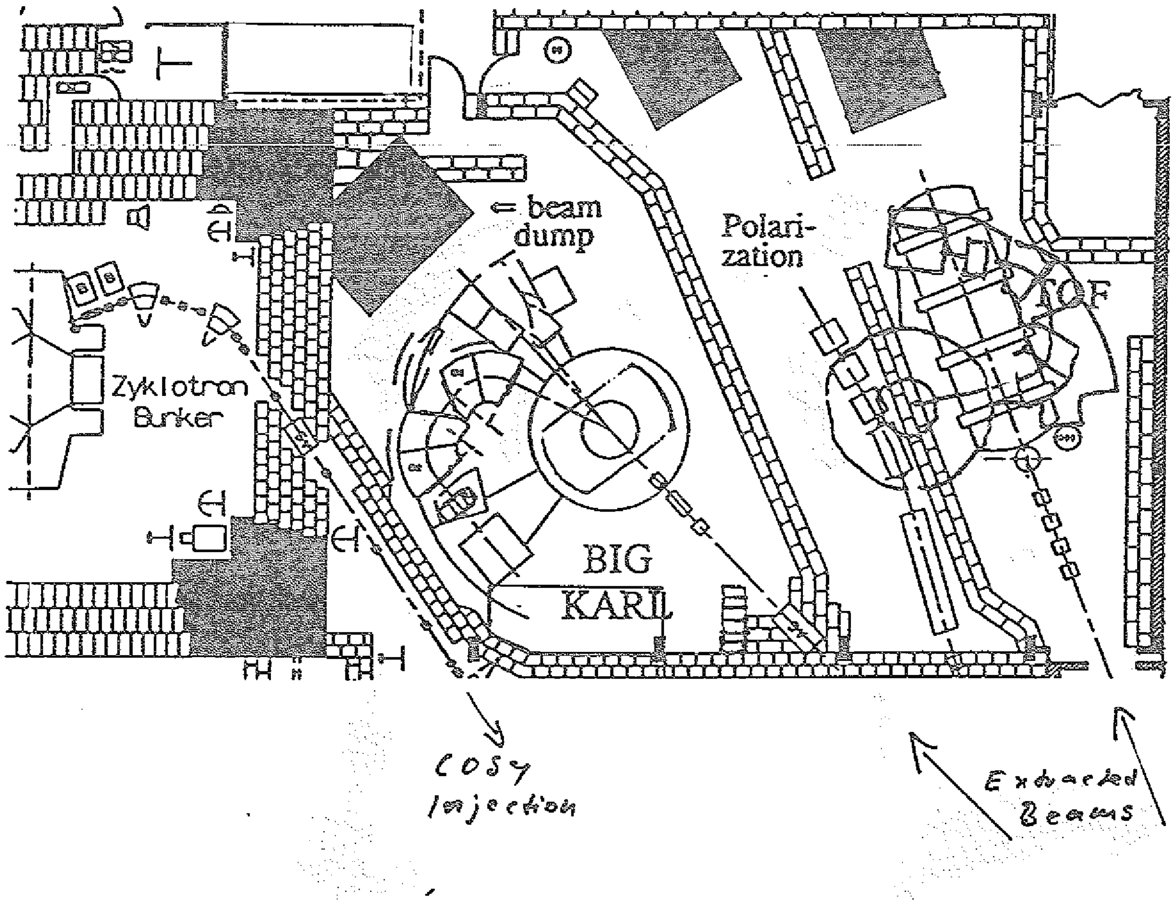

beam dump
Polari- zation
TOF
Zyklotron Bunker
BIG KARL
COSY Injection
Extracted Beams

The Big Karl Magnetic Spectrometer

DESIGN:
$E/\Delta E \leq 10000$
$d\Omega_{max} \approx 10$ msr
$B \approx 1.7 - 17.5$ kG
$\rho \approx 1.98$ m
$D_{variable} = 0 - 24 \frac{cm : \%}{100 \cdot \Delta p}$
$\theta_{lab} = -10° - 140°$

EXPERIMENTS:
$E/\Delta E = 5000 - 10000$
beam ≈ 100 nA
$d\Omega = 3.5$ msr

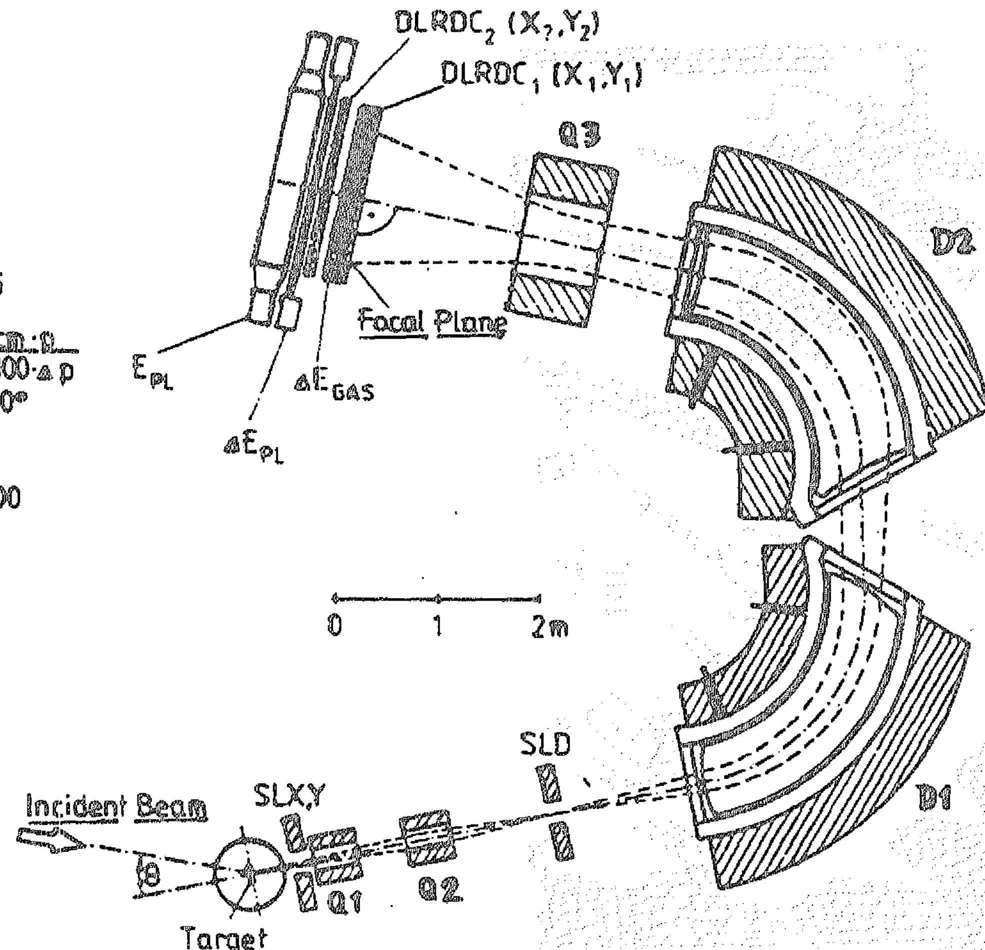

List of proposed experiments

#	Spokesman	int.	ext.	Experiment	p_0 [GeV/c]
1	Ernst		BK	Light Hyper-Nuclei	2.2
2	Ernst		BK	Λ-Production at Rest	1.7
3	Eversheim		Pol.	Parity Violation	0.7 2.3
4	Eversheim	polarised ion source			
5	Hinterberger	TP2		Excitation Function (Dibaryon)	0.7 - 3.3
6	Jahn		BK	Two Meson Production	1.0-2.6
7	Jarczyk	experiment in the injection beamline			
8	Koch	*		Neutral Mesons in Nuclei	0.6-3.3
9	Kuhlmann		TOF	P-P Bremsstrahlung	0.8/1.5
10	Machner		BK	Pionic Atoms	0.8
11	Oelert	TP3		Meson Prod incl Strangeness	1.9-3.4
12	Roderburg		TOF	η and η′ production	1.5–3.3
13	Schult	TP2		Heavy Λ-Hypernuclei	1.3-2.0
14	Scobel		"TOF"	A(p, xn) Cross section meas.	0.6-3.3
15	Turek		TOF	Strangeness in pp→KΛp	2.0-3.0
16	Morsch		BK+TOF	Baryon Resonances	2.8
17	Morsch		TOF	Δ-Resonances	2.3
18	Sistemich	TP2	0-degree facility		

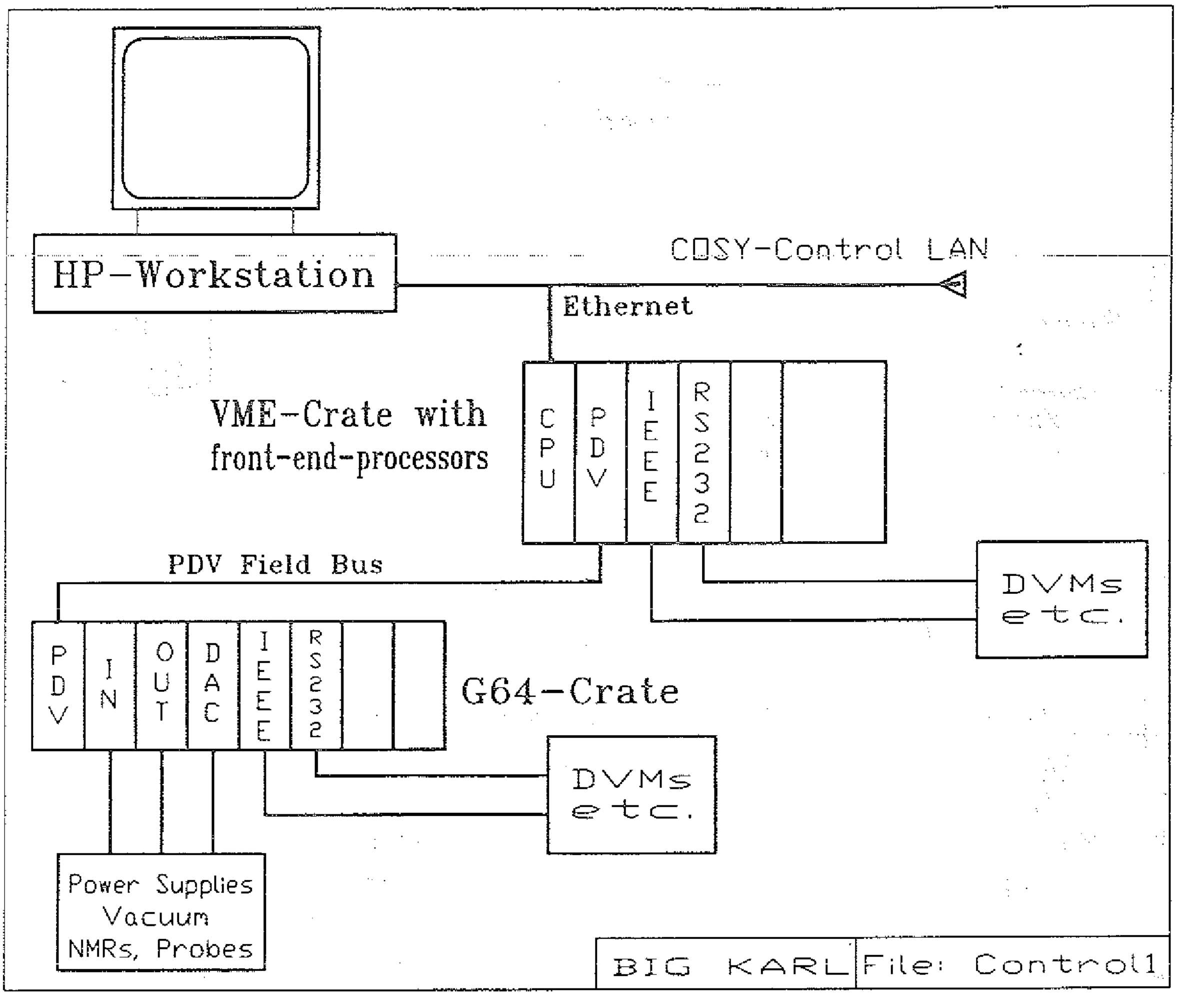
HP-Workstation
COSY-Control LAN
Ethernet
VME-Crate with
front-end-processors
CPU
PDV
IEEE
RS232
PDV Field Bus
DVMs
etc.
PDV
IN
OUT
DAC
IEEE
RS232
G64-Crate
DVMs
etc.
Power Supplies
Vacuum
NMRs, Probes
BIG KARL
File: Control1

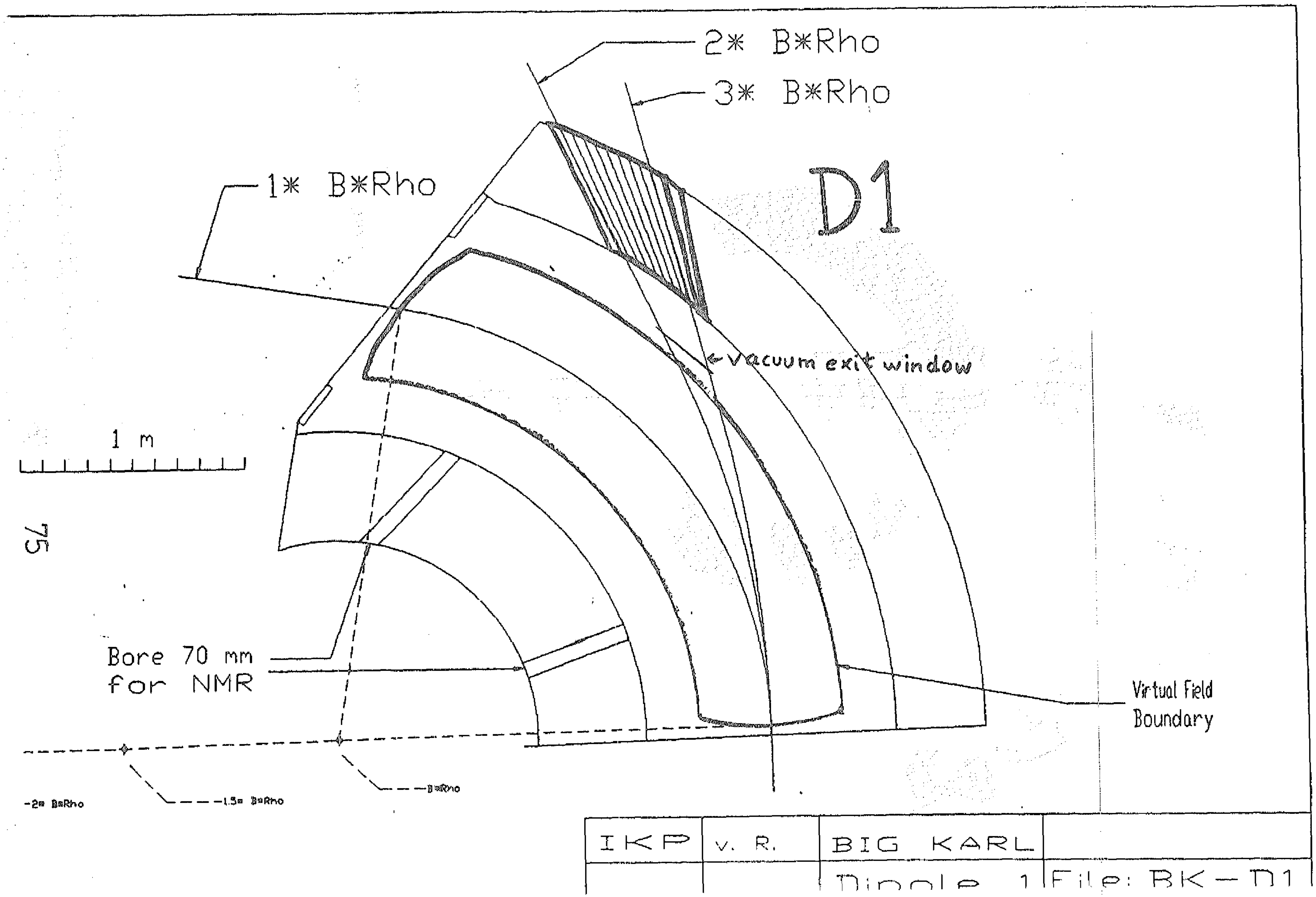
2* B*Rho
3* B*Rho
1* B*Rho
D1
vacuum exit window
1 m
Bore 70 mm
for NMR
Virtual Field
Boundary
-2* B*Rho
-1.5* B*Rho
B*Rho
IKP
v. R.
BIG KARL
Dipole 1
File: BK-D1

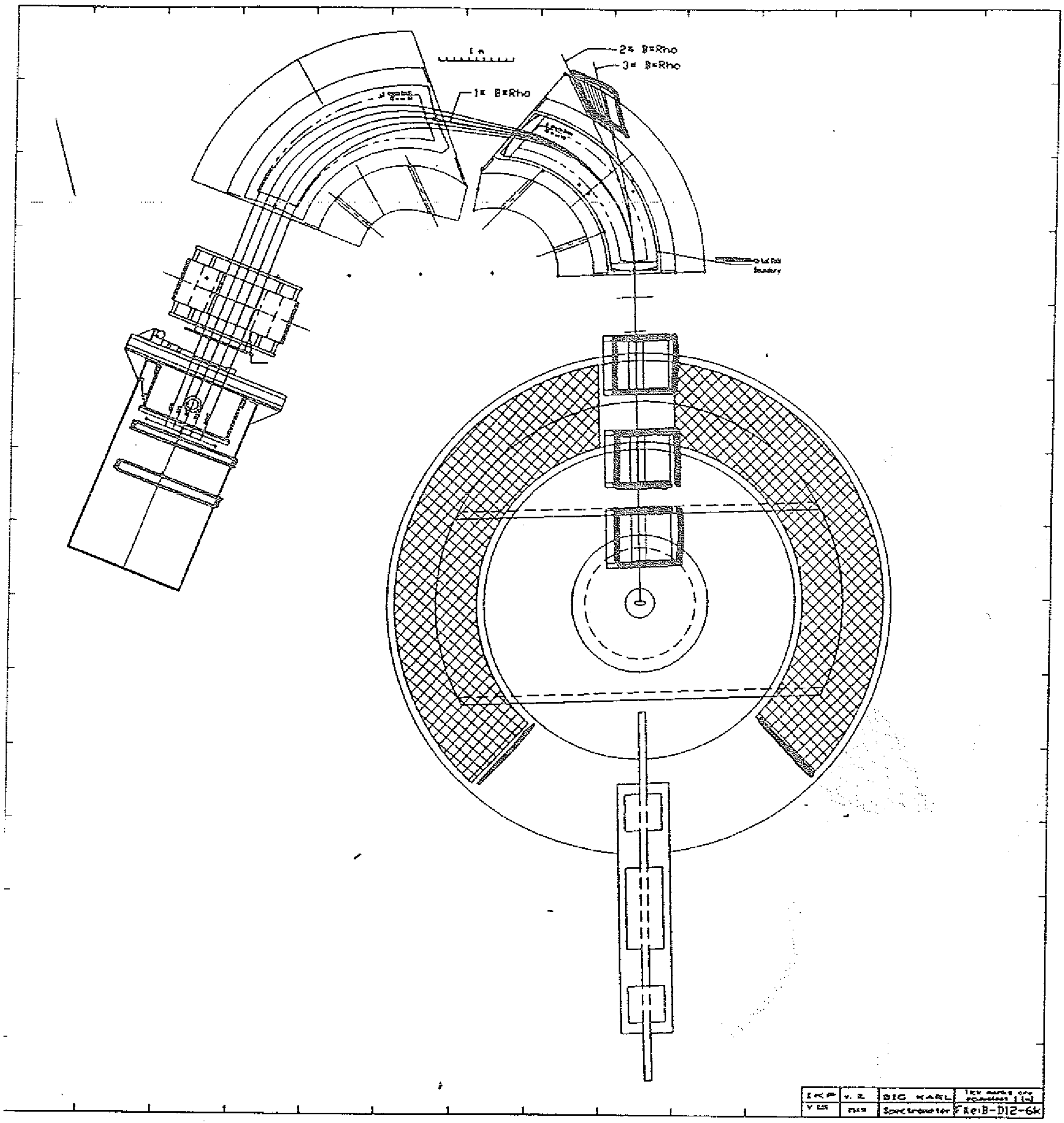
1 m
1= B*Rho
2= B*Rho
3= B*Rho
IKP
v. R.
BIG KARL
Spectrometer
FReiB-D12-6k

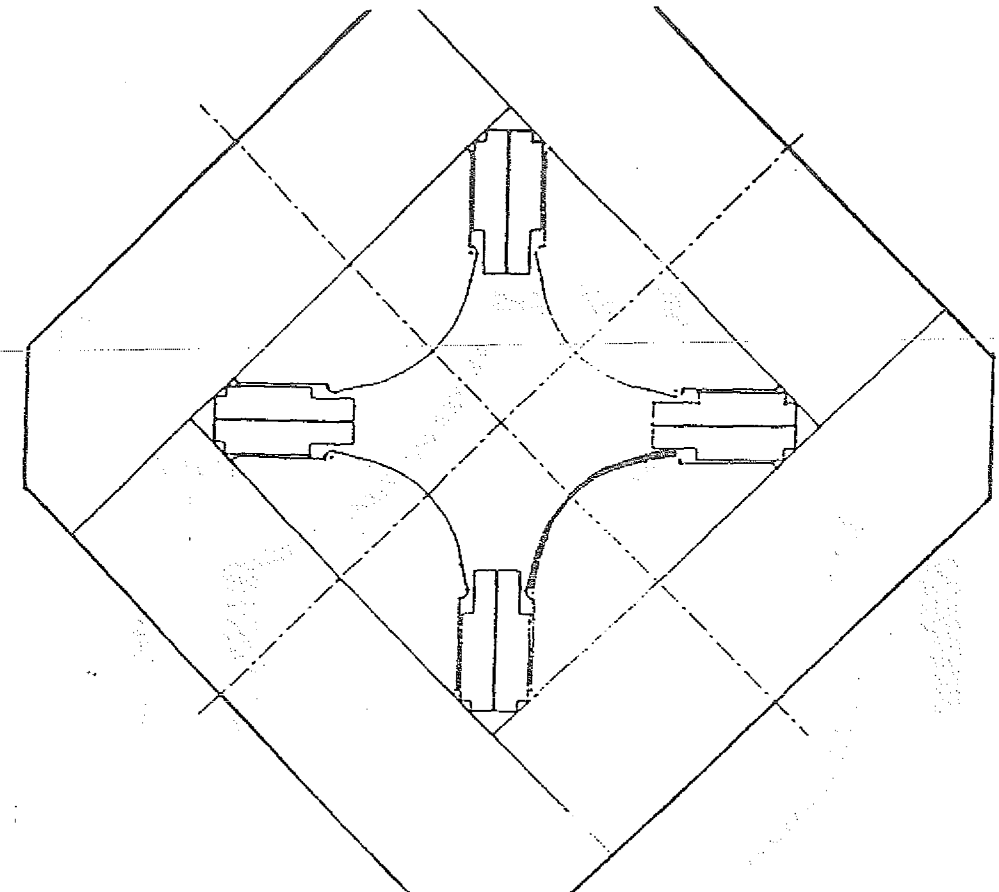

New Entrance Quadrupoles

high focusing strength 8.5 T } needed
high aperture 200 mm }

but { limited space
weight restriction

➡ High pole-tip-field quads ~13 KG

"POISSON" calculations @ 1100 MeV

B_0 = 13 KG 12-Pol 0.1%

B_0 = 8 KG 12-Pol 0.02%

SCHNITT B – B

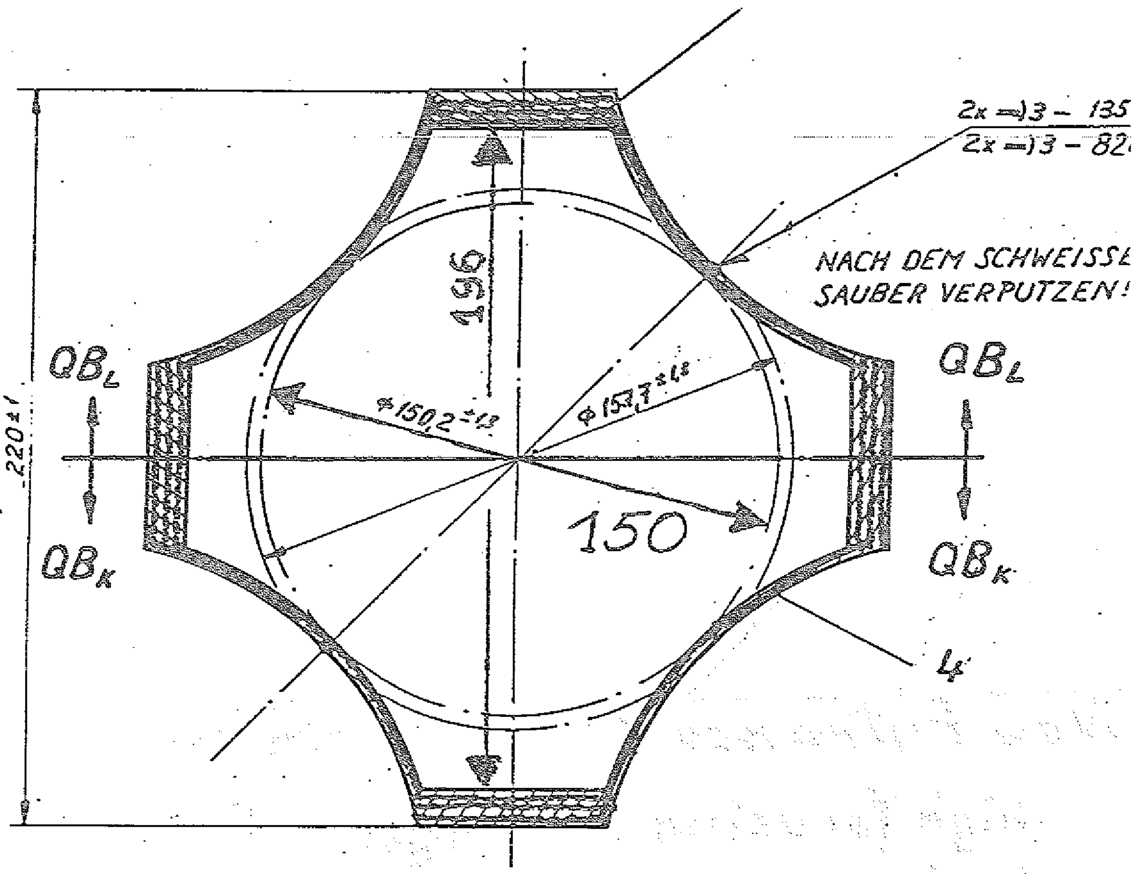

5
2x ⇒)3 – 135
2x ⇒)3 – 82
NACH DEM SCHWEISSE
SAUBER VERPUTZEN!
196
QB_L
QB_K
220±1
ф 150,2±1,8
ф 153,7±1,8
150
4

File used Q3D2Q_STAN_0_PLOT

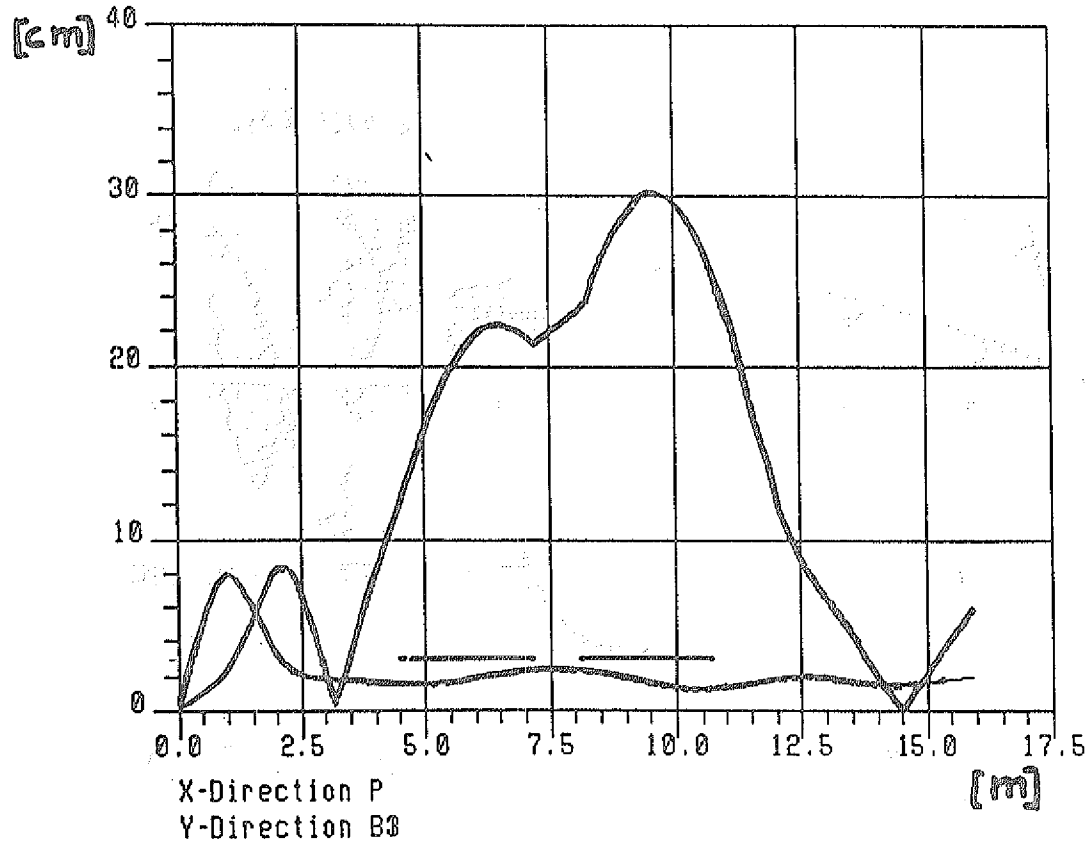

File used Q3D2Q_ANG_0_FIX

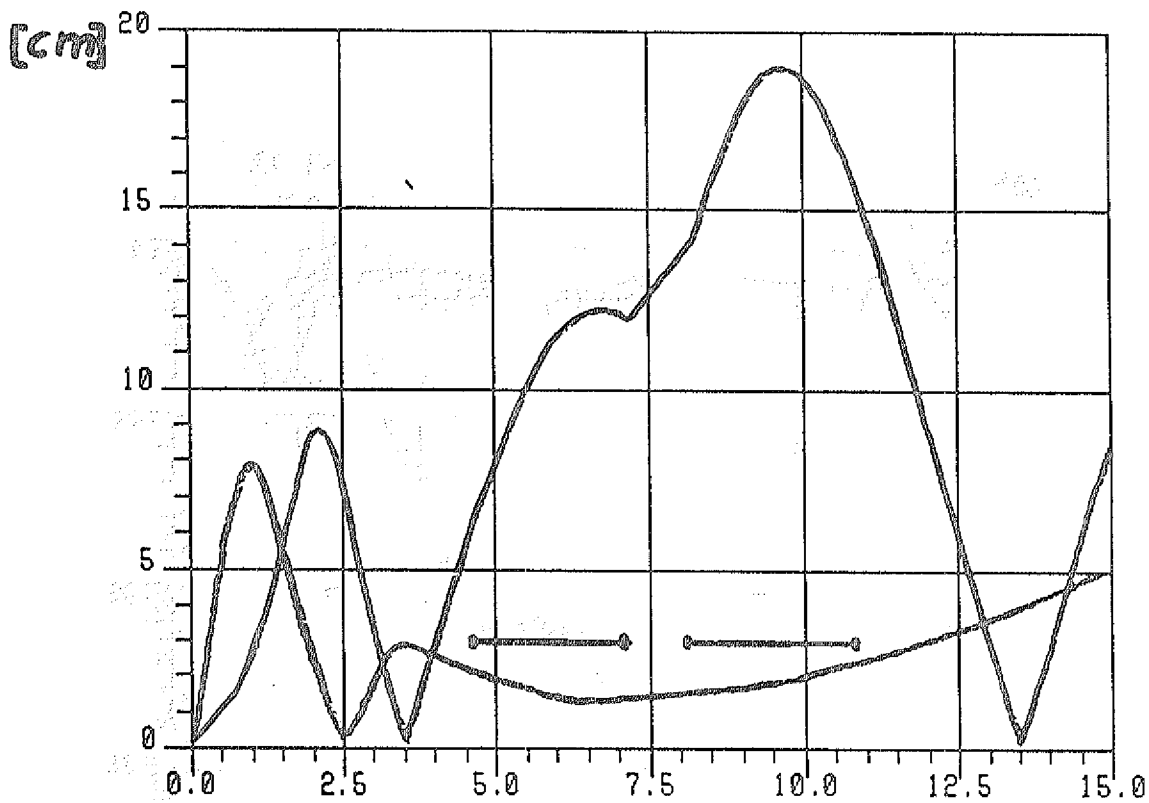

X-Direction P
Y-Direction B8

QQQDDQ- Highlights

- Standard Mode

  Horz. Point-Point

  Vert. Point-Point

  highest resolution

  variable Dispersion

- Angle Sensitive Mode

  Horz. Point-Point

  Vert. Parallel-Point

  scattering angle reconstruction

  small extend of direct beam at the exit window

- Other Modes

  e.g. telescopic mode

Focal Plane Detectors

— New Detectors Under Contruction
  — High resolution in X and Y
  — Multi-hit capability

— Indispensable Tool for Bringing the Spectrometer back into Operation

"The availability of those detectors and of the appropriate data aquisition, that shows on-line the spectra in the focal plane, is a critical prerequisite for the recommissioning of BIG KARL"

DISCUSSION

H. MACHNER noted that, in order to achieve with the spectrometer the 56 mrad acceptance required by COSY 10, an additional quadrupole (to be obtained from DESY) will be placed in front of the target.

H. PLENDL asked whether the beam exit hole that is to be drilled into the magnet material will result in any change in quality.
P. v. ROSSEN replied that, at the relatively low magnetic fields needed for COSY 10, this hole will not be a problem. For other experiments, that hole can be plugged up.

H. MACHNER noted that the induction drift chamber that was placed between Ge Wall and BIG KARL spectrometer in the original proposal has been removed in order to avoid background reactions on the chamber material.

J. Smyrski

Jagellonian University, Cracow

The Focal Plane Detector

A multi–wire drift chamber for the focal plane of the BIG KARL spectrometer with high position and angular resolution is described.

CELL STRUCTURE

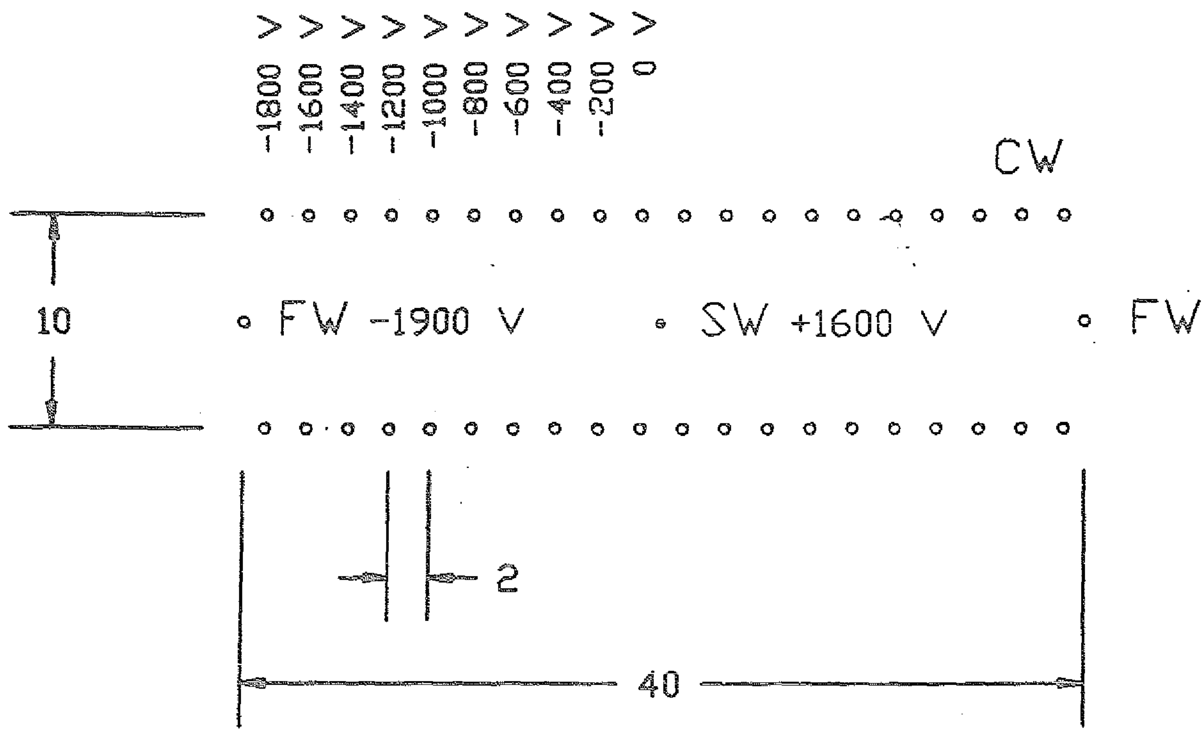

SW - sens wire d = .02 mm gold-plated tungsten

FW - field wire d = .05 mm Be - Cu

CW - cathode wires - // -

Gas mixture: 80% Argon + 20% Ethan (normal preasure)

Maximum dirft time: 400 ns

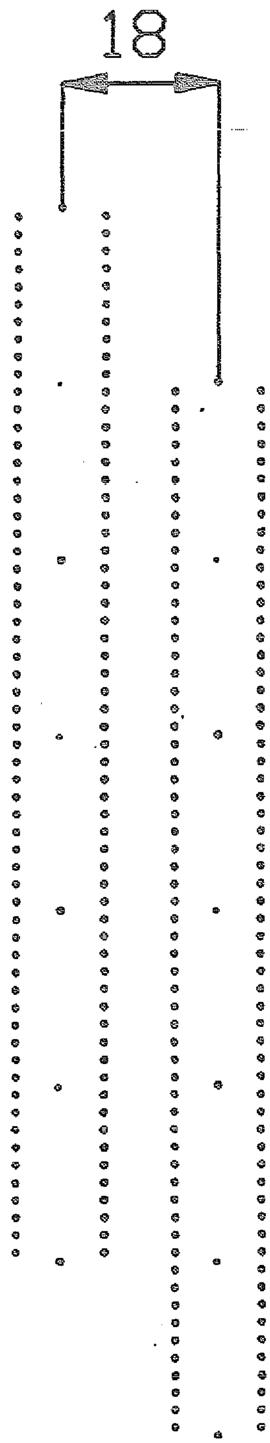

Two measuring planes staggered by half a cell

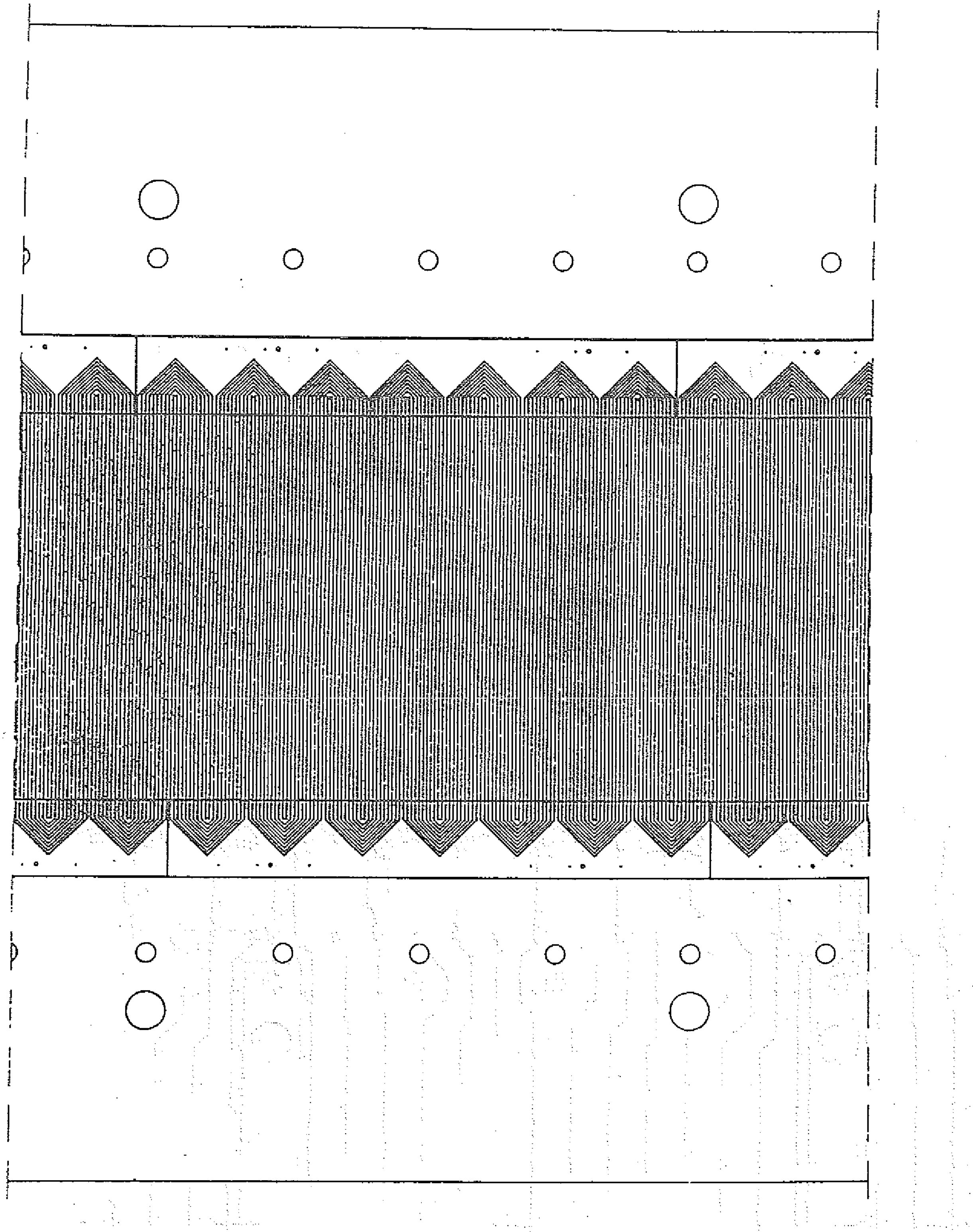

cathode plane

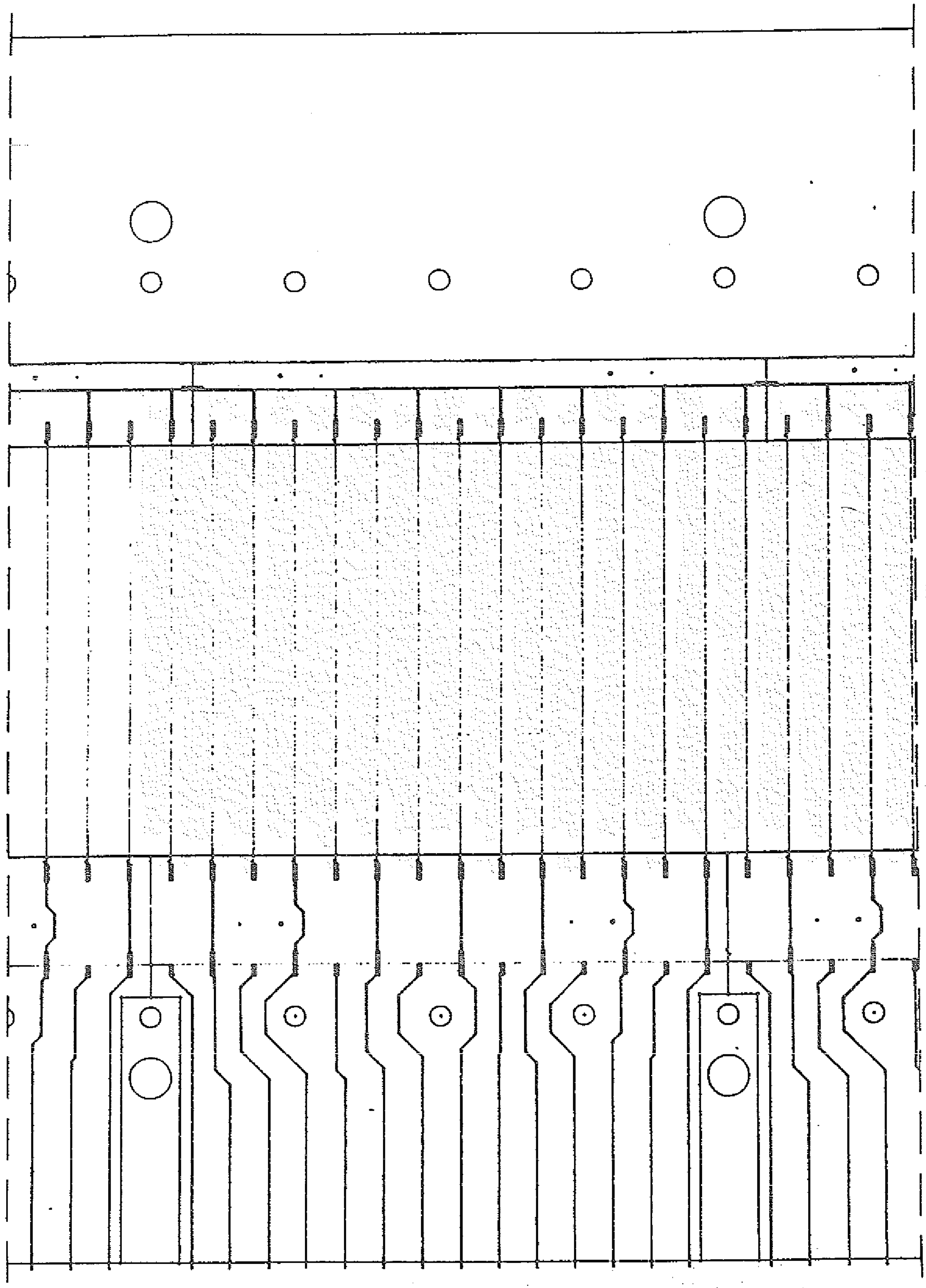

anode plane

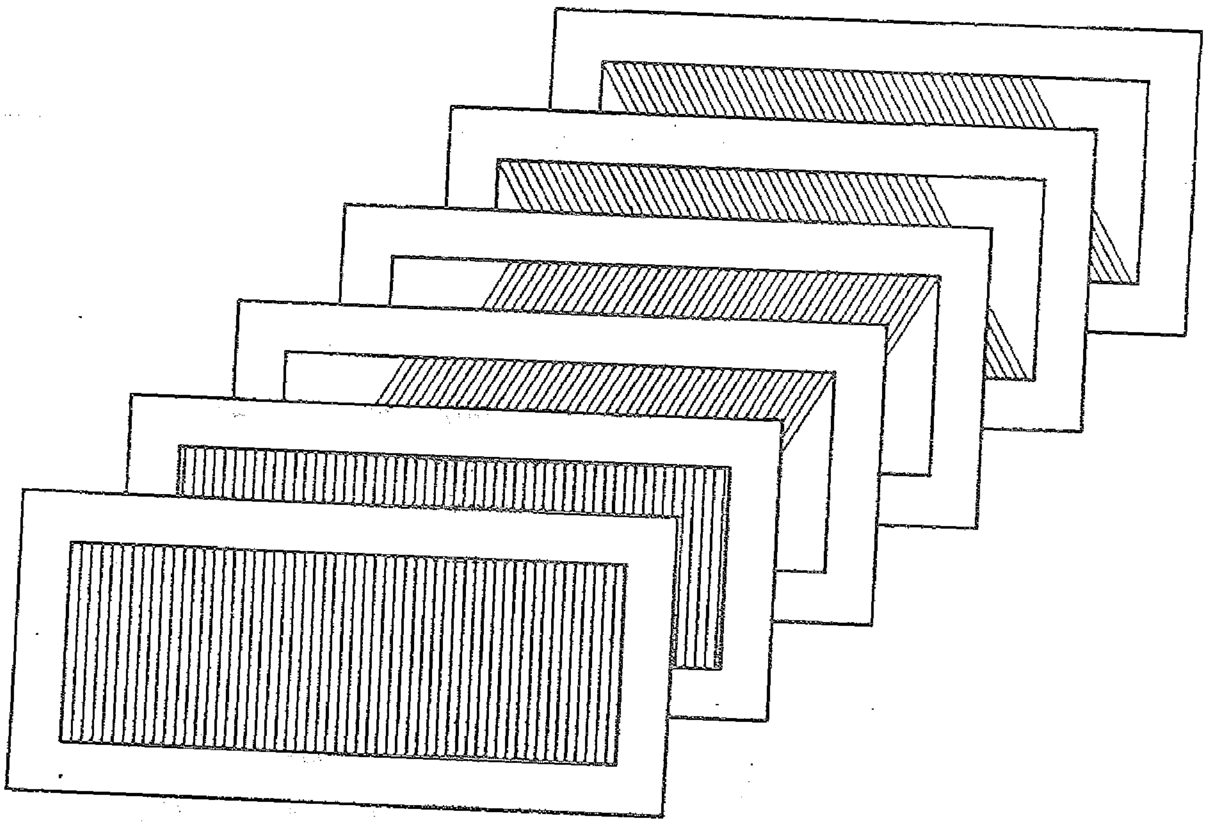

Orientation of wires in one packet

Active area:

20X130 cm^2 for Big Karl detector

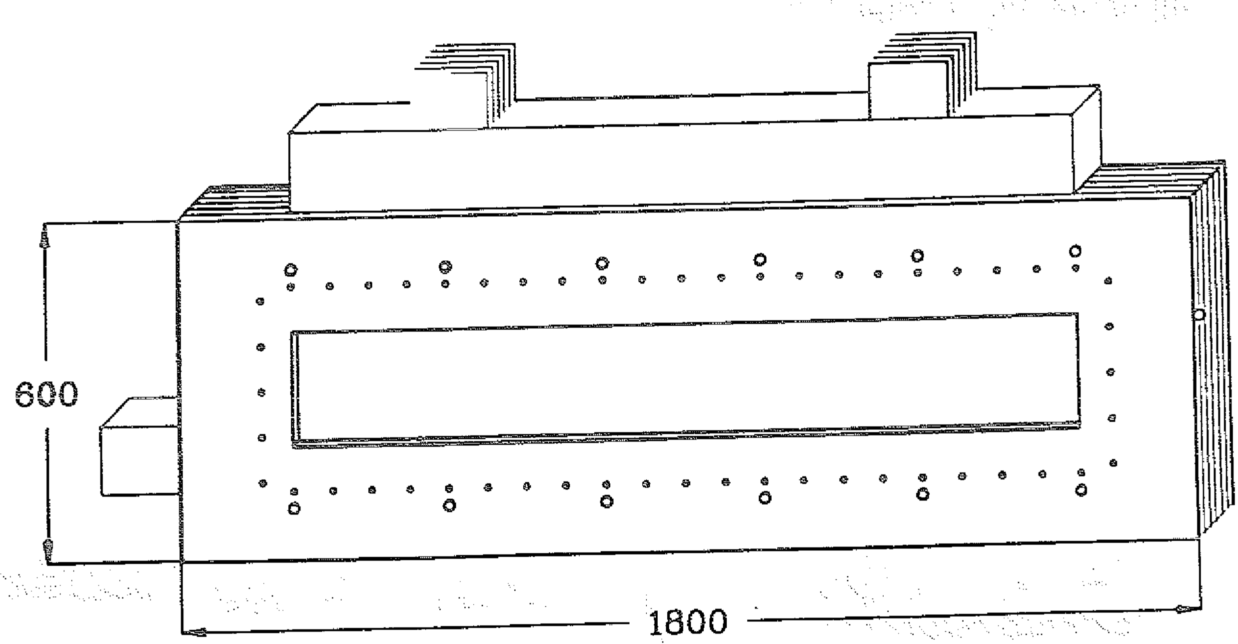

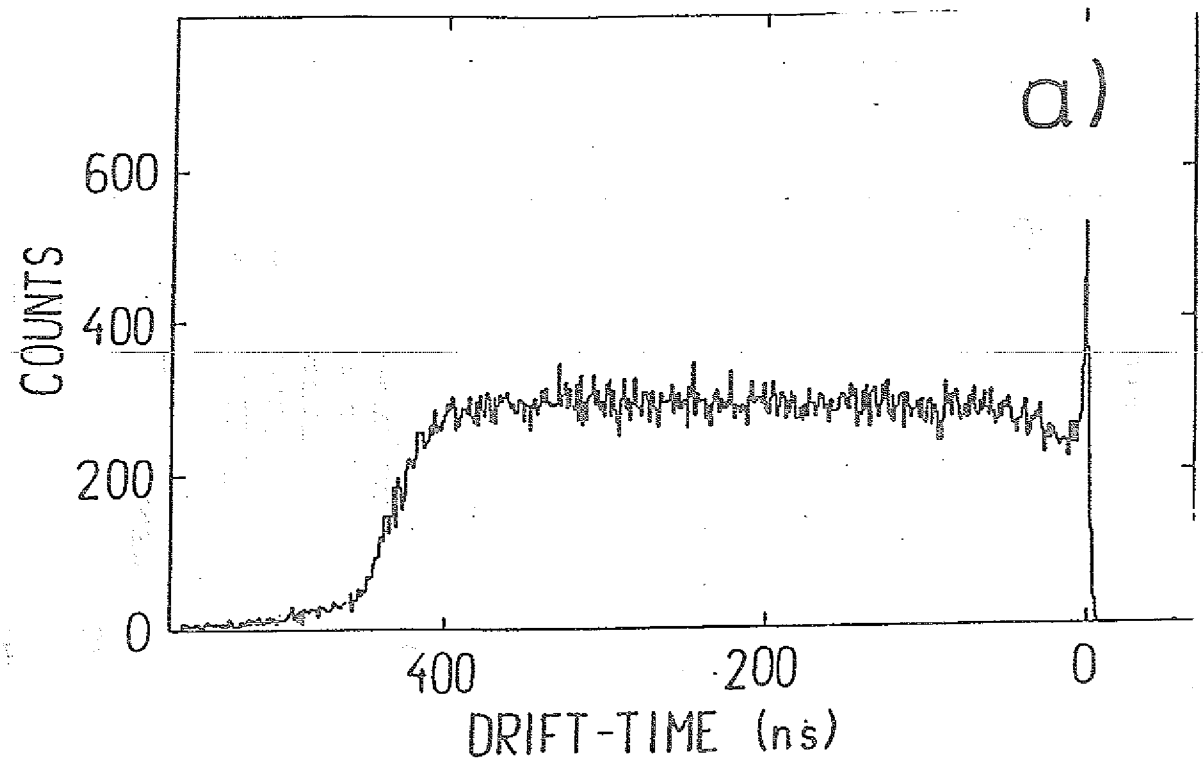
a)
600
400
200
0
COUNTS
400
200
0
DRIFT-TIME (ns)

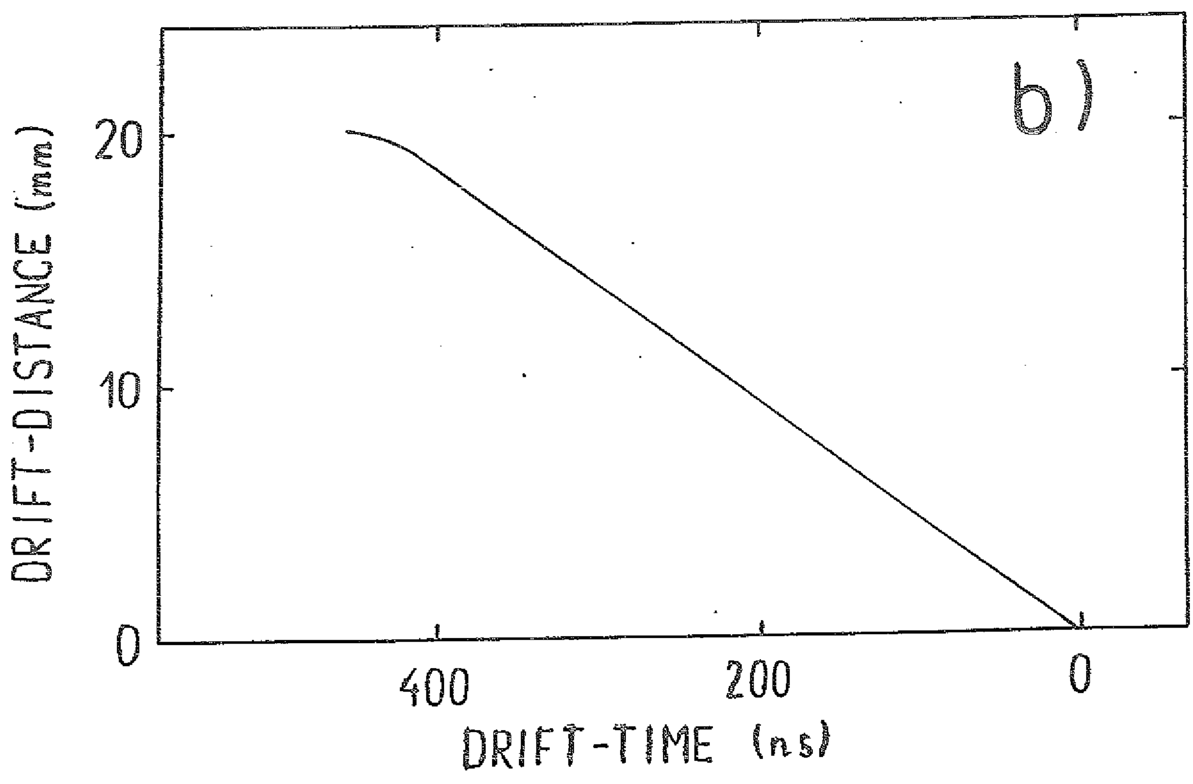
b)
20
10
0
DRIFT-DISTANCE (mm)
400
200
0
DRIFT-TIME (ns)

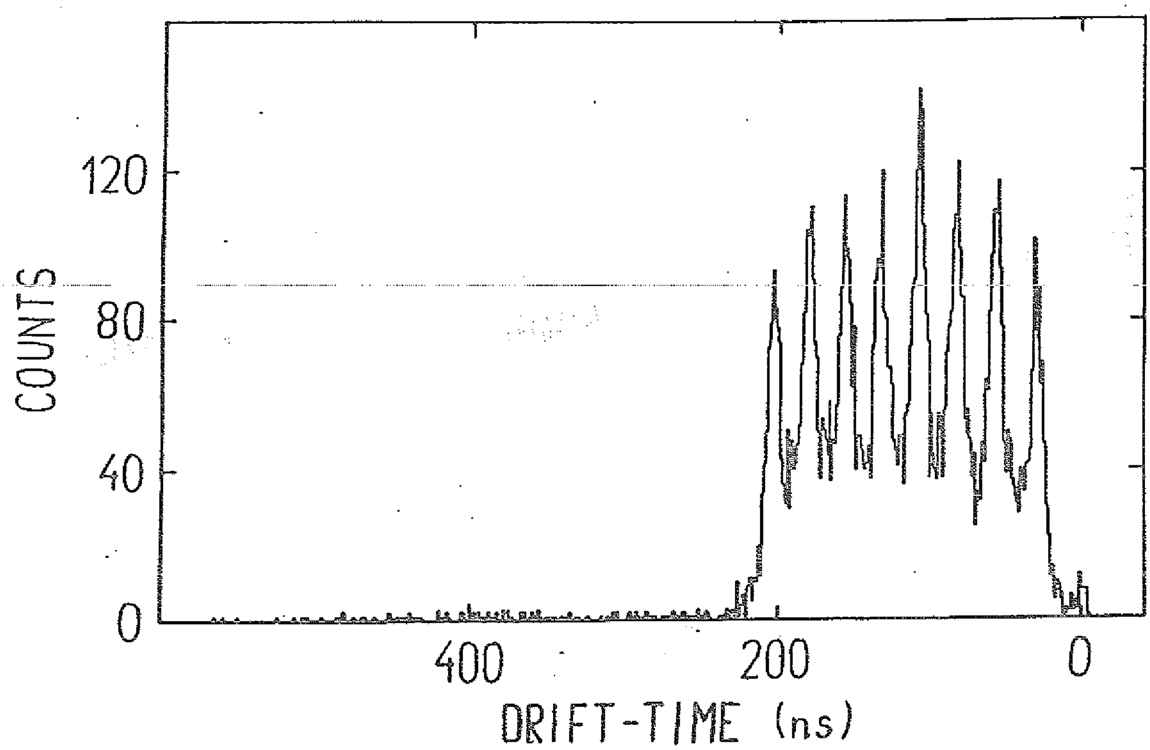

COUNTS
120
80
40
0
400
200
0
DRIFT-TIME (ns)

	COSY 10 requirement:	our detector performance:
Position resolution - horizontally (FWHM)	250 μm	100 μm
Position resolution - vertically (FWHM)	250 μm	250 μm
Double track resolution - horizontally	40 mm	~ 3 mm
Double track resolution - vertically	4 mm	~ 6 mm
Angular resolution (RMS) for 80 MeV protons		2 mrad

DISCUSSION

H. PLENDL: How straight is the focal plane?
P. v. ROSSEN: The focal plane could be made straight by the use of the correction windings, but its not really necessary, as we are measuring both position and angle in the focal plane. That allows us to reconstruct the focal points for larger momentum deviations.

K. KILIAN: What accuracy can be achieved in estimating the entrance angle to the spectrometer?
P. v. ROSSEN: One has to treat the horizontal and the vertical plane separately. Horizontally, the angle–sensitive mode gives you an angle magnification of three which would allow a very precise angle reconstruction. But due to the mixing of target position and momentum for the image in the focal plane, the main error comes from the size of the target spot. A size of 2 mm results in approx. 2 mrad uncertainty plus the uncertainty due to the angle error in the focal plane. From this it's easy to see that the primary beam should have a very small phase space.
Vertically you don't have the linear mixing of momentum and position. For the central momentum one can directly deduce the angle by measuring the vertical position in the focal plane. The vertical extent of the beam spot is, in first order, of no significane. The precision obtainable is around 2 mrad. For the of momentum of the particles one needs to have the angle information as well, as the transformation matrix is dependent on the beam momentum. Thus the accuracy depends directly on the momentum deviation.
For a full evaluation of the errors it is necessary to use at least second order effects, as in second order all coordinates mix.

B.J. Lieb

George Mason University, Fairfax, Virgina

The Hadron Ball

A 4π detector for charged and neutral particles with moderate energy and space resolution and consisting of 32 BGO crystals has been built and used at LAMPF. In the COSY 10 experiment, it is planned to position it around the target to record background events.

LAMPF BGO BALL

C. L. MORRIS
J. McGILL } LAMPF
R. RANSOME
RUTGERS

4π GEOMETRY
in Lab system

20 HEXAGONAL CRYSTALS

12 PENTAGONAL CRYSTALS

2 PENTAGONAL CRYSTALS REMOVED FOR BEAM ENTRY & EXIT.

LAMPF

BGO Ball
side view

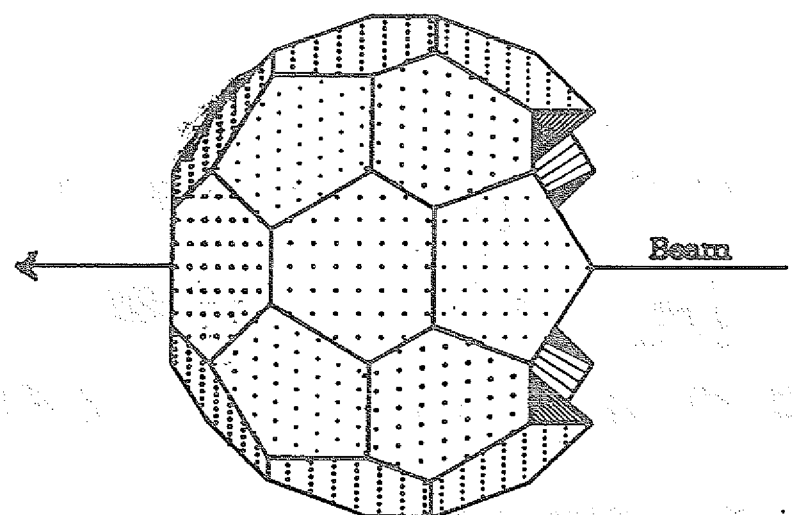

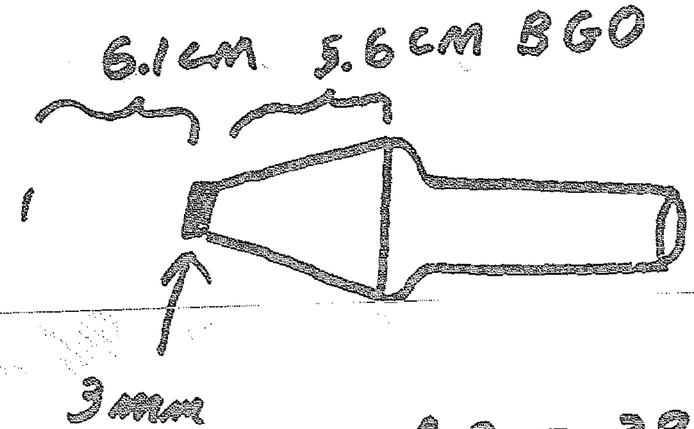

$d\Omega = .39\,sr.$

PARTICLE	ENERGY OF PARTICLE STOPPED	
	PLASTIC:	PLASTIC +BGO:
π	7.2 MeV	92 MeV
P	17	185
^{2}H	23	250
^{3}H	28	305
^{3}He	59	640
^{4}He	66	720

BGO PROPERTIES

$\rho = 7.1\ g/cm^3 \quad \rho\tau = 40\ g/cm^2$

RAD. LENGTH 1.1CM

∴ DET. IS 5.0 RAD LENGTHS

DECAY CONSTANT ~300NS

LOW AFTERGLOW
($<$ 1% OF NaI)

COUNT RATE ~ 80K/S

TIME RESOLUTION ~1NS

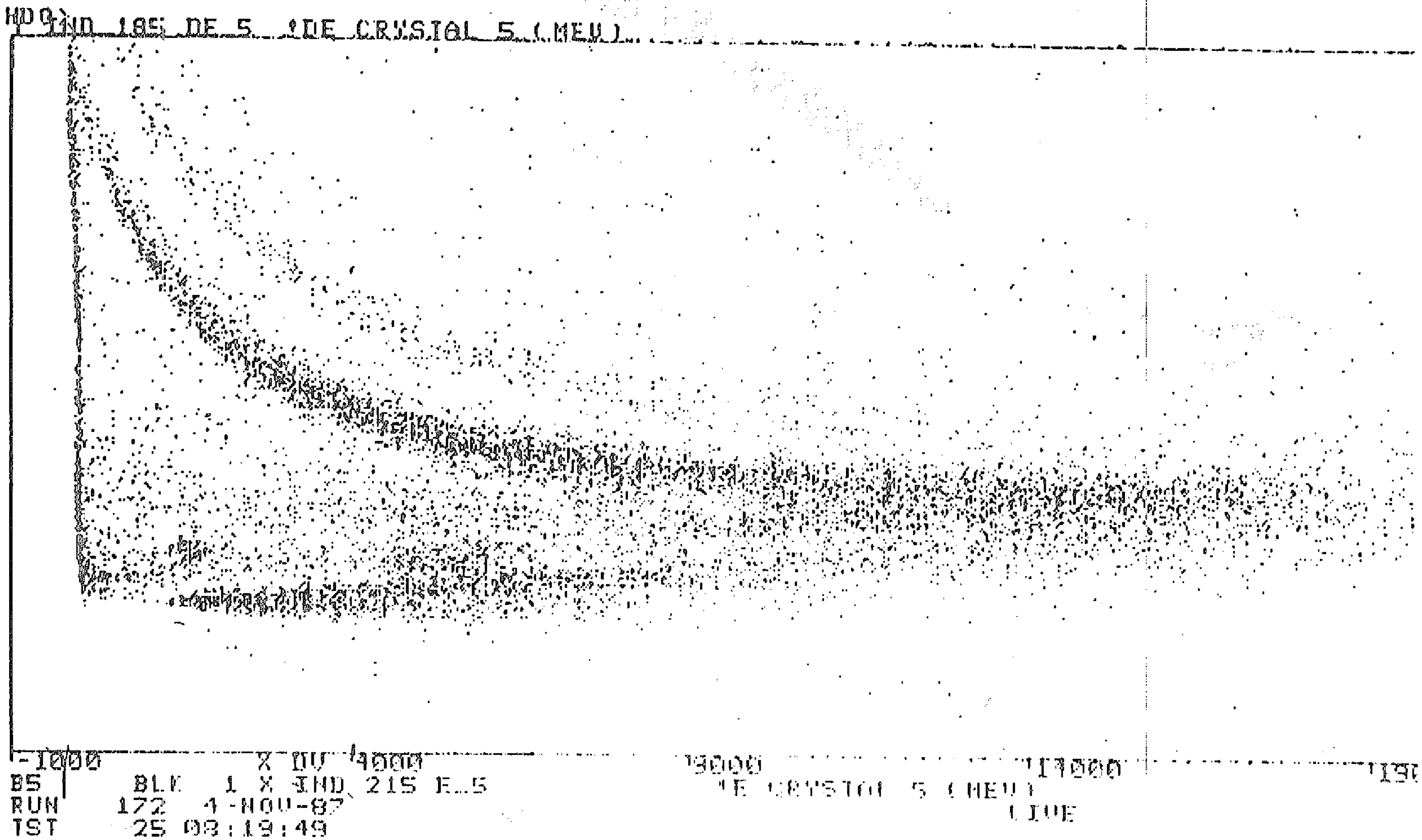

HDG> IND 185 DE 5 (DE CRYSTAL 5 (MEV)
-1000
X DV 4000
9000
11000
BS
BLK 1 X IND 215 E 5
RUN 172 4-NOV-87
TST 25 08:19:49
LIVE

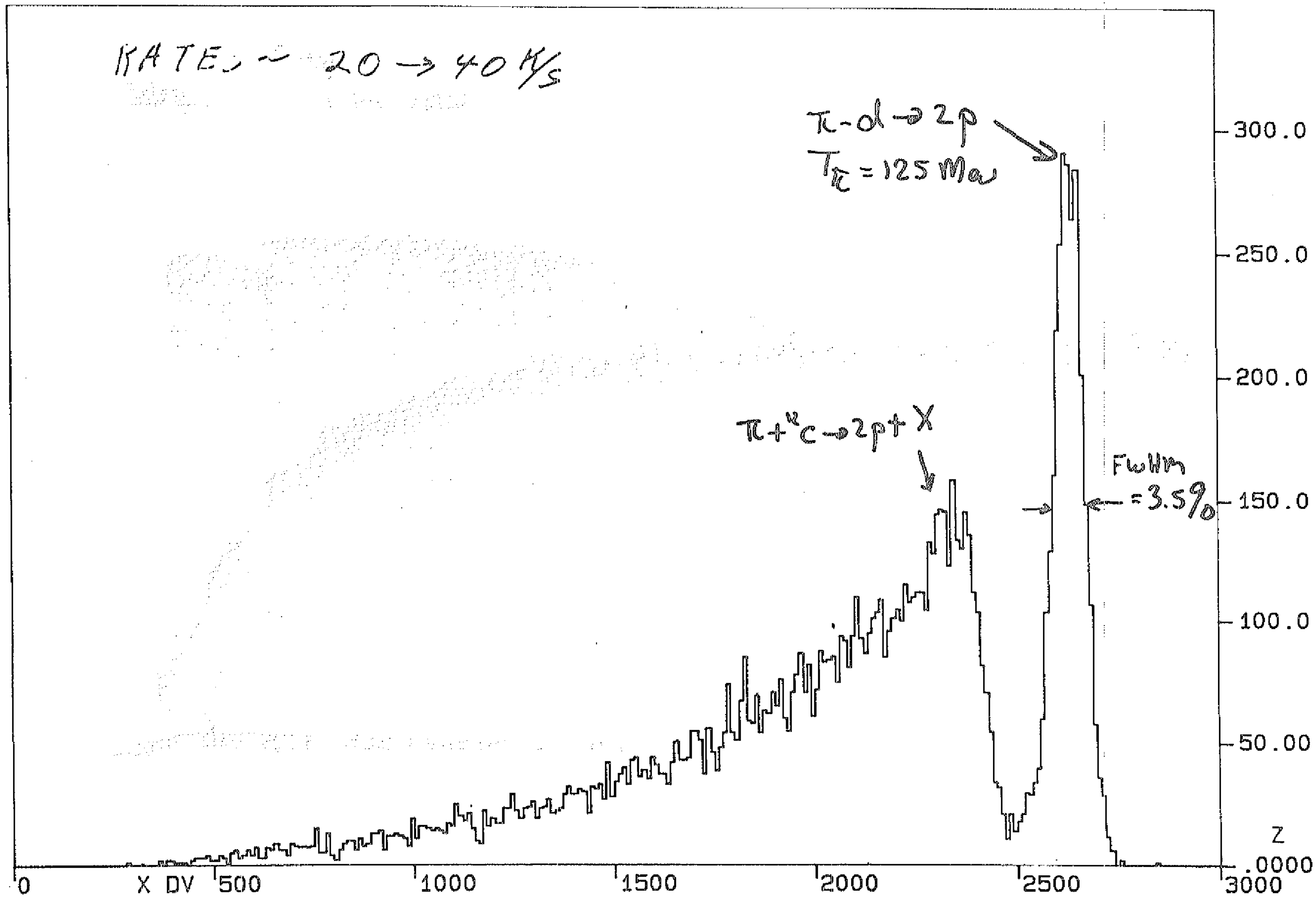

2P BLK 1 X IND 334 ESUM TOTAL ENERGY FROM BALL (.1MEV)
RUN 503 23-JAN-87 SUM= 11775. XLO= 0 XHI= 0 RU0503.HSV
TST 77 15: 13: 16 ADD= 1: 1 FAL= 364888 LST= 0 21-JAN-87 18: 07

104

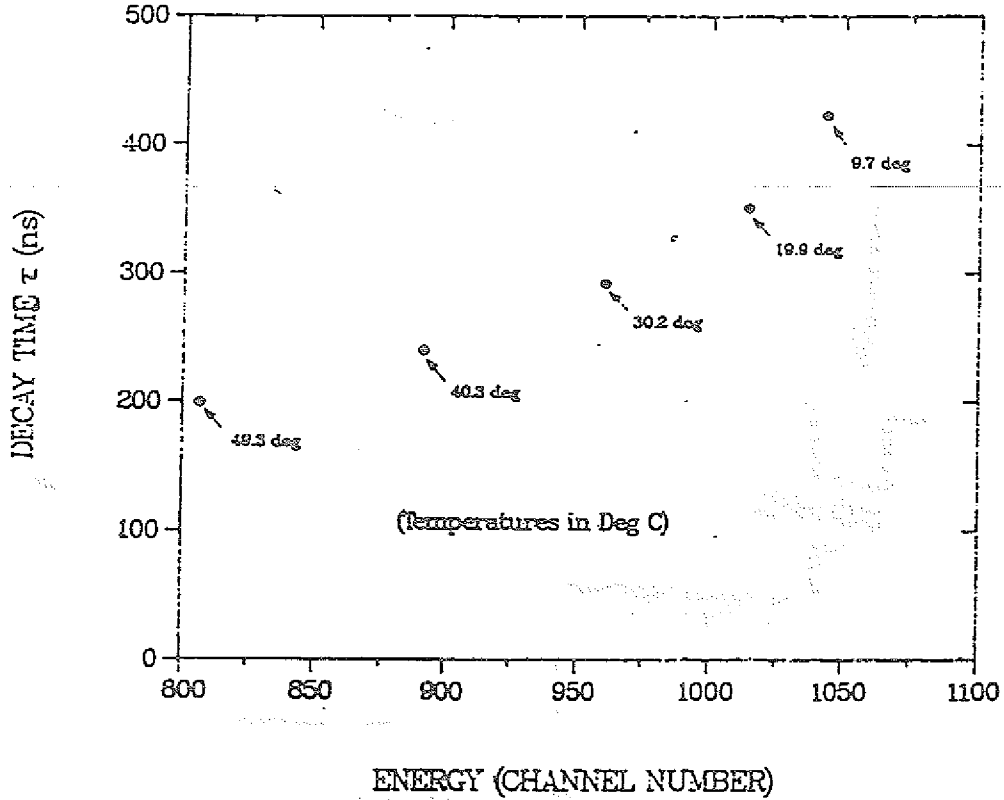
DECAY TIME τ (ns)
ENERGY (CHANNEL NUMBER)
9.7 deg
19.9 deg
30.2 deg
40.3 deg
49.3 deg
(Temperatures in Deg C)

Fig. 2

BGO BALL ELECTRONICS

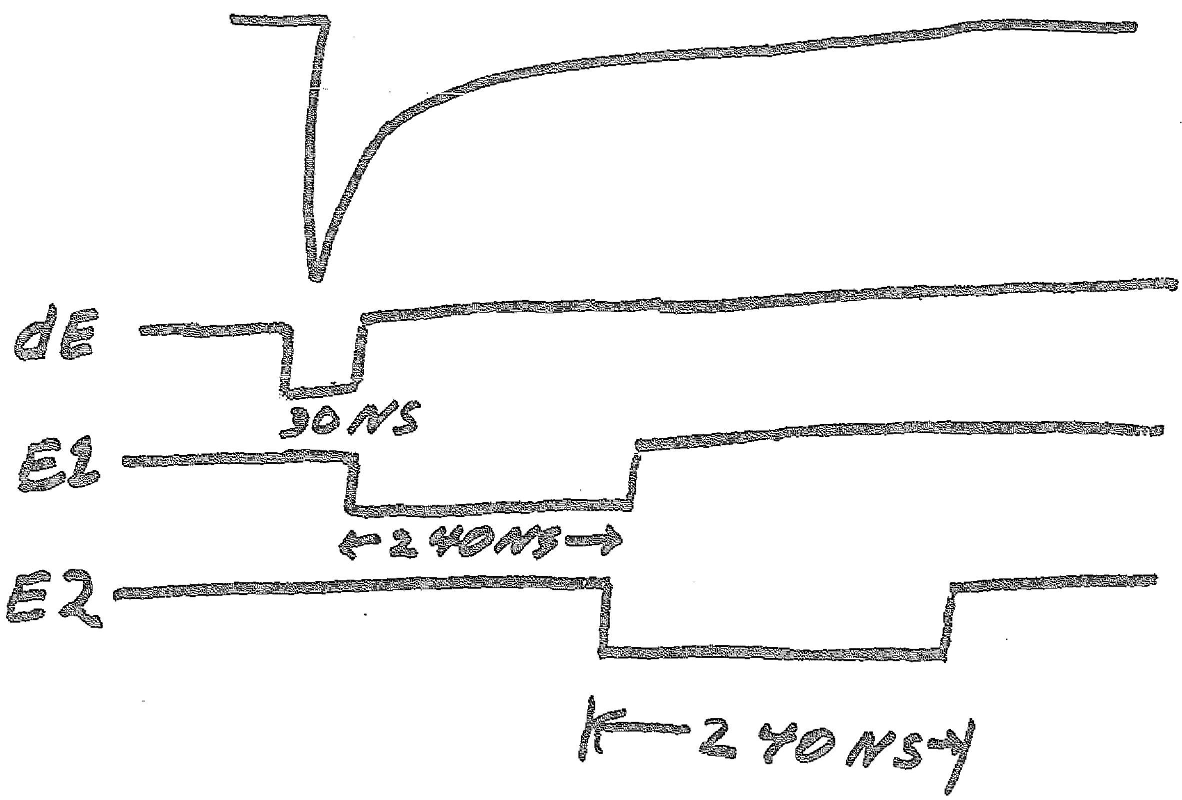

dE & E1 ARE CORRECTED IN SOFTWARE.

$E = E1 + E2$

$R12 = E1/E2$ { PILEUP REJECTION & TEMPERATURE

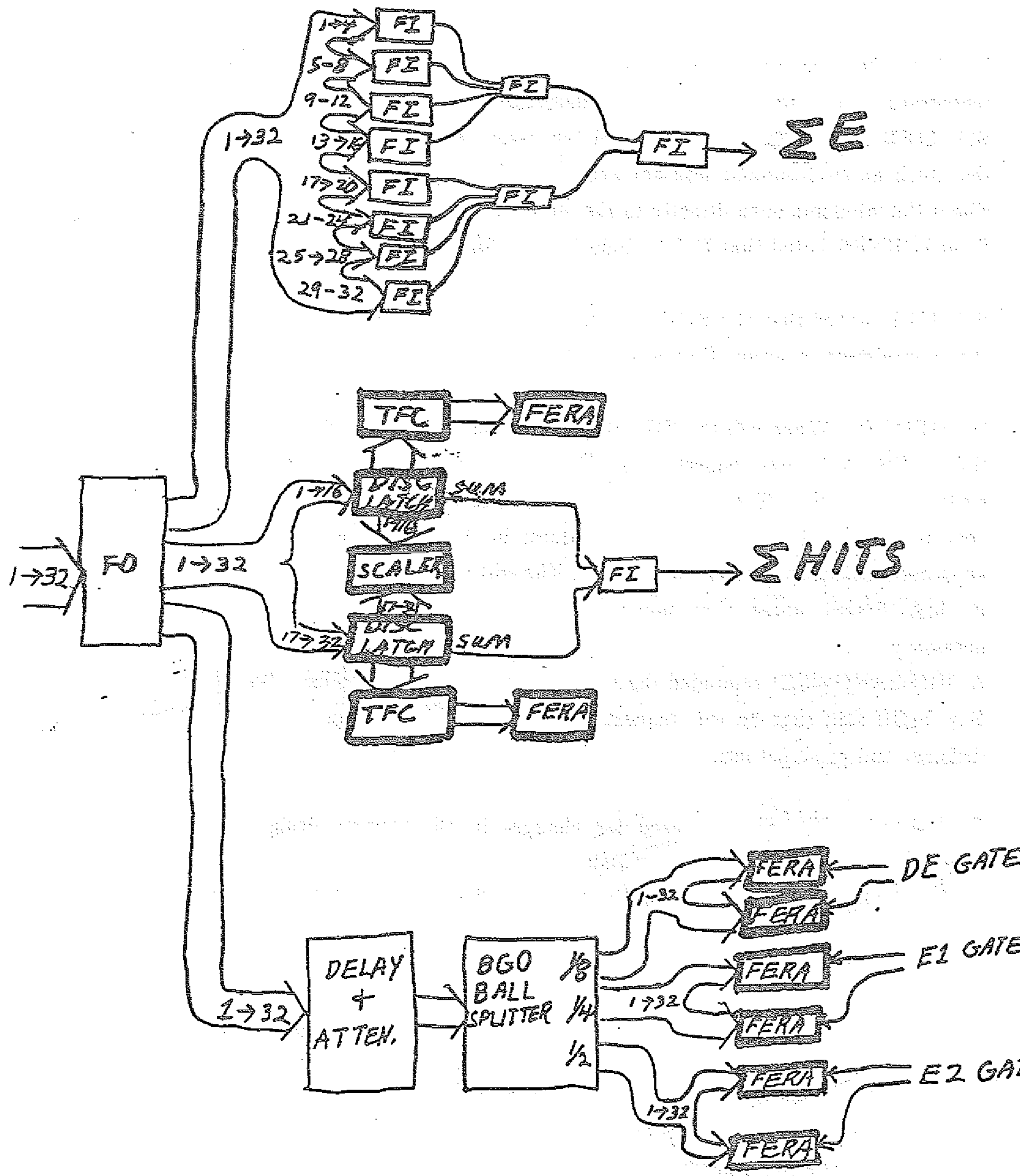

1→32
FO
1→32
1→4
5–8
9–12
13→16
17→20
21–24
25→28
29–32
FI
ΣE
TFC
FERA
DISC LATCH
SUM
SCALER
FI
Σ HITS
1→16
17→32
1→32
DELAY + ATTEN.
BGO BALL SPLITTER
1/8
1/4
1/2
DE GATE
E1 GATE
E2 GATE

DISCUSSION

H. PLENDL: Do special precautions have to be taken to maintain a constant temperature environment for the BGO detectors?
B.J. LIEB said he felt that a normal laboratory environment would be sufficient and that such an environment was not available when the detectors were used at LAMPF, where the lab doors open directly to the mesa.
H. MACHNER noted that LED's could be used for temperature control, if necessary.

B.J. LIEB stated that the BGO Ball comes with a full set of FERA–type electronics, so that a minimum of setup effort will be required.

W. MEILING: When will the BGO detector system be available?
B.J. LIEB: A formal request to LAMPF is needed. [Such a request has since been written and mailed. The editors.] The detector is used no more than a few months per year at LAMPF. [It will be shipped to Mainz in 1992 and be used for several months in an experiment at the MAMI accelerator. The editors.]
H. MACHNER noted that minor modifications could be made on the system, if necessary.
A. BUDZANOWSKI reminded the speaker of the need for detailed drawings.
B.J. LIEB said that he will request any available information from Chris Morris, the designer and principal user.

K. KILIAN reiterated the need for changes in the present design of the Ge Wall structure to accomodate the BGO Ball.
G. RIEPE agreed he will continue to work on this problem with all concerned.

K. Zwoll

ZEL, KFA Jülich

and

W. Meiling

T.U. Dresden

The Data Acquisition System

The architecture of the data acquisition system that has been designed in collaboration with the IKP data analysis group is outlined.

COSY Data Acquisition System for Physical Experiments

W.Erven, J.Holzer, H.Kopp, H.W.Loevenich, W.Meiling [1], K.Zwoll
Forschungszentrum Jülich, Zentrallabor für Elektronik, FRG
M.Karnadi, R.Nellen, K.-H.Watzlawik
Forschungszentrum Jülich, Institut für Kernphysik, FRG

- Introduction

- System architecture
  - General layout
  - Digitizing level with CAMAC, FASTBUS, VME
  - VME Eventbuilder
  - Host Computer System

- Conclusion

[1] On deputation from Technische Universität Dresden, Abteilung Physik, FRG

In "CANU" (COSY-Arbeitsgemeinschaft Nordrhein-Westfälischer Universitäten), a collaboration of COSY users, the data acquisition system has been discussed since 1990

==> Summary of Recommendations

Main Demands on the Data Acquisition System

- Open architecture to allow use of future components with better performance
- High flexibility to satisfy changing demands of physical experiments
- Application of approved standards in hardware and software
- Usage of available modules and systems
- Minimum effort for own module developments
- Dedication of one data acquisition system to each experiment

Main Features of the COSY Data Acquisition System

- Application of well-proved modular instrumentation systems: CAMAC, FASTBUS and VME
- Intercrate connections based on the VICbus
- Distributed intelligence using controllers based on the CPU family 680x0 and the OS-9 real-time operating system
- Application of workstations for experiment control, data storage and data analysis
- Use of standardized communication protocols with TCP/IP, Telnet, FTP, and NFS

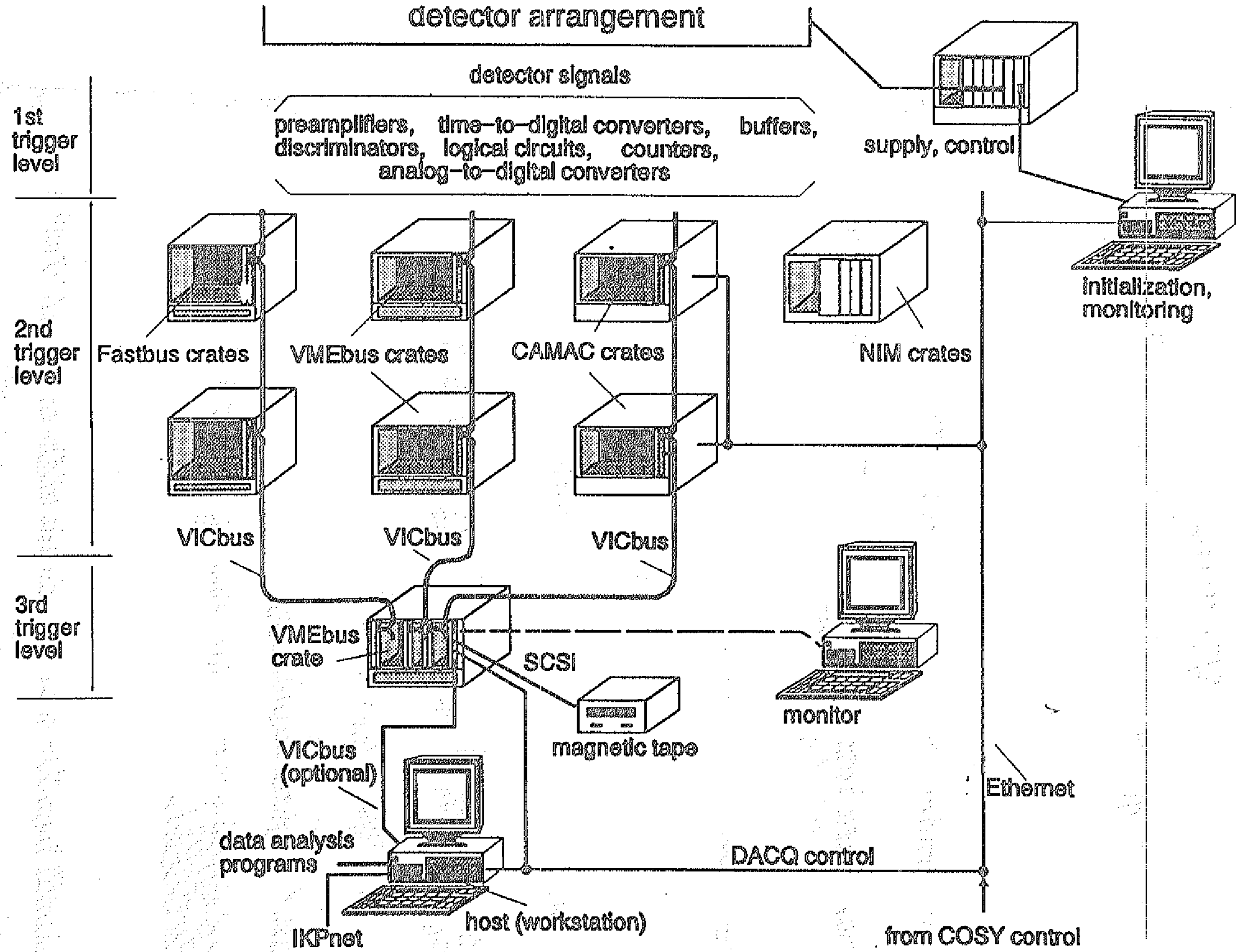

Overall System Architecture

VICbus
An Emerging International Standard for Parallel Inter-Crate Connection

- VICbus under standardisation in IEC-TC1 SC26
- Transparent interconnection of VME-backplanes with 64 twisted-pair cable
- Multimaster and master-slave relation
- Up to 31 nodes connected to the bus
- Distances up to 100 m in maximum
- Asynchronous and synchronous data transmission protocols with transfer rate up to 33 Mbyte/s
- Interrupt structure defined
- Fault tolerant capability
- Gate-array implementation supported by CES Geneva

- General bus for workstations with exposed VMEbus
- Possibility of connecting other parallel systems

Intelligent CAMAC Crate Controller with A2 Functionality and VICbus Interface

- Development in cooperation with CES/Geneva
- Transparent operation in relation with a VME CPU running under OS-9 and CAMAC ESONE library
- Local intelligence with fast list processor and list compiler on the VME CPU
- Stand-alone OS-9 system with LAN connection and NFS

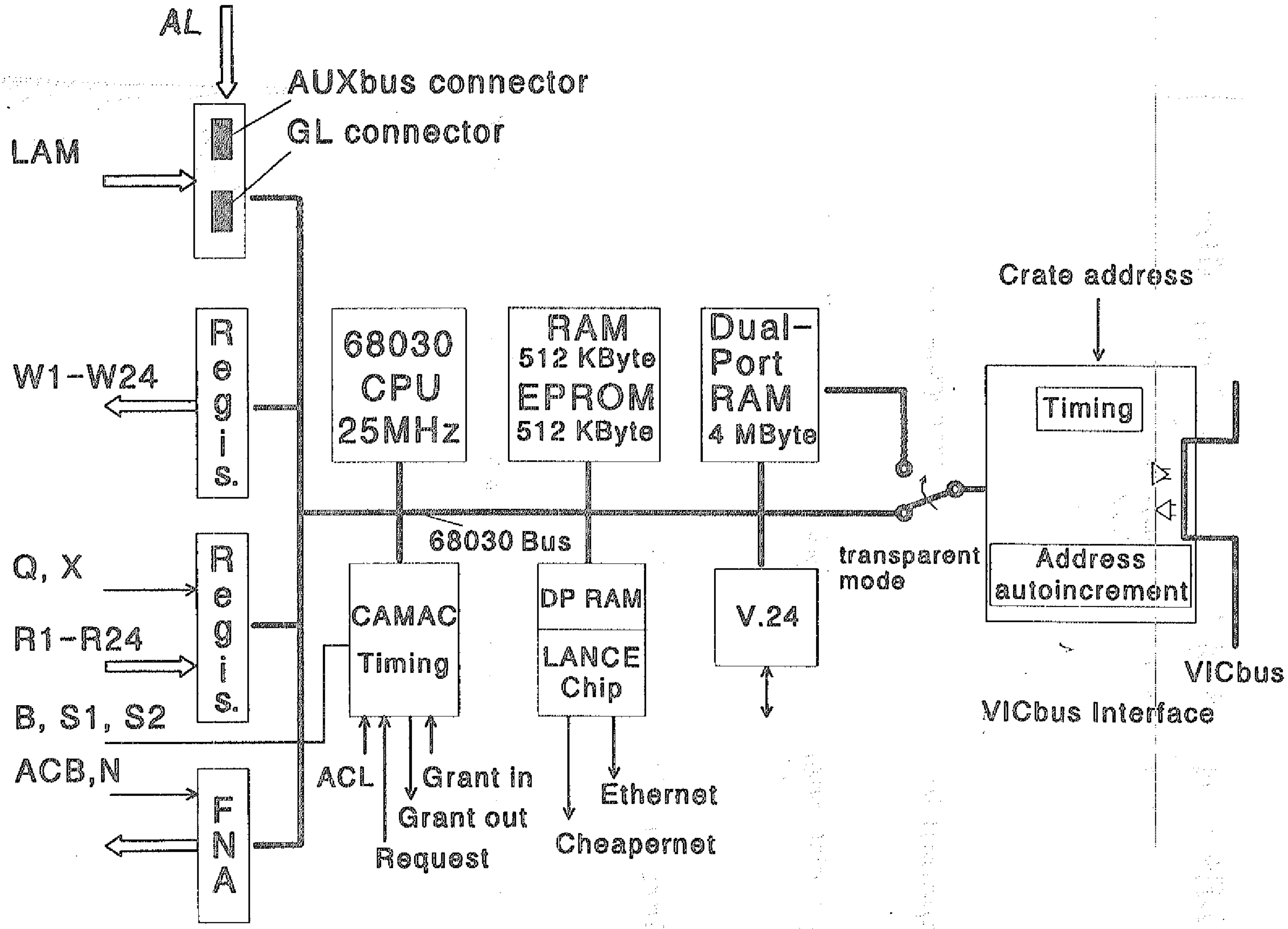

Intelligent CAMAC Crate Controller with
A2 Functionality and VICbus Interface

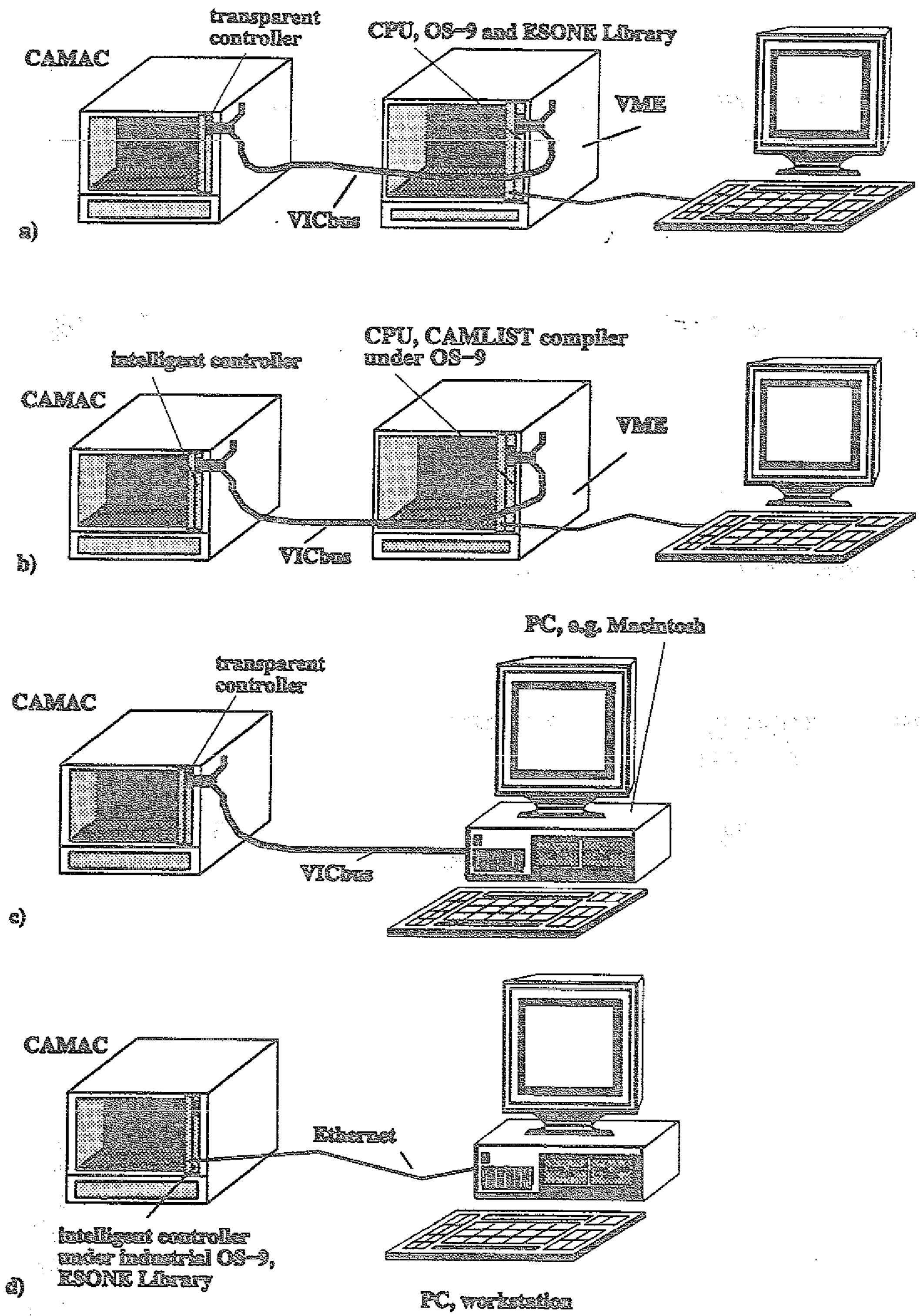

Different system configurations with CAMAC Controller

FASTBUS Instrumentation

- In general, modules with on board data reduction should be preferred (Kinetics and Philips)

- Aleph Event Builder (AEB) with GSI - Software (TDAS)

  Starter Kit : FASTBUS Crate + AEB(OS-9) + PC

- FASTBUS VSB Interface (FVSBI) from OPAL with VME CPU (C - Library), <4Mbyte/s

  Starter Kit : FASTBUS Crate + FVSBI + VMV + VME CPU (OS-9), NFS or Winchester

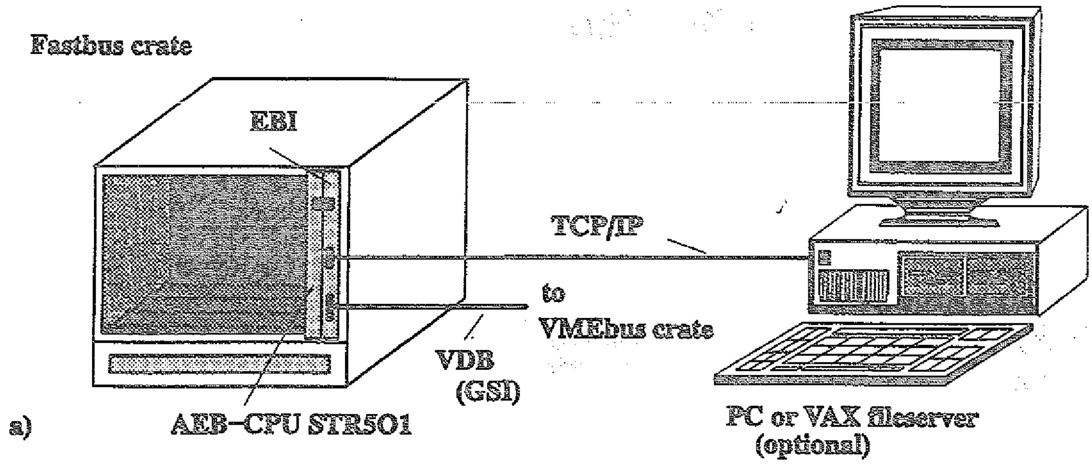

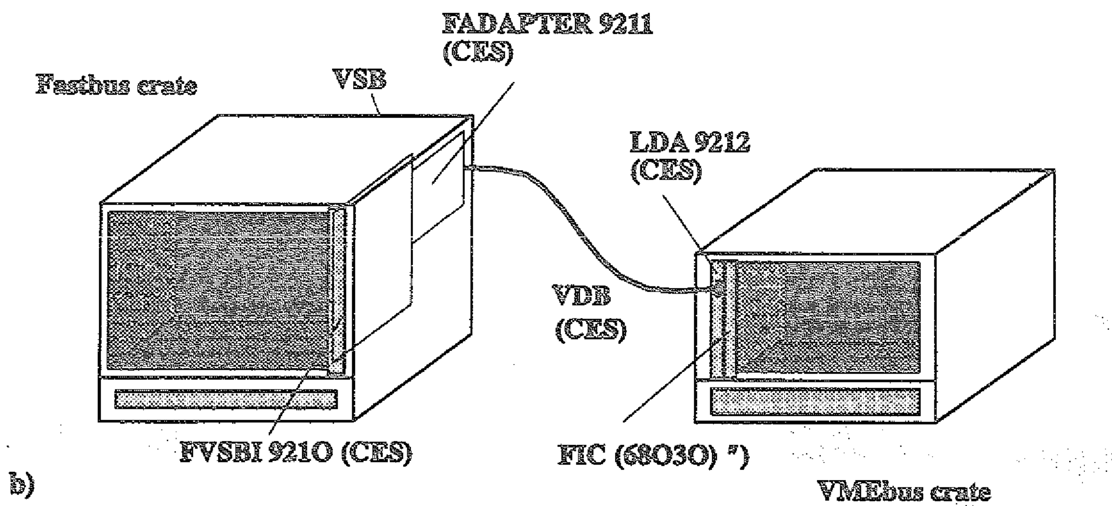

Starter kits for different FASTBUS controllers

Event Builder - a Multiprocessor System based on VME

- High data throughput due to optimized assembler code programs and system-wide buffer structures hidden from OS
- Set-up, monitoring, control and programming support running under OS-9 real-time operating system
- Permissibility of high data rates (>300 Kbyte/s)
- VSB/VICbus interface
- Additional adaption of several CPU modules to a synchronisation bus
- SCSI connection to external mass storage unit
- Optional connection between VICbus and host computer

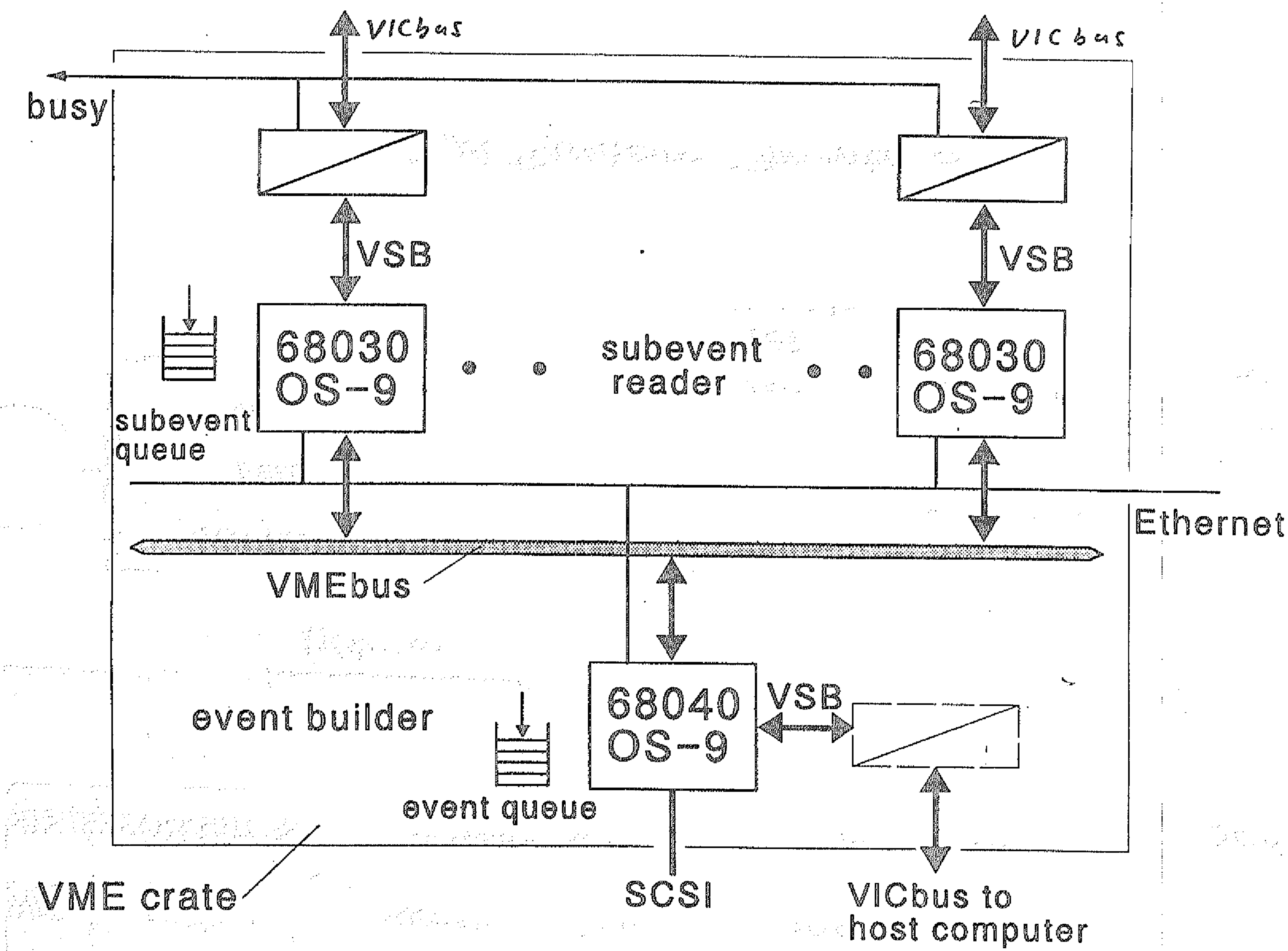

VME – Eventbuilder

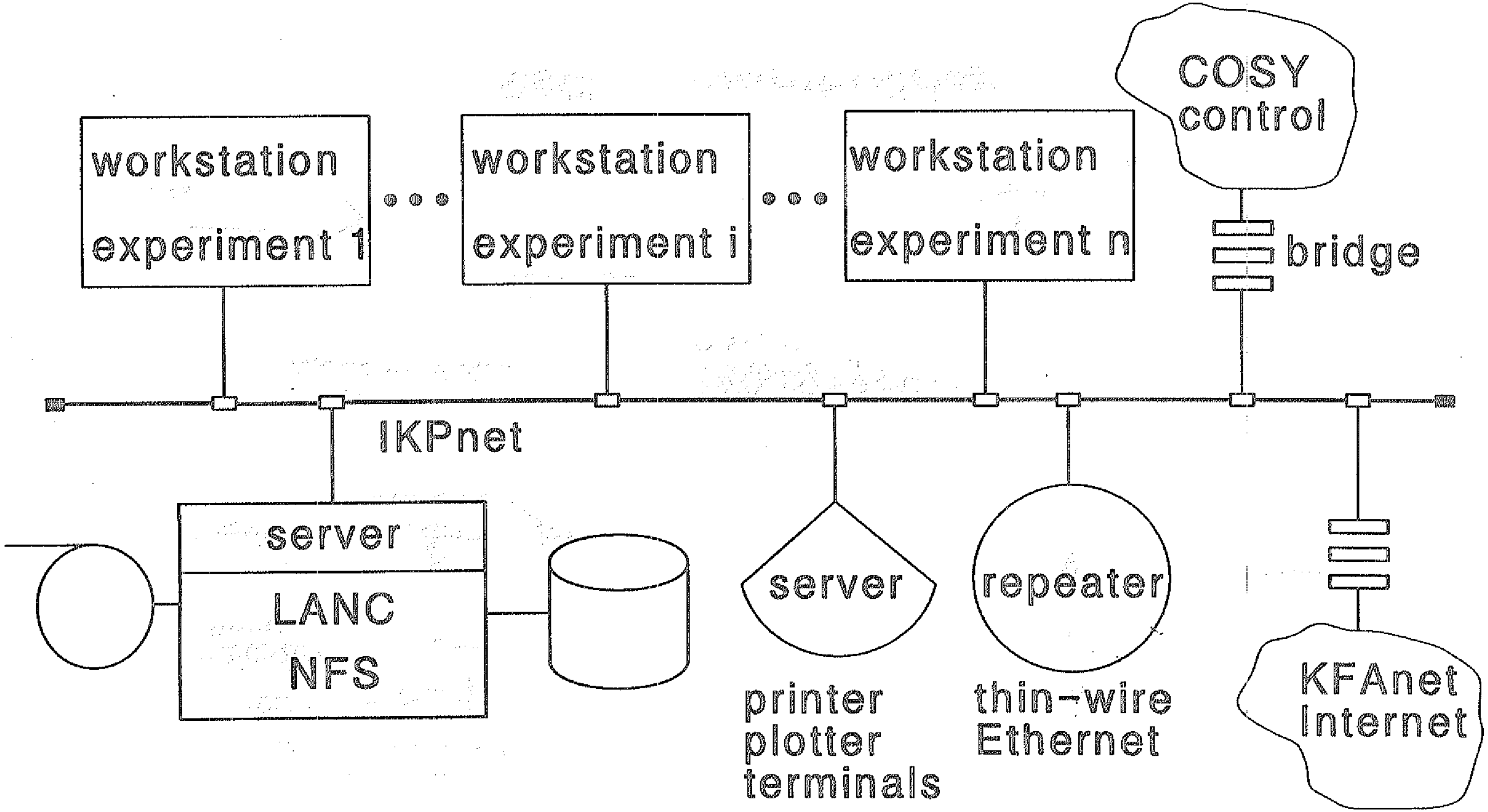

Host System Structure

Programming

— Standalone OS-9 Workstation

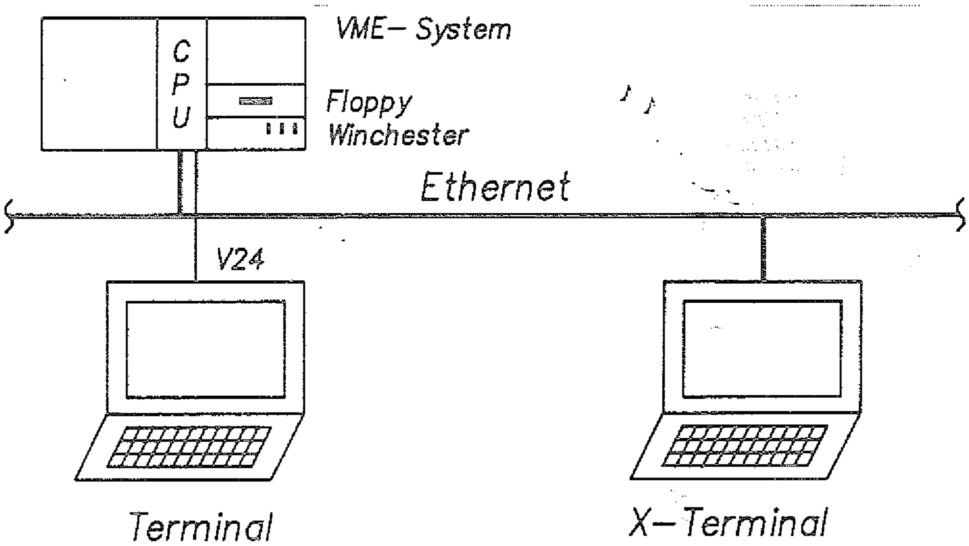

— Industrial OS-9 diskless VME with network server (NFS)

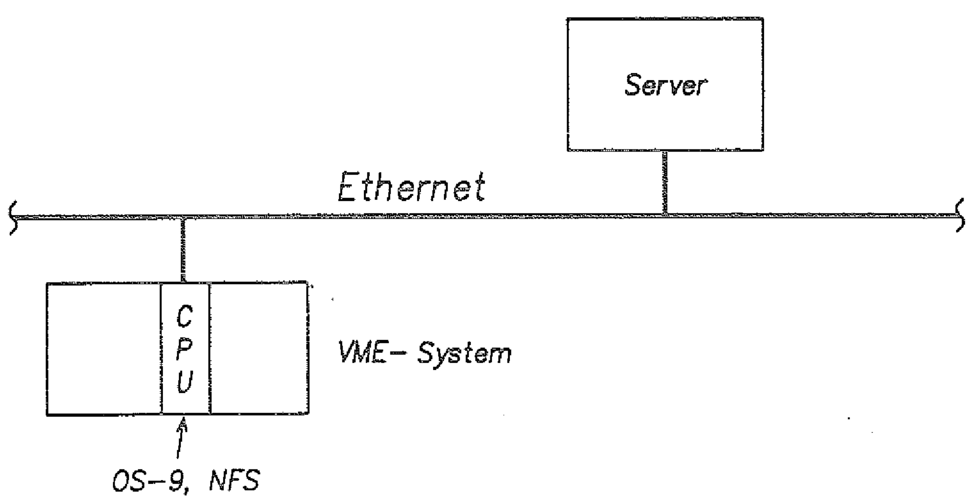

K03-20H4E

— UNIBRIDGE cross-software with network access

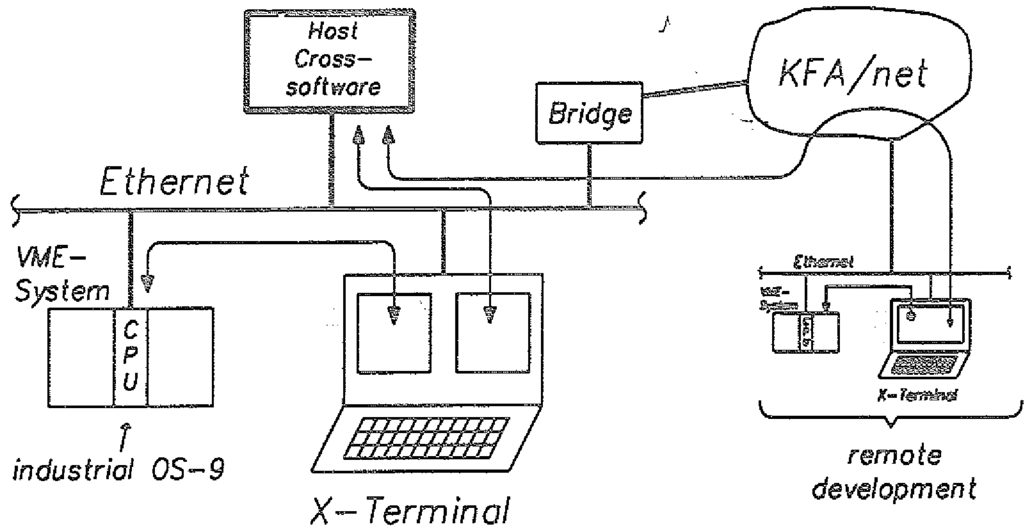

K03-24H4 E

COSY Data Acquisition System for Physical Experiments

W. Erven, J. Holzer, H. Kopp, H.W. Loevenich, W. Meiling[1], K. Zwoll
Forschungszentrum Jülich, Zentrallabor für Elektronik, FRG
M. Karnadi, R. Nellen, K.-H. Watzlawik
Forschungszentrum Jülich, Institut für Kernphysik, FRG

Abstract

For nuclear physics experiments at the internal and external beam of the Jülich Cooler Synchrotron COSY, a three-level data processing and acquisition system shall be developed. Signals from various detector arrangements are digitized and preprocessed by CAMAC, FASTBUS and VME modules. A multiprocessor system based on VMEbus is used for event-building, data recording and buffered data transfer to the host computer. All crates are connected by parallel VICbus. For this, an intelligent CAMAC crate controller with VICbus is under development. Microcomputer-based VME modules are equipped with CPU's of the 680X0 family, working under OS-9 real-time operating system. The data acquisition system is mainly based on commercially available modules. For experiment control and data analysis, workstations as part of a local cluster are provided. Proprietary standards developed at CERN, together with OSF open standards will be implemented. TCP/IP protocols for VMEbus masters and host computer serve for initialization and command transfer.

I. Introduction

The Cooler Synchrotron COSY, under construction in Jülich, will deliver protons in the energy range from 40 to 2500 MeV for medium energy nuclear and particle physics experiments. In the synchrotron and storage ring of COSY the protons, which are injected from the cyclotron JULIC, are cooled by two facilities: an electron beam cooling system at low proton energies and a stochastic cooling arrangement at higher beam energies. The accelerated proton beam is characterized by high phase space density, allowing experiments with well-defined beam momentum, high spatial resolution and low background. Various external target stations are possible supplied by the extracted beam, using particle detectors in combination with the magnetspectrometer BIG KARL or with the Time-Of-Flight (TOF) spectrometer, which is being constructed [1]. Furthermore, at the internal beam, physical experiments are prepared which enable measurements with extremely thin targets and low background.

In the experimental environment, scintillation and semiconductor detectors, drift chambers and Cerenkov counters are used. The number of detector channels is not higher than about 1000 in each detector component. "CANU" (COSY-Arbeitsgemeinschaft Nordrhein-Westfälischer Universitäten), a collaboration of COSY users, recommends a common structure for the data acquisition system serving COSY experiments [2]. The main features of this are described as follows:

- Each experiment or target station should have "its own" data acquisition system.
- Readily available hardware with proven concepts, hardware standards and approved software packages should be applied as far as possible to obtain minimal cost and risk.
- An open architecture and modular design of hardware and software should guarantee adaptability to modified requirements of physical experiments and to more advanced components.

Based on these recommendations the structure of the COSY data acquisition system was defined, which is described in the following sections.

II. System Architecture

A. General Layout

The configuration of the COSY data acquisition system is schematically shown in Fig. 1. For digitizing the detector signals, CAMAC and FASTBUS modules are applied. If available, suitable VMEbus modules can be used. The subevent data blocks are read out by subevent readers which are located in the event builder VMEbus crate. Under control of the event builder the subevent data blocks are preselected, framed to event data blocks and stored onto magnetic tape. Data analysis will be done by use of workstations which are available as host computer cluster for all COSY experiments.

The interconnection of CAMAC crates and FASTBUS crates is based on the VME Inter-Crate bus (VICbus). Therefore, some expense was necessary to develop a CAMAC crate controller with VICbus connection (see Fig. 2).

It should be mentioned that all intelligent crate controllers and VMEbus master boards are equipped with microprocessors of the 680X0 family, running under the realtime operating system OS-9. Further, Ethernet is used for control and event data transfer to the experiment workstation.

[1] On deputation from Technische Universität Dresden, Abteilung Physik, FRG

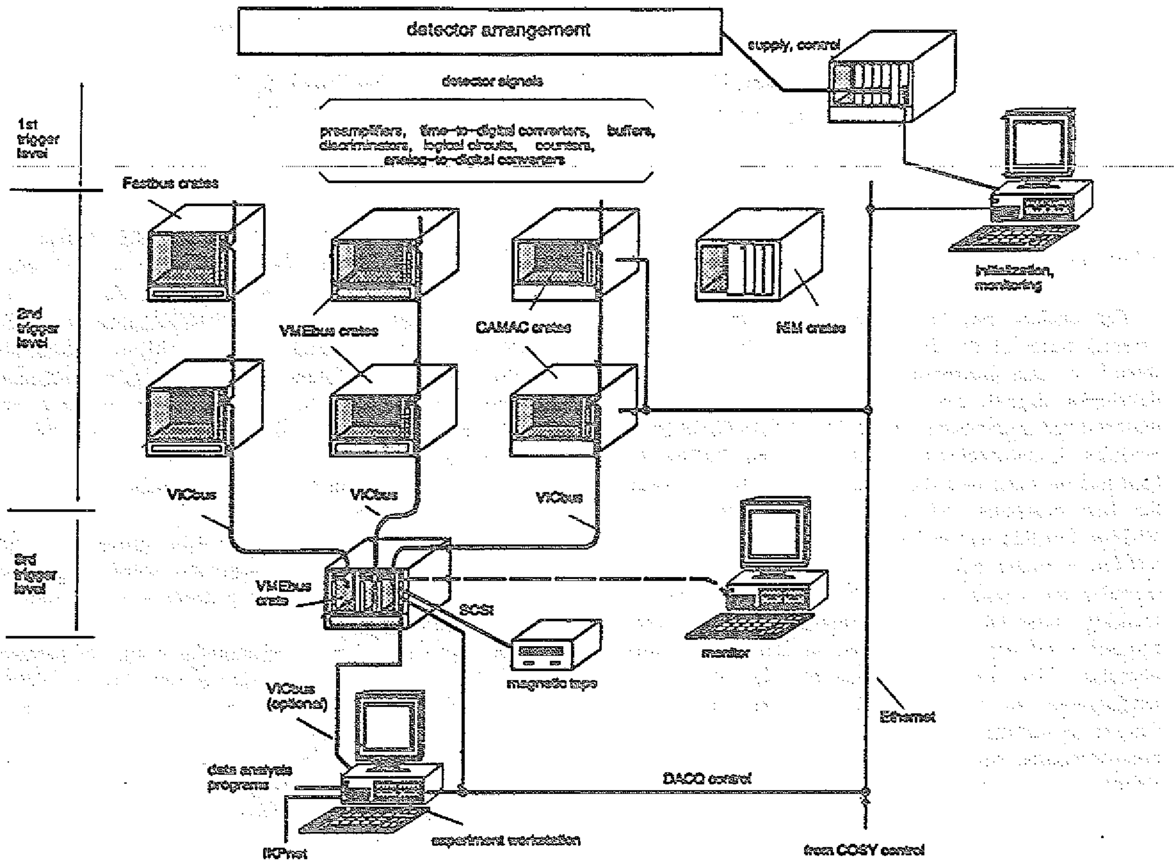

Fig. 1 The COSY data acquisition system.

B. The VICbus: An emerging international standard

In the past several approaches of proprietary bus designs for connecting control equipment systems to each other over parallel buses have been published. A new attempt to specify a standardized bus for this purpose was undertaken by a small crew from companies and research centres with the VICbus document [3]. The VICbus was initially designed for interconnecting VME crates in a transparent or non transparent way to fulfil the growing need of larger experimental and process control equipment. Due to its wide-spread scope in the future it also gives the facility to interconnect other systems than VME. In the case of CAMAC, the VICbus has been chosen for replacing the CAMAC Branch Highway with its expensive cabling and connector technique. Furthermore, the standardization effect leads to an economic and high performance interfacing technique for workstations and computers with exposed VMEbus as I/O port. Some companies are going to implement the appropriate software drivers.

VICbus uses standard flat cable with low-cost connectors. Signal multiplexing allows use of 64 twisted-pair cable. The VICbus is capable of spanning the length of up to 100 meters with a different timing for short (< 30m) or long (30m-100m) cables. Up to 31 devices are permitted on a single VICbus segment. Though the need of the arbitration mechanism for multimaster environment is foreseen, it is not used by us, because for our application only a multislave system with a single master is needed.

The VICbus data transmission protocols are two fold. In the "compelled mode" with an end to end acknowledgement, normal data rates are possible. The "non-compelled mode" offers higher speed data transfers in a pipelined operation mode up to 33 Mbyte/s.

To simplify the design of a VICbus interface, an ASIC has been developed by the company CES. This ASIC includes the logic for crate number decoding and for mapping an individual interrupt to the 32 different interrupts on the VICbus as well as most important interface registers.

If the VICbus is used for data acquisition with several VICbus segments connected to a single VME crate, a VICbus to VSB interface is required, which will be developed in the near future.

C. The CAMAC System

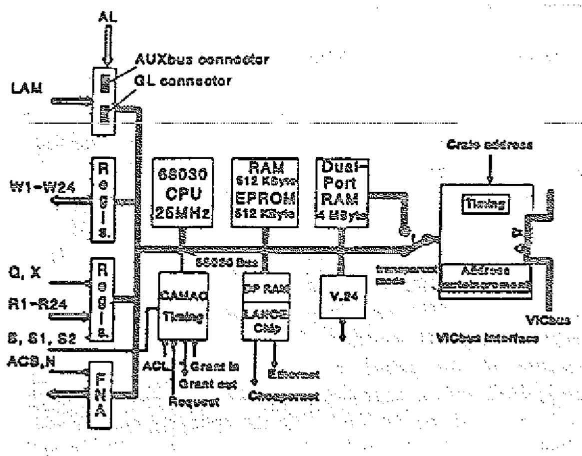

Fig. 2 Schematic diagram of the intelligent CAMAC crate controller with CC-A2 functionality and VICbus interface.

Within the framework of the data acquisition system, a CAMAC crate controller in cooperation with CES Geneva has been developed. Fig. 2 gives a blockdiagram of the controller. To avoid the difficult programming of a bit-slice processor, the execution of CAMAC routines is divided in two parts. The first one performs the CAMAC Dataway cycle and supports the blocktransfers with highly integrated PAL's. The more complex tasks are executed by a standard microprocessor (Motorola 68030) which runs, whenever possible, in its own cache memory. The controller follows CAMAC EUR 6500 specifications and can also be used as an auxiliary controller, in order to give a smooth migration from existing CAMAC systems to a state-of-the-art equipment.

The controller is optimized for a fast readout blocktransfer without any deadtime between CAMAC cycles. In "short cycle" operation mode, the performance is enhanced by generation of a non-standard Dataway cycle of 600 ns duration. To decouple the VICbus readout from the internal operation of the microprocessor, a dual port RAM has been implemented.

The processor part has enough resources to support a stand-alone operation under OS-9 with network connection over Ethernet, TCP/IP and NFS.

In the transparent mode of operation a 2 Mbyte address range of the VICbus can directly be mapped to the NAF-Command bits and some auxiliary control bits. This leads to a very simple and economic implementation of the system without overhead due to use of a microprocessor and associated circuits.

The VICbus interface supports the auto-address increment mode to pass blocks of data to or from several contiguously addressed locations of the dual port RAM. Only the address of the first location is specified, and thereafter the actual address is incremented during a read or write cycle. The VICbus controller part has been implemented by standard logic devices, PLD's and the above mentioned special gate array from CES.

Following the CAMAC specifications, a library has been written consisting of a subset of the ESONE CAMAC routines and implemented according to the CAMAC implementation for the OPAL Experiment. But instead of the CES Branchdriver (CES CBD 8210) the VICbus interface with the CAMAC crate controller is supported in the transparent mode. At CERN, the library has been used with RTF (Real Time Fortran). In our application mainly C is desirable; therefore some little changes and adaptations must be foreseen. In a second step, a CAMAC list processor will be implemented to enhance the execution speed of the CAMAC operations. The readout of CAMAC equipment is then performed by user written CAMAC lists. This is a text file that represents a list of basic CAMAC operations (called CAMLIST) to be executed when a trigger occurs. A CAMLIST compiler which is based mainly on a CERN implementation [4,5], generates a code which is executed by the intelligent version of the CAMAC controller.

D. FASTBUS Instrumentation

To fulfil the requirements for the FASTBUS systems we have chosen a two fold solution:

- For high performance requirements we will integrate the "AEB - ALEPH Event Builder" [6]. Especially the electronics for the experiment development by the TOF (Time-Of-Flight) collaboration will use this solution with a preliminary software approach [7].
- For moderate performance we have chosen the "FVSBI - FASTBUS to VSB Interface" FASTBUS controller [8] which gives an adequate solution for data rates up to 4 Mbyte/s at a reasonable price (over than 50% less than the AEB). The software is a C - Library which exposes the main functionality of the U.S. NIM Committee FASTBUS library [9].

We recommend the use of the new family of FASTBUS ADC's and TDC's with on board data reduction, such as: zero suppression and pedestal subtraction, to achieve an acceptable overall data acquisition speed.

For both solutions we will develop interfaces to adapt the individual controllers to the VICbus.

E. VME Eventbuilder

The basic building blocks of the VME event builder crate are commercially available single-board VME microcomputer boards (see Fig. 3). Each single-board computer is dedicated to a specific function. So the subevent readers are responsible to collect the event data from the front-end electronics (CAMAC, VME, FASTBUS) via the respective controllers and VICbus. The use of one subevent reader for each VICbus segment allows simultaneous readout of the several front-end controllers.

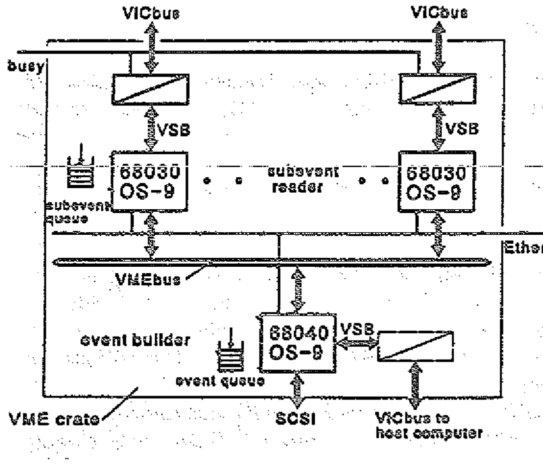

Fig. 3 Schematic diagram of a VME Eventbuilder crate.

To separate I/O traffic from the VMEbus and thus to reduce the required VMEbus bandwidth, the VSB is used for connecting the VICbus. For this purpose a set of line driver modules interface the VSB to VICbus and vice versa. These modules are also responsible for connecting the subevent readers with the trigger electronics. The design of the driver modules will be carried out to adapt CPU boards with different functionality as far as the VSB interface is concerned.

To limit the number of software versions we decided to focus on two board types for the subevent readers. The FIC 8232 (from CES Geneva) was chosen for high performance applications and the Eurocom 6 (from Eltec, Mainz, FRG) as a cheaper version for moderate user demands. Both are equipped with a 68030 CPU running at 25 MHz, as well as Ethernet connection and 4 Mbyte of RAM. Since the subevent readers also function as VMEbus masters, they can send their formatted data to a global event buffer in the event builder CPU, which formats the data in a common data structure (ZEBRA with experiment specific extensions). User written routines can manipulate the raw event data. A SCSI interface serves as the data channel to Exabyte or IBM Summit tapes. Some selected events can also be transferred via the Ethernet TCP/IP connection to the host. Furthermore the standard VICbus connection can offer a high-speed data channel to the experiment computer. The new 68040 based VME CPU boards give sufficient power for the event builder function. Until now we have the choice between a two processor board manufactured by CES, or single processor boards from Eltec or Motorola. In any case, the OS-9 operating system should be the basis of the VME system software. For monitoring, control and tests, tasks in the context of OS-9 will be implemented. For fast event data collection and transfer through the system, all the details of the OS-9 system should be hidden from the appropriate user programs. As programming support, we are installing the UniBridge cross-software from Microware on an Ultrix DEC station, which is accessible over the network facilities of the research centre in Jülich.

F. Host Computer Architecture

In the experiment environment workstations will be used for experiment control and data analysis. These workstations require high CPU performance, a minimum of 16 MB memory, powerful 3D graphic supported by a local graphic processor and regarding I/O channels, Ethernet, SCSI for local disks and tapes as well as connection to the VMEbus. Also in the future FDDI will be aspired. For the first generation of COSY experiments a workstation cluster with a central server and workstations as satellites are scheduled. Because of the actual orientation of our collaboration, VAX/VMS with a migration to RISC/UNIX is desirable. In the first period, on the VAX side the operating system VMS with LAVC, DECNET and LAT is used, and the connection to the UNIX world is realized by employing VMS/ULTRIX connection with NFS, RPC and ARPANET (TCP/IP, FTP, Telnet). Within the cluster the server is related to central services for workstations, in particular supporting common system disk, batch and network service, clusterwide user disks and other system services according to libraries and general data acquisition and evaluation software.

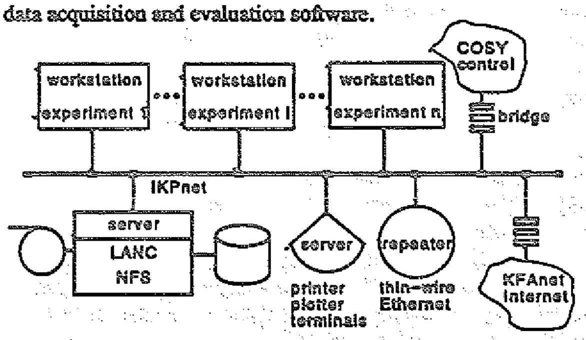

Fig. 4 Host configuration with Ethernet backbone.

Workstations for the experiments possess local disks and tapes respectively. These disks are used for paging and swapping of files, experiment specific data acquisition software and as container for OS-9 VME software accessed by NFS.

UNIX stations are equipped with local system disks, and the access to the central server will be provided by NFS. The world-wide network communication, including electronic mail is realized by INTERNET as well as BITNET.

G. Host Software Structure

In general, the capabilities of acquisition software according to the requirements for the first generation of COSY experiments [1] comprehend experiment control and data analysis. Experiment control consists of functions such as remote set-up of digitizing and auxiliary systems, run control with error handling, including communication with COSY Control as well as monitoring concerning the system status and its dynamic behaviour. Data analysis comprises on-line sort and analyzing of event data, its graphical representation with histogramming functions, track recognition, 3D imaging of detector arrangements and tracks from variable angles of view.

The essential criteria for the design of this software are:

- scalability, with the aim, that for each experiment or target station an independent acquisition software of similar structure can be used, fulfilling the represented requirements,
- portability and compatibility with respect to the operating system and hardware architecture,
- common user interface as far as the handling and operating is concerned.

Regarding physics requirements, the employed software will be proprietary standards, MODEL [10] and PAW [11], established in nuclear physics. On the other hand standards will be implemented, especially TCP/IP and NFS for the communication with the VME systems as well as X-Windows/OSF-Motif as common user interface and GKS or PHIGS for graphics application.

On the host side, all operations will be processed asynchronously regarding the event data flow. Depending on the event rate and the CPU load, a variable, statistically representative selection of events will be fed for data analysis.

An event covers one or more subevents. Each subevent is dedicated to one digitizing system and has an individual data structure. On the other hand, each digitizing system consists of a set of multichannel modules, selected randomly for each event to deliver data. Consecutive events have different data length.

In the software, logical links for set-up and control of digitizing and auxiliary systems as well as the arrangements of event data to the individual channels of detector components will be achieved by:

- hardware configuration data sets, wherein the digitizing and auxiliary systems are assigned to the detector components according to its type and the individual equipment,
- set-up data for initialization comprising all in the experiment active systems including the actual set-up parameters,
- assigning to each type of digitizing system an readout routine with defined subevent structure and an according subevent decoding routine.

The acquisition software will be of modular structure in such a way, that independent experiment control and data analysis functions are combined to processes with access to a common database.

All processes will be controlled by a common user interface. Independent processes can be activated from one or more workstations or terminals. On the contrary, data flow dependent processes like event buffer distribution, event decoding or on-line sorting are running synchronously in the background.

The database will be realized by the ZEBRA Data Structure Management Package [12], wherein for event data ZEBRA Exchange Format will be used, with defined event and subevent data structure. All other data, especially evaluated event data will be stored in ZEBRA Native Format.

In the first step, a basic functionality will be realized for all experiments. Additionally software interfaces and tools will be provided for experiment specific extensions.

III. Conclusion

This paper reflects the conceptual design for the data acquisition system at COSY started in 1990. It is based on application of existing or emerging international standards in hardware and software. Some hardware for this is being developed to fulfil the requirements of the VICbus, especially the CAMAC controller and a VICbus to VSB interface.

The key future work will focus on the overall software structure and its implementation. In this respect the GSI-GOOSY software system [13], which is now under consideration, will in main points meet our requirements as far as the front end controllers and the multiprocessor system are concerned. The host system software, as outlined in one of the previous paragraphs, will be based on software packages developed at CERN.

IV. Acknowledgements

Many persons in the CANU Commission and at the Forschungszentrum Jülich have contributed to the design of the data acquisition system. Especially helpful were discussions at CERN with several people from on-line computing group, PRIAM Project, Crystal Barrel, OBELIX, WA89 and OPAL. The authors also wish to acknowledge the contributions of people from GSI.

V. References

[1] E.Kuhlmann, H.Machner "Data Acquisition Requirements of Collaborations Preparing First Generation COSY Experiments", CANU et al, Kommission Datenaufnahme, Internal Paper, 1991.

[2] COSY-Arbeitsgemeinschaft Nordrhein-Westfälischer Universitäten CANU, Kommission Datenaufnahme COSY, "Summary of recommendations as of March 4, 1991, Internal paper".

[3] C.F.Parkmann, "VICbus, Inter-Crate Bus for the IEC821 VMEbus ", Draft Specification Revision 0.95, International Organisation for Standards, International Electrotechnical Commission (IEC), Joint Technical Committee 1, Sub-Committee 26, Working Group 8, CERN, Geneva, Switzerland, Nov. 1990.

[4] J.A.Dykema et al, "The VME Event Builder", Proc. of VMEbus RESEARCH, Proc. of International Conference and Exhibition, ETH Zürich 11,12,13 Oct. 1988, North-Holland, ISBN 0447005244, pp. 203-210.

[5] S.Cittolin, M.Demoulin, W.Jank, J.P.Porte, D.Samyn, B.G.Taylor, H.von der Schmitt, "MacUA1 MACINTOSH-

BASED DEVELOPMENT SYSTEM", CERN-UA1 Technical Note 90-01, Geneva, Switzerland, Jan. 1990.

[6] A.Marchioro et al, "The ALEPH Event Builder, A Multi-User FASTBUS Master", IEEE Trans. of Nucl. Science 35, vol. 1, pp. 316-320, Feb 1988.

[7] T.Plaich et al, "Acquisition, Analysis and Control Software for the Experiments in CAVE B^{G+B}", GSI Annual Report, 1989.

[8] M.Weymann, "The FVSBI - FASTBUS to VSB Interface, short description", CERN/EF, Geneva, Switzerland, Oct. 1989.

[9] U.S. NIM Committee, "FASTBUS STANDARD ROUTINES", U.S. Department of Energy, Office of Energy Research, DOE/ER-0367, May 1988.

[10] C.Boissat, W.Bozzoli, P.Burkimsher, R.Jones, J-P.Matheys, G.Monarrechi, T.Nguyen, D.M.Sendal, P.Vande Vyvre, A.Vascotto, D.Weaver, "MODEL A Software Suite For Data Acquisition", CERN 1211 Geneva 23, Internal Paper.

[11] R.Brun, O.Couet, C.Vandoni, P.Zanarini, M.Goossens, "PAW-Physics Analysis Workstation", CERN Program Library Entry Q121, Version 1.07, CERN Geneva, Switzerland, Oct. 1989.

[12] R.Brun, J.Zoll, "ZEBRA users guide", Version 3.53, CERN Computer Centre Program Library, Jan. 1987.

[13] H.Essel et al, "An integrated data acquisition and analysis system at GSI", IEEE Trans. of Nucl. Science, vol. 36, no. 5, pp. 1523-1527, Oct. 1989.

DISCUSSION

J. KOONIJN asked about the possibility of on–line data reduction at higher rates when needed.
K. WATZLAWIK replied that on–line data reduction is not provided for at the present time because of the cost involved, but that it can be added at a later time.

H. MACHNER asked when the system would be available to the experiments.
K. ZWOLL replied that this will be by the end of this year.

K. Watzlawik

IKP, KFA Jülich

The Host Computer

The part of the data handling system that will permit on–line data analysis is described.

COSY EXPERIMENT DATA PROCESSING

Hardware Architecture

Workstation Cluster with central server and workstations as satellites:

- Architecture: VAX/VMS with a migration to UNIX

- Operating System
  VMS with LAVC, DECNET, LAT and
  VMS/ULTRIX-Connection with NFS, RPC, ARPANET
  (TCP/IP, FTP, SMTP and Telnet)

Server:
- common system disk,
- batch, printer/plotter queues, network service,
- clusterwide user disks,
- common user system with libraries,
  general data acquisition and evaluation software.

Experiment Workstations:
- high CPU performance,
- min. 16 MB Memory,
- powerfull 3D-Graphic, local garaphic processor,
- I/O channels:
  Ethernet, SCSI for local disc and tape,
  connection to VMEbus, in future FDDI,
- local page/swap files, exp. specific data acquisition software,
  container for VME/OS9 software.

Workstation Cluster

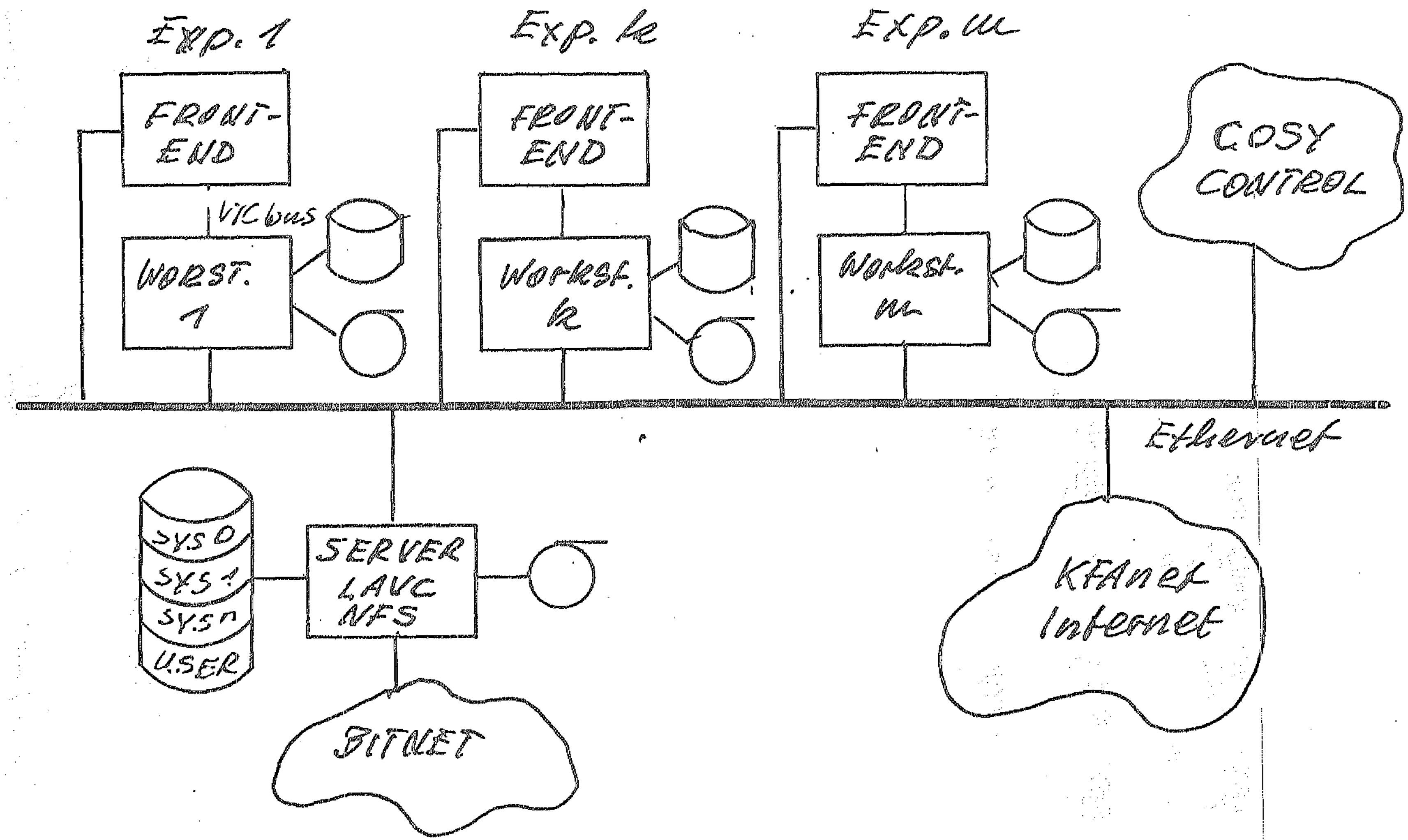

Summary

- VAX/VMS Workstation Cluster
  for the present applications and
  for the 1. generation of COSY experiments,

- RISC/UNIX (ULTRIX) Workstation Cluster
  for the 1. off-line data reduction,

- RISC/ULTRIX migrations or RISC/VMS
  for advanced COSY experiments,

OSF and POSIX standards are recomendet

Off-line Data Evaluation Requirements

Assuming that
- one experiment of 2 weeks runtime with 100kBps (1KB/event) produces 100GB of raw data,
- availability of COSY for experiments are 50%,
- availability of the Experiment are 80%,

hence it follows for IKP COSY Experiments
- data rate in evarage 24 KBps,
- 750 GB of raw data per year (about 200 EXBYTE 8500 cassettes).

Off-line Data Evaluation:

1. Data Reduction --> local in the IKP

   (2.5h CPU of IBM 3090 for 200 MB raw data)

   - CPU power about 10 MFlop (LINPACK n=100, one IBM 3090) for IKP COSY Experiments,
   - reduction factor 3 to 4,

2. Data Reduction --> local in the ZAM

   event reconstruction, track fitting
   (12H CPU of IBM 3090 for 200 MB of raw data)

   - CPU power about 50 MFlop (five IBM 3090),
   - disk capacity about 40 GB,
   - reduction factor 15.

3. Data Reduction --> local in the IKP

   correction, visualisation

   - graphic performance
   - disk capacity.

Networks, IKPnet

Requirements:

- local INTERNET subnets for COSY Experiment Networks,

- separation of Ethernet cables by Bridges or Routers with the aim to optimize the distribution of network trafic,

- experiment networks must be independet from KFAnet (Router, Gateways),

- FDDI for data transfer to ZAM for off-line evaluation.

EXP. NETWORKS, IKPnet

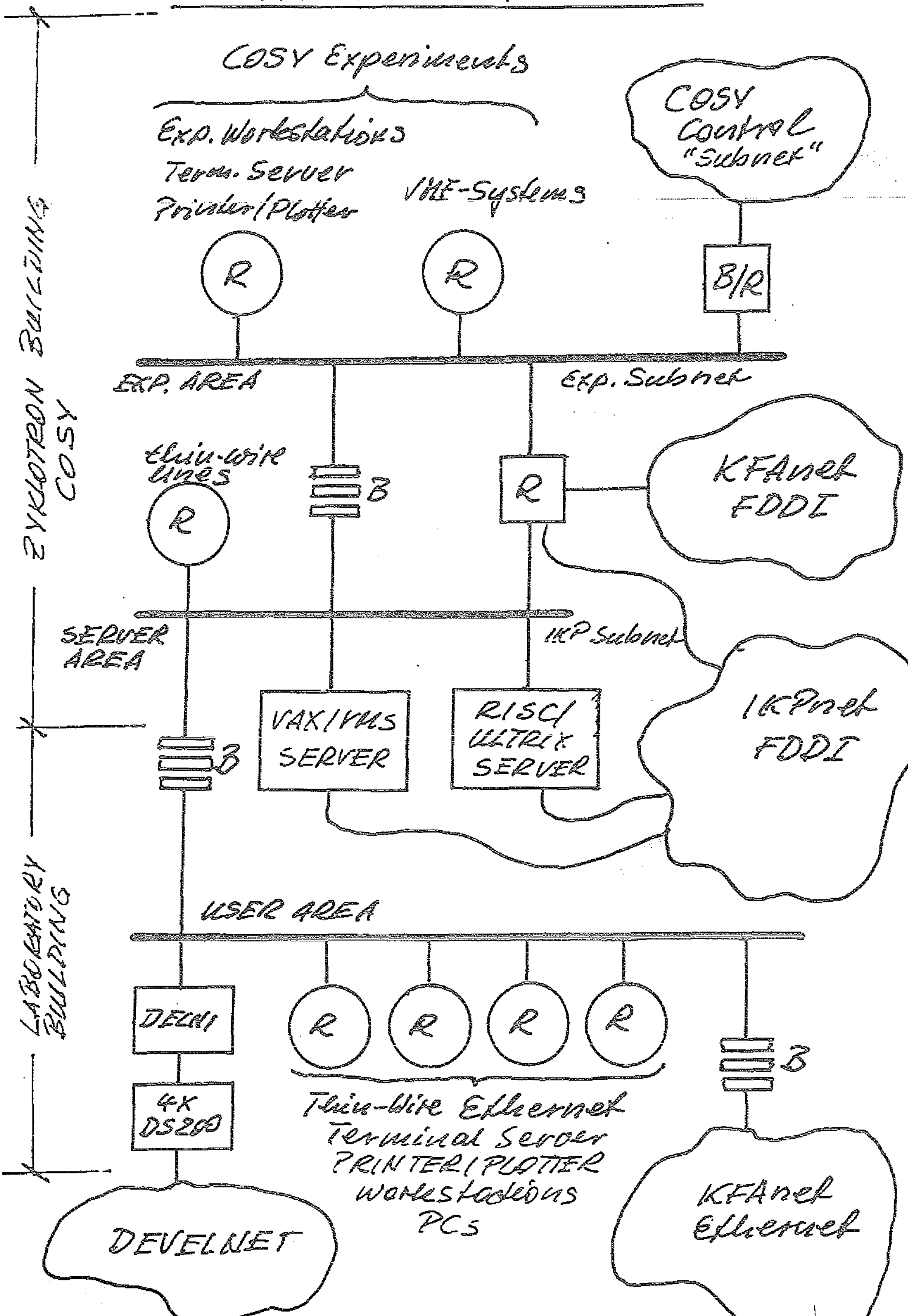

On-line Data Acquisistion Software

Capabilities, Functionality

Experiment Control

- remote setup of digitizing and auxiliary systems (HV power supply, trigger...),

- run control,
  control of front-end hardware, error handling,
  communication with COSY control,
  control of auxiliary hardware (gas supply for DCs, MWPCs, vacuum and target control....)

- monitoring concerning system and experiment run status (scaler, data end event rates ....)

Data Analysis

- on-line sort and analysis of event data,

- graphical representation of data,
  histogramming, track recognition,
  3D imaging of detectors and tracks form
  variable angle of view.

Genaral Software Structure

Software Tools

Proprietary, in nuclear physics established standards developed at CERN:

- MODEL - organisation of data flow, control operations,
- ZEBRA - Data Structure Management Package for the Database
  KUIP Kit for User Interface Package
- PAW - Standard package for Data Analysis,
- CERNLIB, HBOOK (Interface to Histogramming)
  HIGZ (High level Interface to Graphics and ZEBRA)
  HPLOT (Plotting Interface)

Open Standards

- TCP/IP, NFS for the communication with VME and COSY Control,
- X-Window/OSF-Motiv as common User Interface,
- GKS or PHIGS for graphics applications.

Organisation of Data Flow

Setup, control of digitizing and auxiliary systems as well as arrangements of event data to channels and detector componets will be organized by:

- Hardware Configuration Data Set
  digitizing systems
  auxiliary systems

  type, no of systems — aquipment
  subdedectors ↔ no of mudules, channels

- Setup Data
  enabled Modules and channels, pedestals
  sort configurations

- each type of digitizing (auxiliary) system are assingned to a individual
  Setup Routine,
  Readout Routine with defined subevent structure
  Subevent Decoding Ruotine.

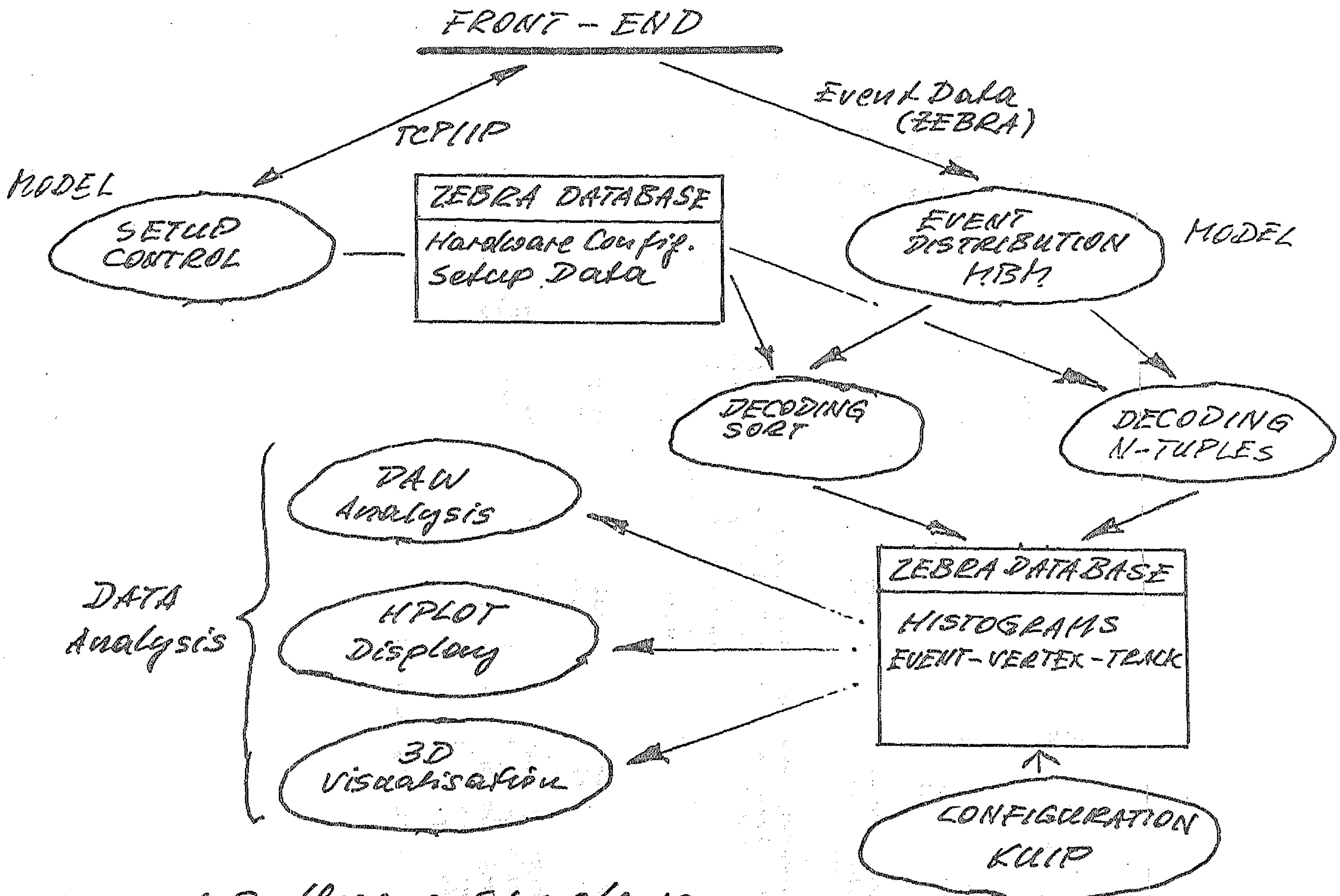

General Software structure

DISCUSSION

H.MACHNER: What portion of the hardware would the experimenters have to provide?
K.WATZLAWIK: The front end and the work stations, which are available now at a cost ranging from 20 000 to 80 000 DM.

It was also pointed out that stand-alone systems will be incorporated into the cluster and that work stations not in use at the time of an experiment can be used for on-line data analysis.

H.MACHNER stated that, for COSY 10, more than one work station would be needed, either in stand-alone mode or connected to SERVER.

H.MACHNER asked why different systems are to be used for data acquisition and for off-line data analysis.
K.WATZLAWIK replied that there is no sufficient computing power available at this time. With the 64 bit RISC architecture, which will be available in the near future for VMS as well as for ULTRIX, both on-line data acquisition and off-line data evaluation can be realized with the same work station.

K.ZWOLL noted that computing at IKP at present is VMS-based, but that computing in the future will be UNIX-based.

H.PLENDL: When will the UNIX system be available?
K.WATZLAWIK: We are now at a stage where a break in computer architecture is occurring: About two years from now, the new system will be user-ready, but in the mean time we must get by with the old one.

K.Watzlawik also stated that he plans to use the CERN software for data analysis without modification.

D. Filges and P. Cloth

IKP, KFA Jülich

Monte Carlo Studies

A Monte Carlo code based on the Bertini code is available for detector simulation studies. Its usefulness is demonstrated on a calculation that was done for the COSY 10 experiment.

D. Filges
G. Sterzenbach
KFA - IKP

26.6.91

Monte Carlo Studies

- The Jülich Monte Carlo - MC3 - for Detector Simulation

- MC-Simulations of the Detector System for the COSY-10 Experiment

• Collaboration Meeting COSY-10
KFA-Jülich, 26.6.1991

Log. of Monte Carlo MC3

MC3 Run

- Start run
  - initialyse the program
  - read the problem input (CMD, USRCMD)
  - record start of run (SOR, USRSOR)

- Event loop
  - Start event (SOB, USRSOB)
  - Source (feed stack)
  - Stack loop
    - Tracks, collisions, decays (Scores)
  - End event
    - process the Scores (MCADET, USRDET)
      - (digitize, apply trigger logic)
    - fill histograms & record end of event (EOB, USREOB)

- End run (EOR, USREOR)
  - output histograms & record end of run
  - call CMD for postprocessing

MC3 organisation

Page 1

Frame routines

controll input/output and program flow

Physics routines

SORS — generate source particles
import source particles from files
generate primary collisions (PSM)

Geometry — provide a region for each point
find distance to boundaries
(default is CG-L2 package)

Decay — provide particle decay

SLOW — provide particle energy loss

COLISN — provide nuclear interaction
(Bertini INC + EVAP in preparation)

physics routines call ANAEVT to interface with the analysis package

MC3 organisation Page 2

Analysis interface

ANAEVT is called when
- source particles are generated
- for each particle track
- after each collision
- after particle decay
- after particles escape
- after particle death (E-cut)

ANAEVT records
- $\vec{x}, t, \vec{P}, E$ type of particles
- + delE delt delx (for tracks)
- + collision type

scores recorded depend on input requests

particle types, regions or surfaces can be selected by input

Scores are stored on common /HIT2/

Start run

Initialyse problem independant data:
- Particle property table
- Decay table
- etc.

---

call CMD to read the problem description
- Geometry description
- Material description
- Source particle/ collision description
- MC3-MCA interface description (SCOREs)
- MCA digitiser description (DEFDET)
- Application input (via USRCMD)
- Histogram definitions

---

call SOR to generate Start of run trigger
and initialyse the analysis

call USRSOR for application specific inits
in user code

Event loop

Start event

- clear particle stack
- report start of event, clear Scores(SOB)
- reset user event analysis (USRSOB)

Generate source particles

- call SORS for beam particles
- call SRSCOL for source collision (PSM)
- push particles on stack and call ANAEVT

Stack loop (until stack is empty)

- pull top stack particle
- perform particle tracking loop
  calling ANAEVT to record Scores

End event

- call MCADET (USRDET) to process Scores
- call EOB (USREOB)
  to fill histograms and
  record end of event

Particle tracking loop

```
find distance for the next track
   call Geometry to find region
      and distance to boundary
   find dist. to collision
   find dist. to decay
-----------------------------------------------
fly minimal distance
adjust xyz E t P⃗
score track
-----------------------------------------------
select action: esc. bound. coll. decay
-----------------------------------------------
when               | then
   collision       |   call COLISN
   decay           |   call DECAY
-----------------------------------------------
score action
restore final state particles (if any)
-----------------------------------------------
when               | then
   boundary        |   loop back
```

all scores are done in ANAEVT

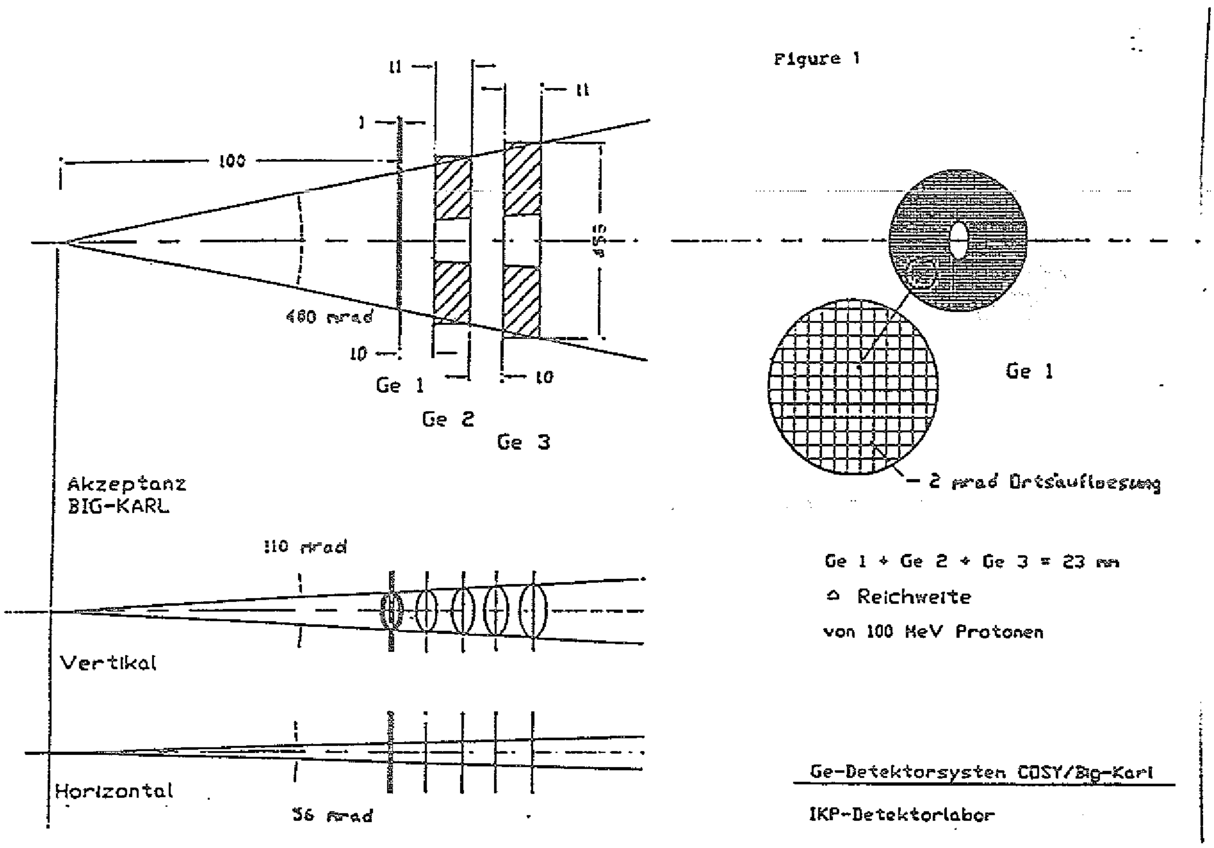

Geometry used: simplified setup

- first Germanium detektor Ge1 for detection of protons
- surface subdivided into a grid of 200 x 200 meshes
  ⇒ angular resolution of 2 mrad

Parameters Used

- energy resolution simulated by a Gaussian with
  $\sigma = \pm 100$ keV

- 2 different assumptions for angle straggling
  $\sigma = \pm 1$ mrad Gaussian
  $\sigma = \pm 5$ mrad Gaussian

- proton beam momentum 834 MeV/c
  (slightly above pion threshold)

MC-Simulation

- PSM-Model for the reaction

  $p \cdot n \rightarrow \pi^{0} \cdot p \cdot p$

- Calculation of the four momenta of the two protons

⇒ Evaluation of missing mass spectrum of the pion

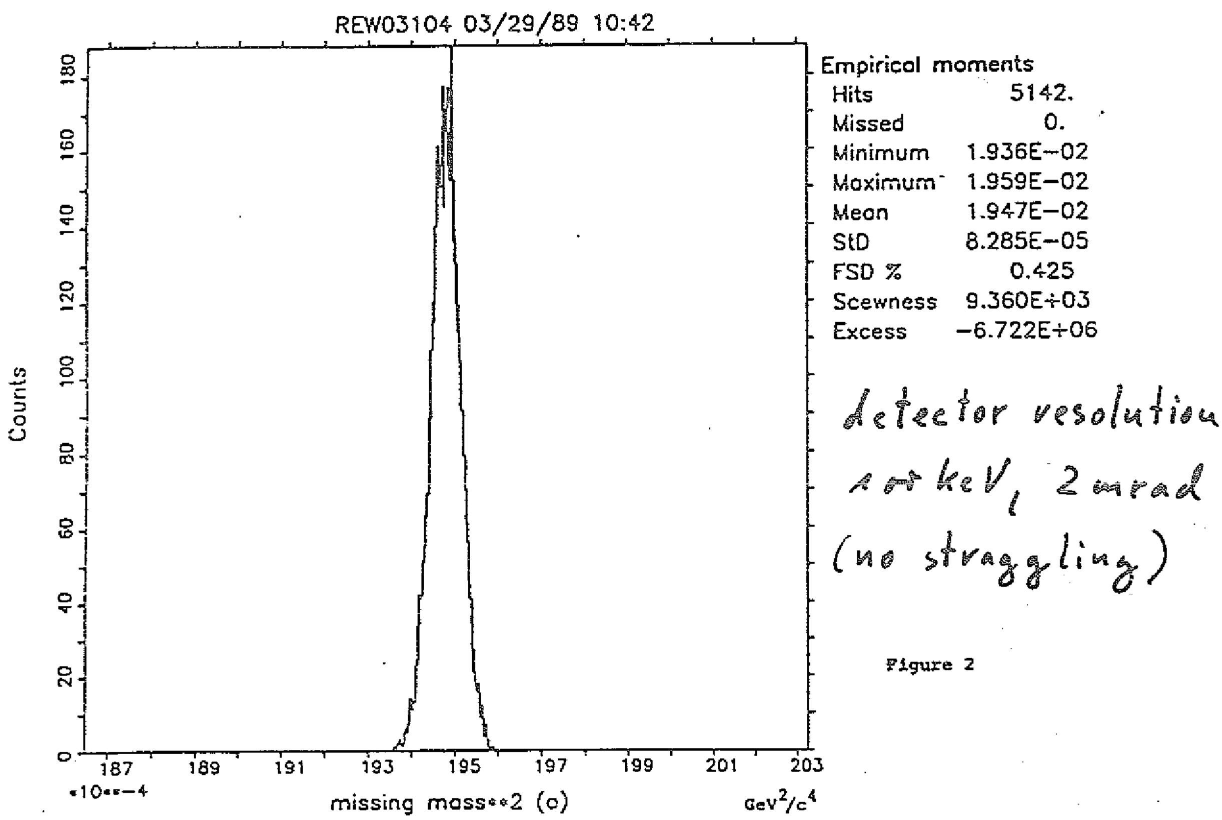

Figure 2

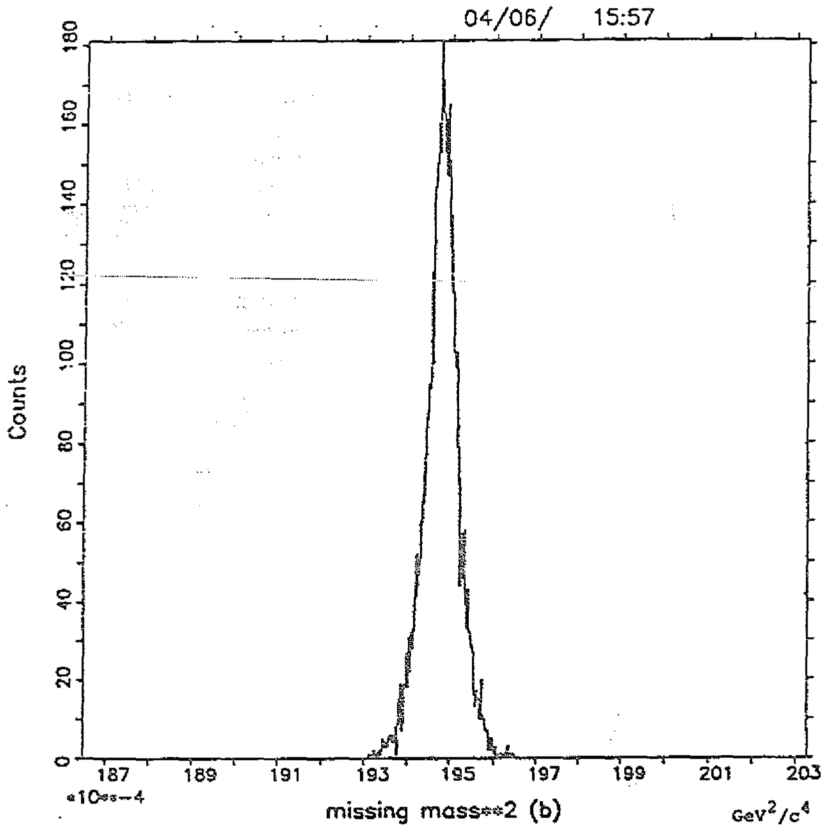

Empirical moments

Hits	5124.
Missed	0.
Minimum	1.931E-02
Maximum	1.965E-02
Mean	1.947E-02
StD	8.947E-05
FSD %	0.459
Scewness	7.409E+03
Excess	-4.922E+06

only straggling 1 mrad

Fig. 3a

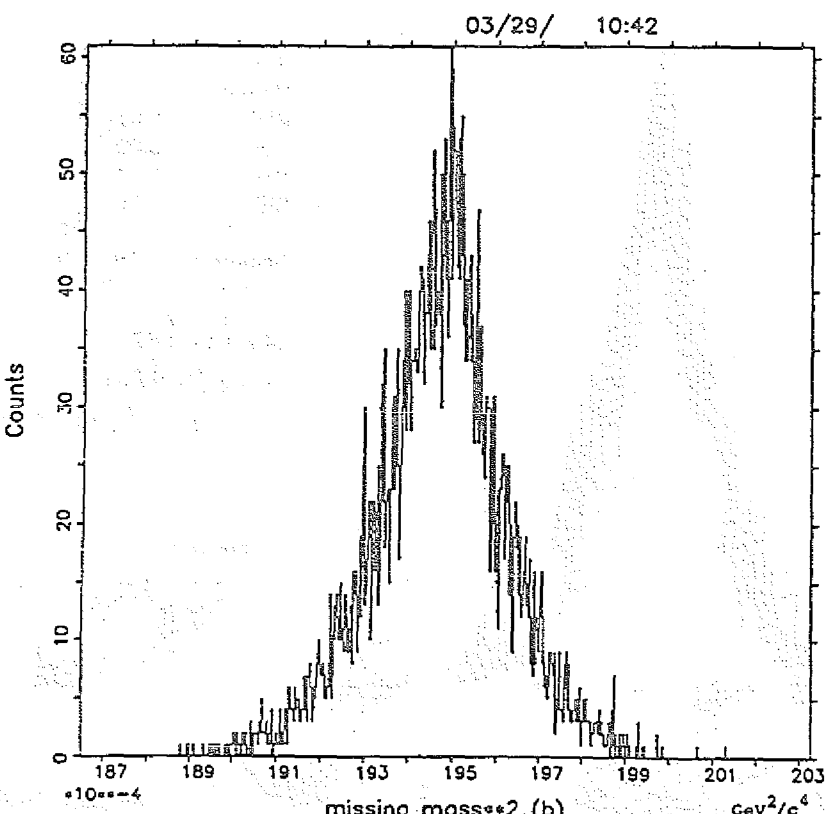

Empirical moments

Hits	5136.
Missed	6.
Minimum	1.888E-02
Maximum	2.013E-02
Mean	1.946E-02
StD	1.697E-04
FSD %	0.872
Scewness	1.096E+03
Excess	-3.832E+05

only straggling 5 mrad

Figure 3b

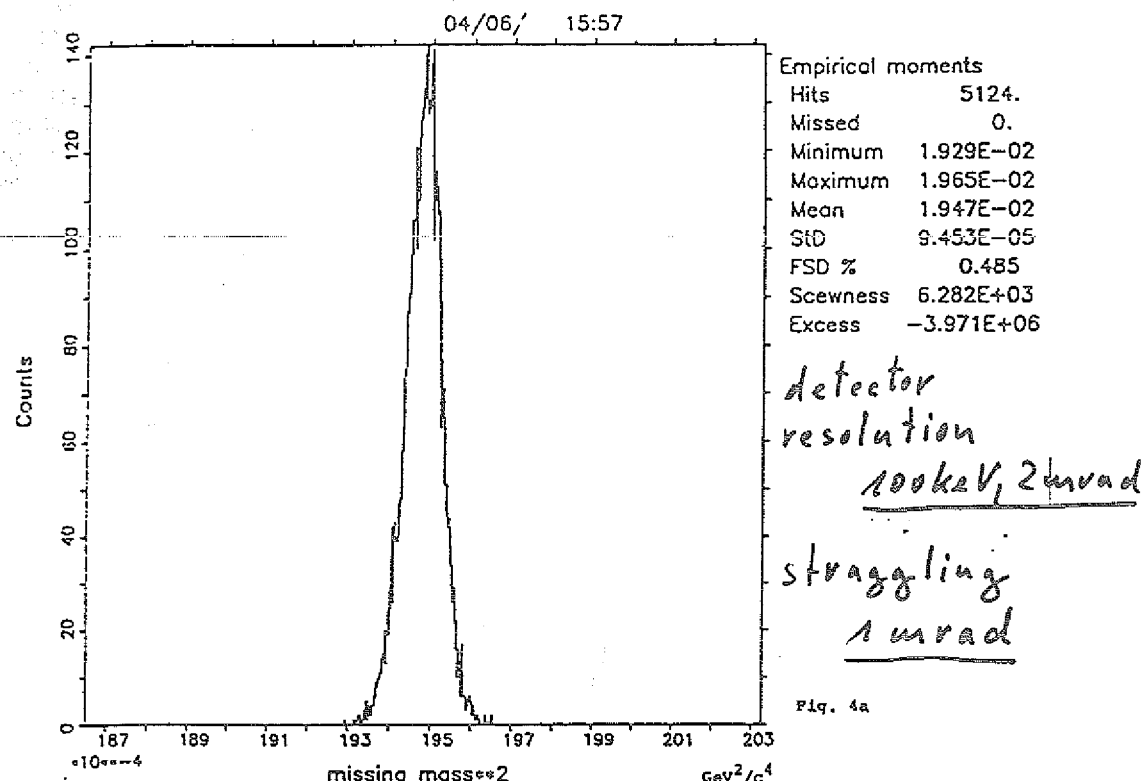

Fig. 4a

$FSD = 0.48\,\% \Rightarrow \sigma_{mass} = 0.335$ MeV

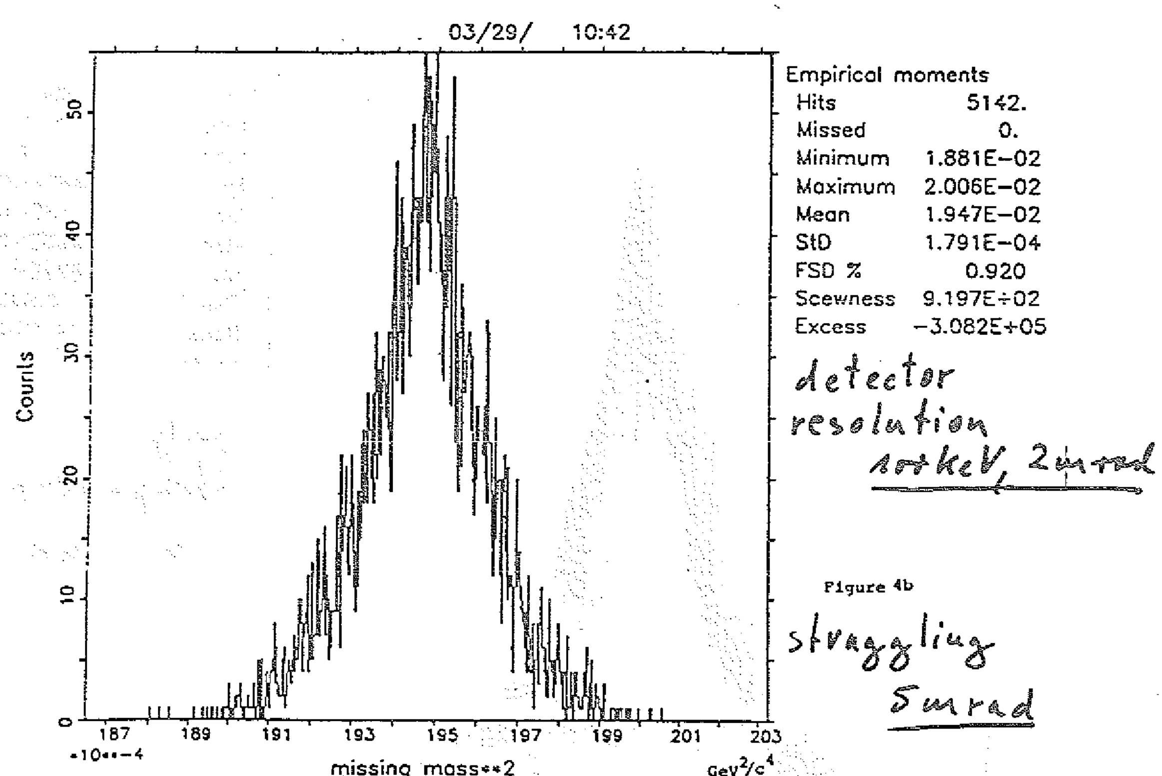

Figure 4b

$FSD = 0.92\,\% \Rightarrow \sigma_{mass} = 0.64$ MeV

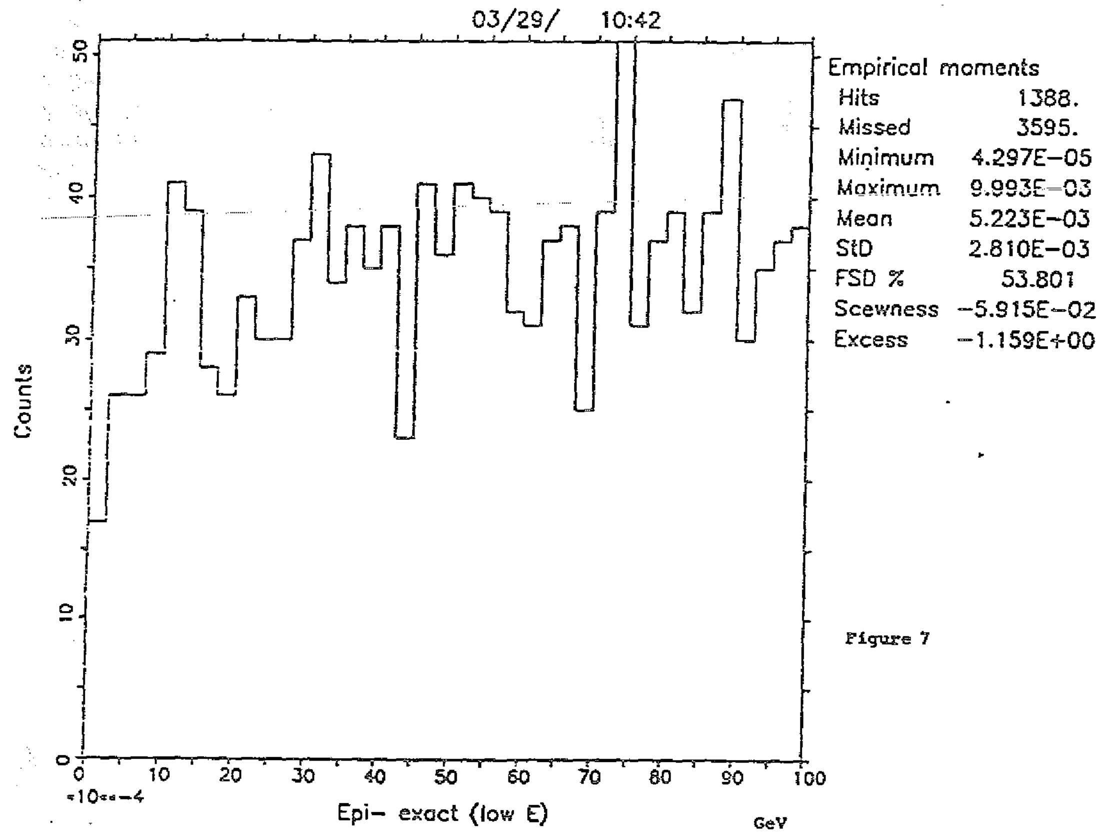

Figure 7

Fraction of events with pions < 1 MeV
(1 % of total number of events in the target)

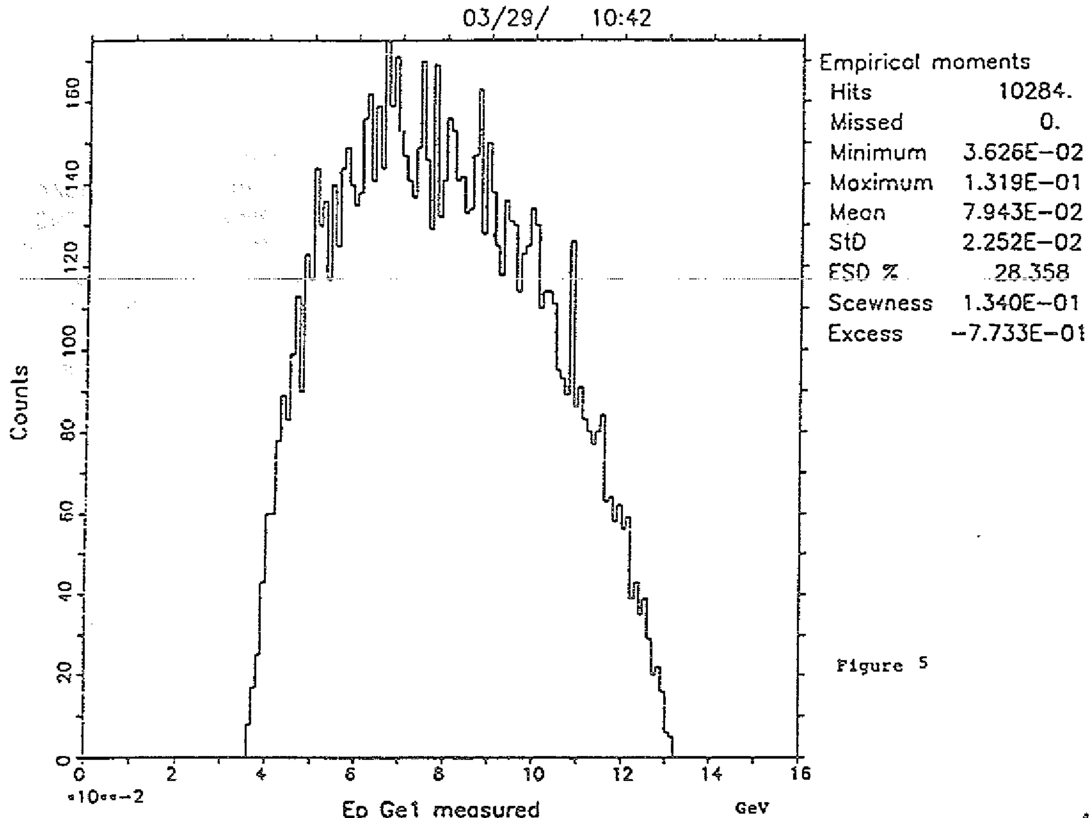

Figure 5

Energy spectrum of protons (detector res. 100keV, 2mrad)

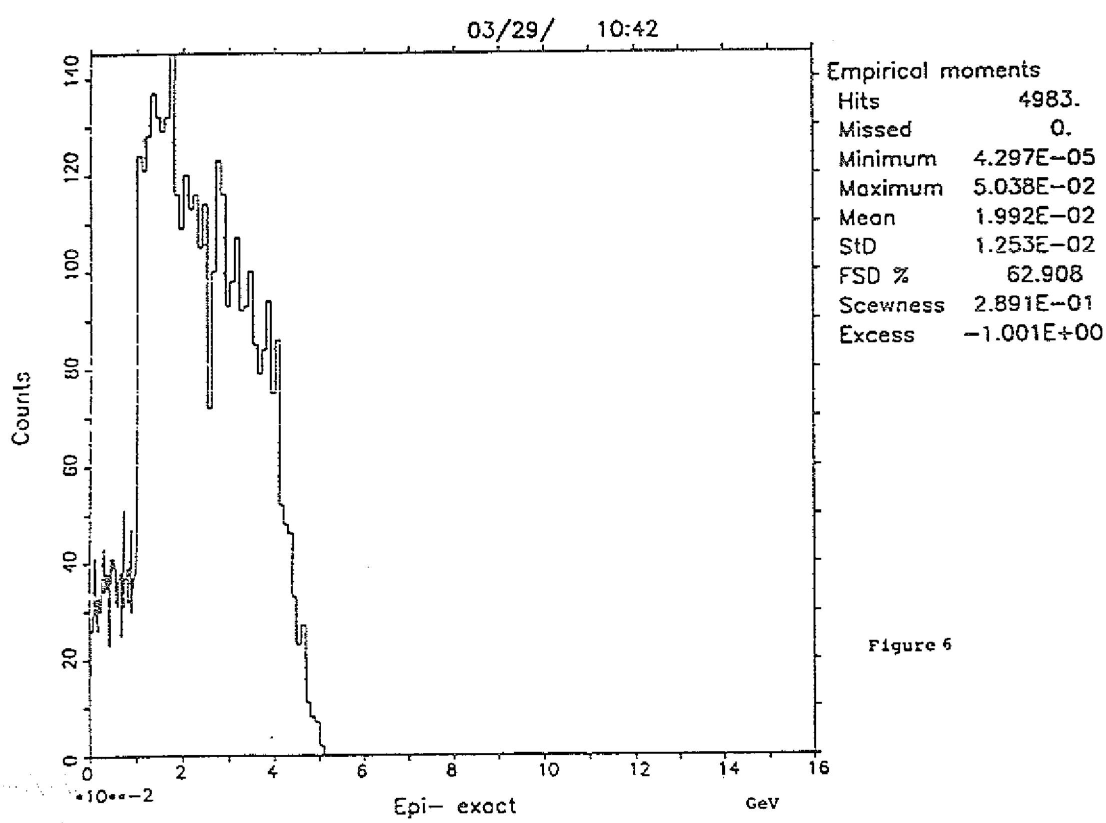

Figure 6

Energy spectrum of pions

DISCUSSION

K. KILIAN pointed out that the resolution that can be achieved with the beam, the spectrometer and the focal plane detector as currently designed and with a thin target is of the order of 0.5 MeV. Compared to the pion–nucleus binding energy in the atomic 1s state ($\approx$ 1 MeV) and the level width ($\sim$ 100 keV) that is not good enough, he noted, because one cannot correctly reconstruct.
Should one, therefore, reconsider the old detector arrangement and put high–resolution wire chambers after target and Ge Wall?
Or should one rely only on the Ge Wall and use the spectrometer merely as an "active beam dump"?
H. MACHNER noted that there will then be problems with the beam halo and that one needs to use the spectrometer together with the Ge Wall in this experiment.
P. v. ROSSEN noted that we do not yet know for sure what kind of beam COSY will deliver.

H. MACHNER: Monte Carlo calculations need to be made for the new detector arrangement.
D. FILGES agreed to the need for such calculations.

K. KILIAN stated that he would consider the experiment to be successful, if it just showed evidence for the production of pionic atoms in a hadronic interaction, even though the goal of the experiment is to determine the energy and width of the levels of such pionic atoms. He also noted that ^{40}Ca is a nice target, because one does not expect to see core excitation.
H. PLENDL added that ^{48}Ca would be a good additional target, because neutron skin effects may become evident.
J. KOONIJN stated that, according to his calculations, one can expect the line width for ^{48}Ca to be narrower than for ^{40}Ca.

H. Machner

IKP, KFA Jülich

A Pre–Experiment

A study of the reaction $\vec{p} + {}^2H \rightarrow {}^3He + \eta$ with a 4π geomertry, an experiment that will allow the testing of the components of all detector and data handling systems separately, is proposed. The intrinsic interest of this experiment is also discussed.

Why is η physics interesting?

- η and η' belong to the $J^{PC} = 0^{-+}$ system (nine mesons). Because of SU(3) symmetry breaking, the physical states are octet-singlet mixtures

$$\eta = \eta_8 \cos\vartheta_P - \eta_1 \sin\vartheta_P$$

$$\vartheta_P \approx 10^\circ$$

$$\eta' = \eta_8 \sin\vartheta_P + \eta_1 \cos\vartheta_P$$

- One expects from SU(3) arguments the following mass relations to be valid:

$$\eta + \eta' = 2K \qquad 1506 \neq 335$$

MeV/c^2

$$\phi + \omega = 2K^* \qquad 1801 \neq 1784$$

$s\bar{s}$-content in η and η'.

0^- (pseudoscalar):

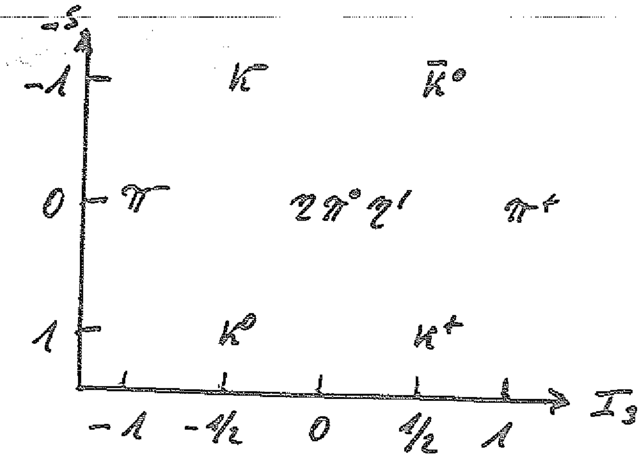

1^- (vector):

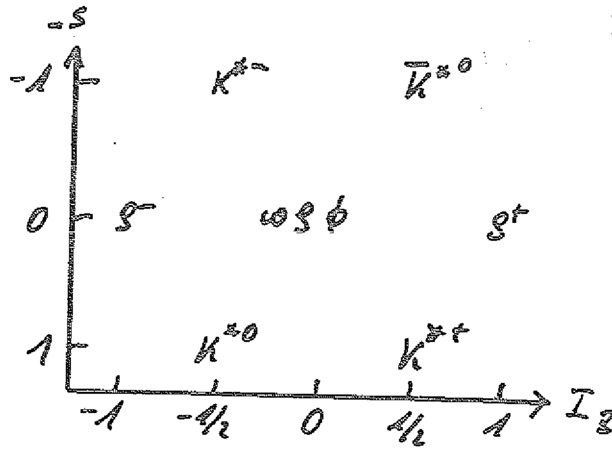

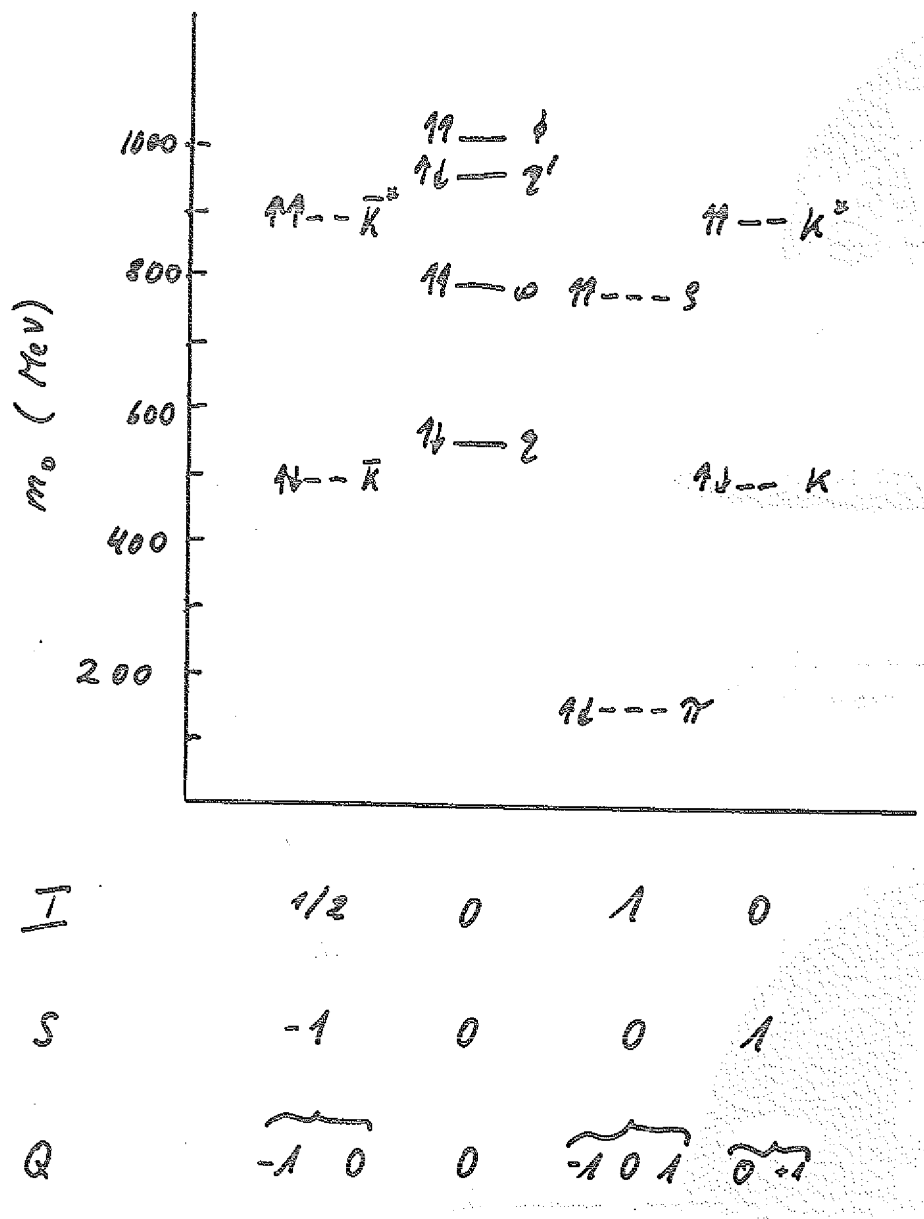

pseudoscalar } mesons
vector

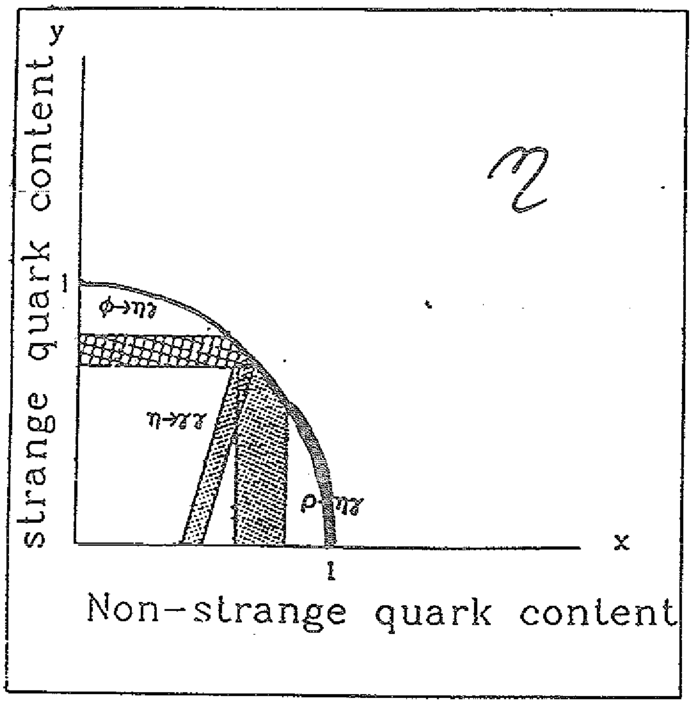

From SU(3) symmetry

$|\eta\rangle = \frac{1}{\sqrt{6}} |u\bar{u} + d\bar{d} - 2s\bar{s}\rangle$

$|\eta\rangle = \frac{1}{\sqrt{2}} |u\bar{u} + d\bar{d}\rangle$

$J = 0, I_3 = 0, I = 0$

charge = 0, S = 0

same as for ω, then

J = 1

Fig. 1 η cuark content [4]. x and y are defined in the formula:

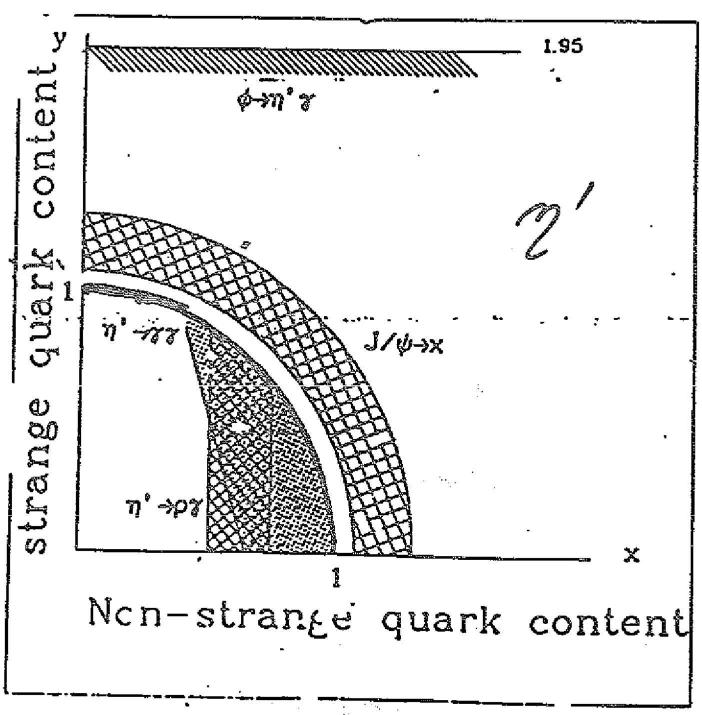

$|\eta'\rangle = \frac{1}{\sqrt{3}} |u\bar{u} + d\bar{d} + s\bar{s}\rangle$

$|\eta'\rangle = |s\bar{s}\rangle$

$I = 0, I_3 = 0, S = 0$

$J = 0$

same as for φ, then J = 1

Fig. 2 η' quark content [4]. ('updated for φ->η'γ [5] and for J/Ψ -> vector + pseudoscalar meson [6])

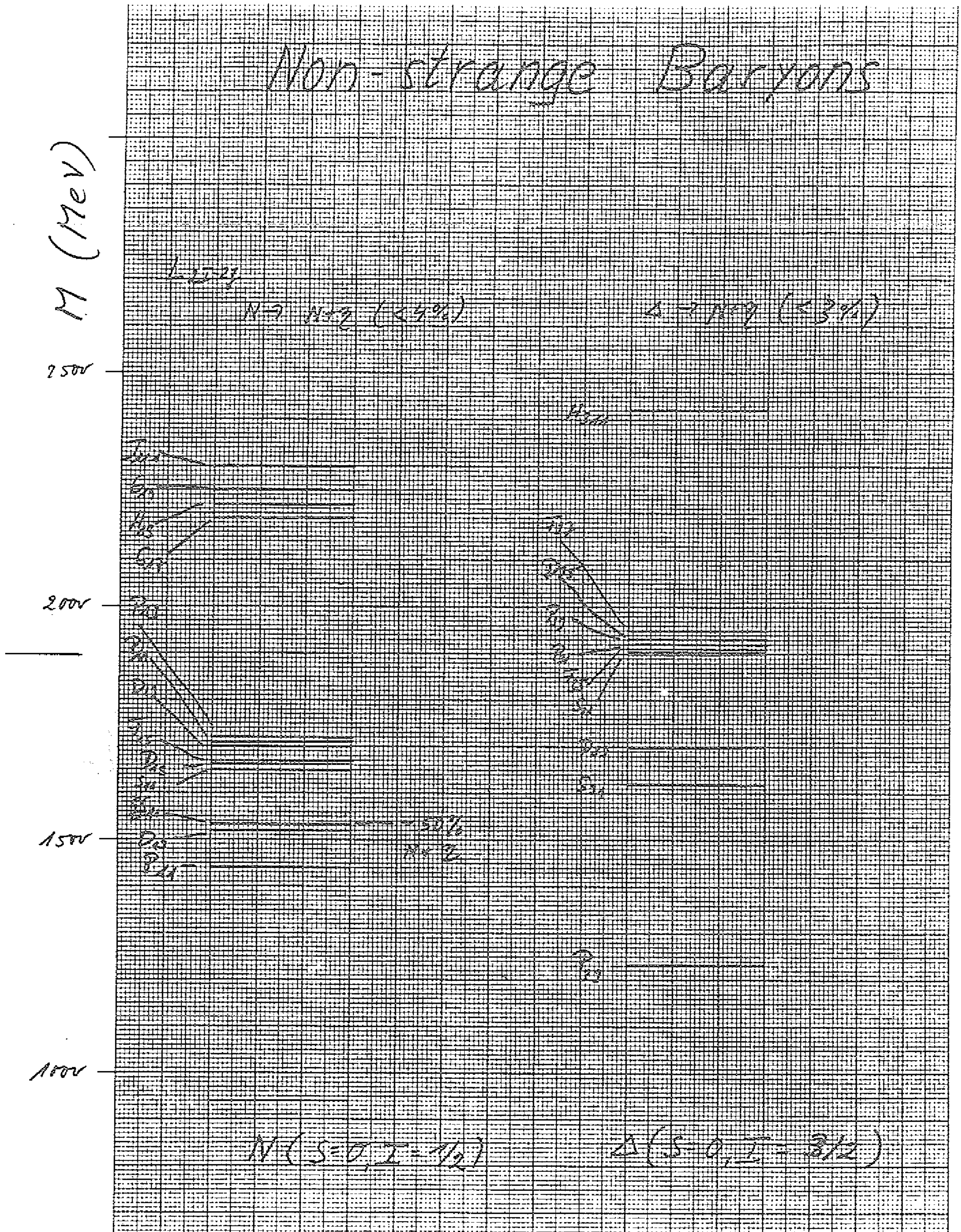

A 4 210x297 mm

MADE IN GERMANY

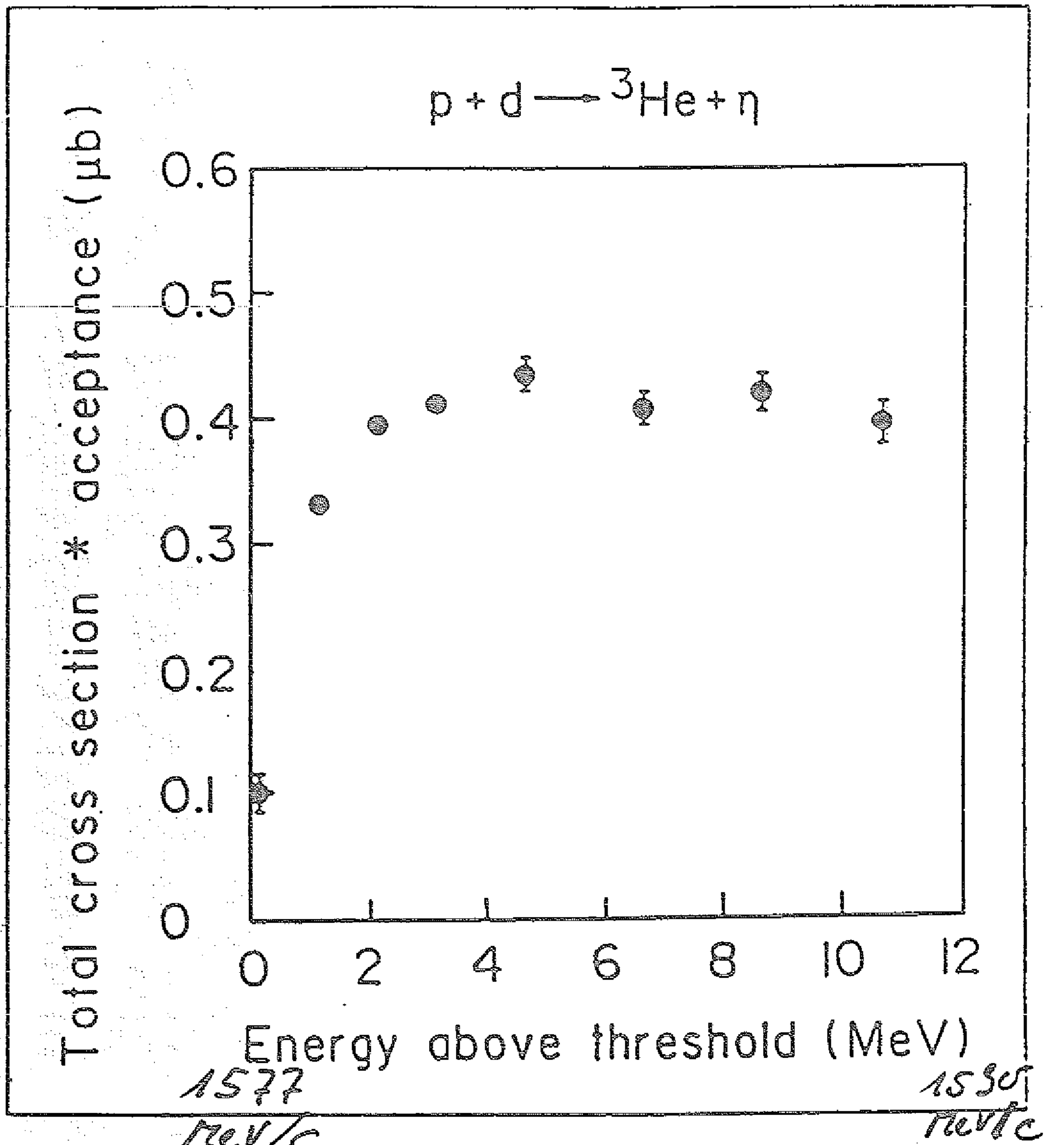

Fig. 3: Top view of one arm of muon detection for $\eta \rightarrow \mu^+ \mu^-$.

Impuls - Reichweite
in Germanium

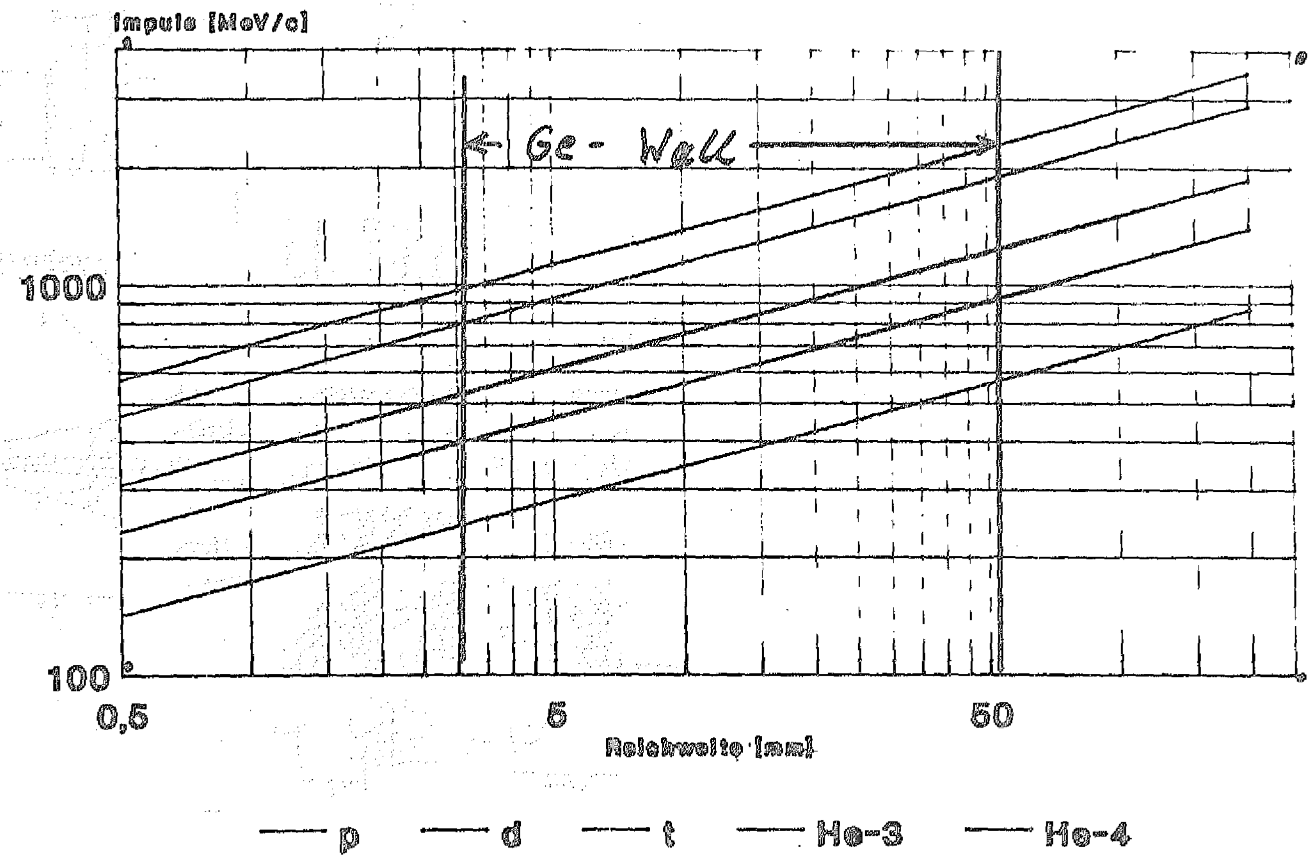

175

50x50 je 32 pie slices

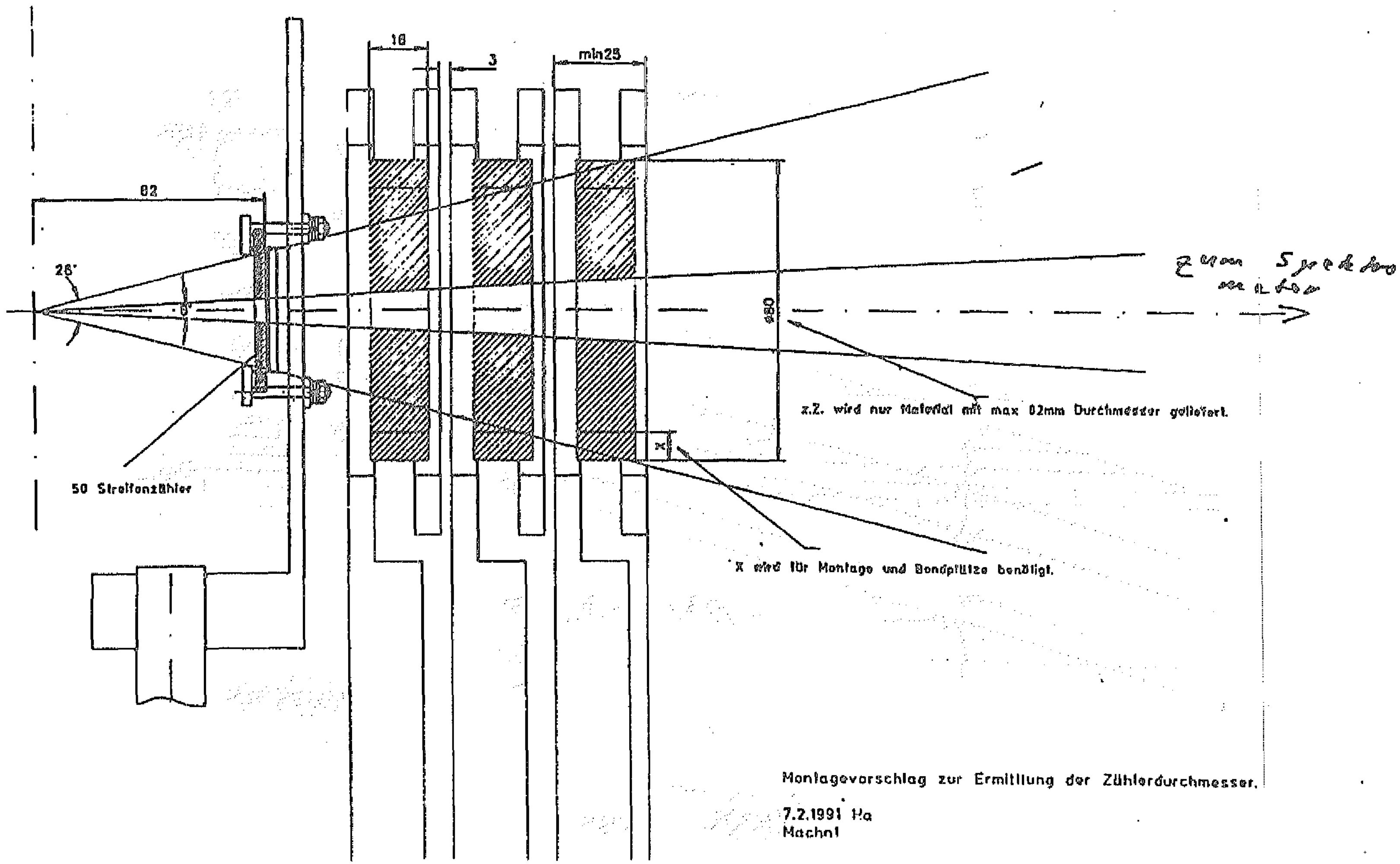

Ge detector system for $p\,^2H \to {}^3He\,\gamma$, with 4π solid angle in COM-system.

$p_p = p_{meg.} \approx 1740$ MeV/c

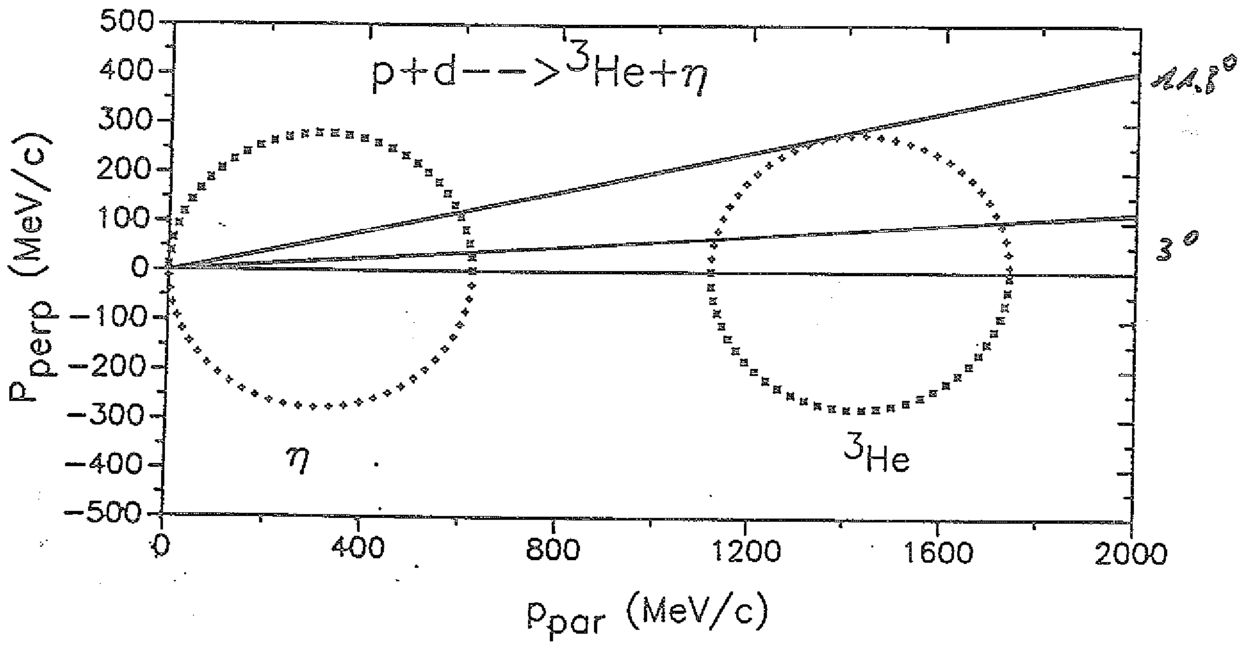

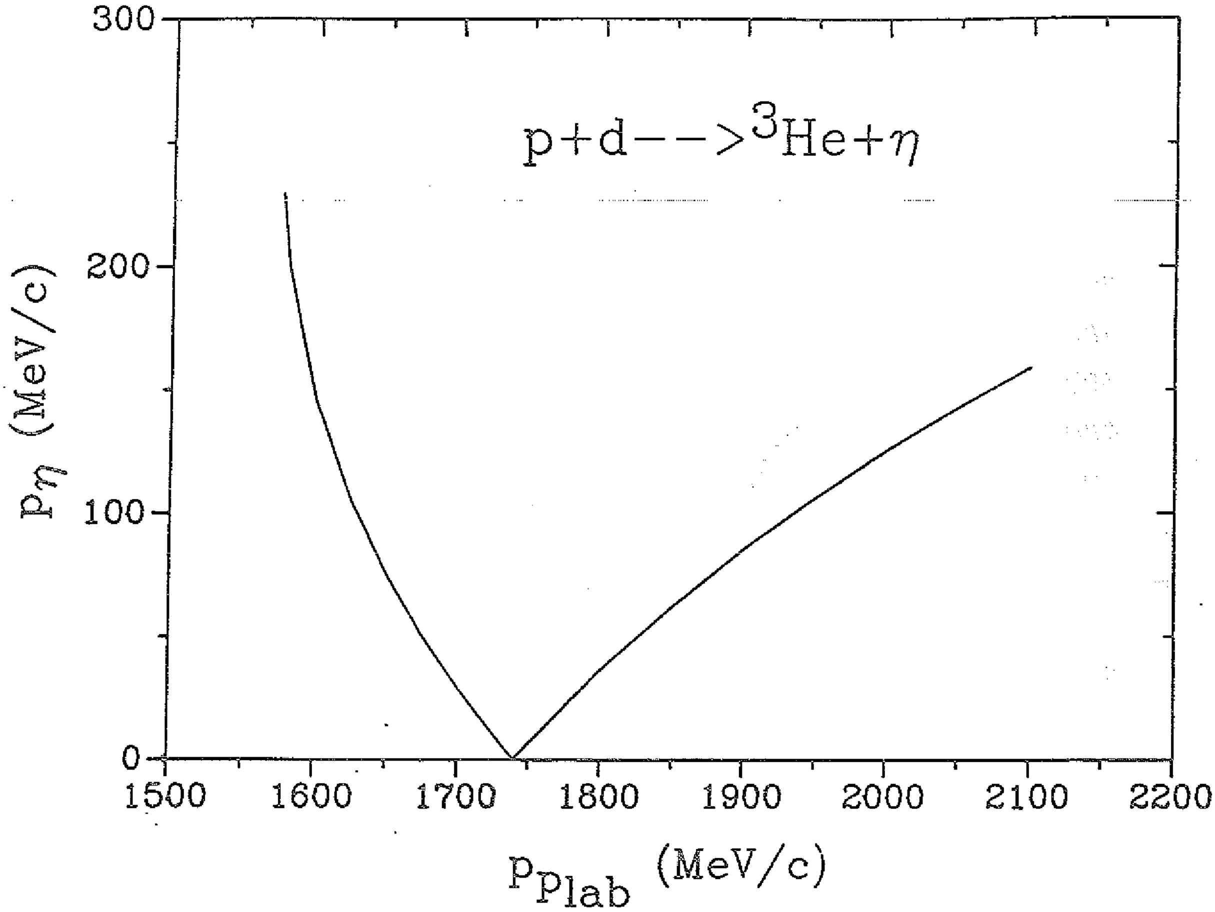

p+d-->3He+η
pη (MeV/c)
300
200
100
0
1500
1600
1700
1800
1900
2000
2100
2200
pPlab (MeV/c)

$p+d \rightarrow {}^3He+\eta$

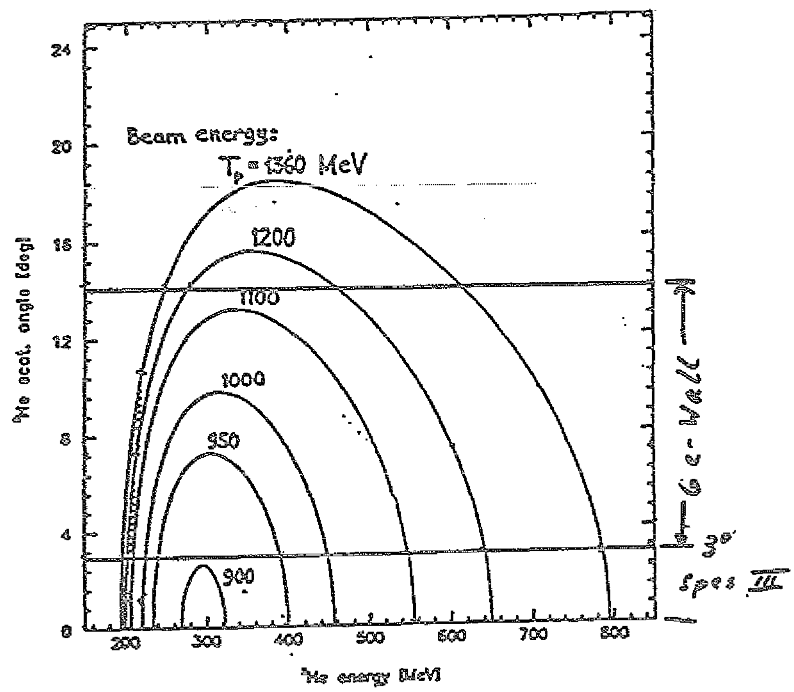

$p+d \rightarrow {}^3He+\eta$

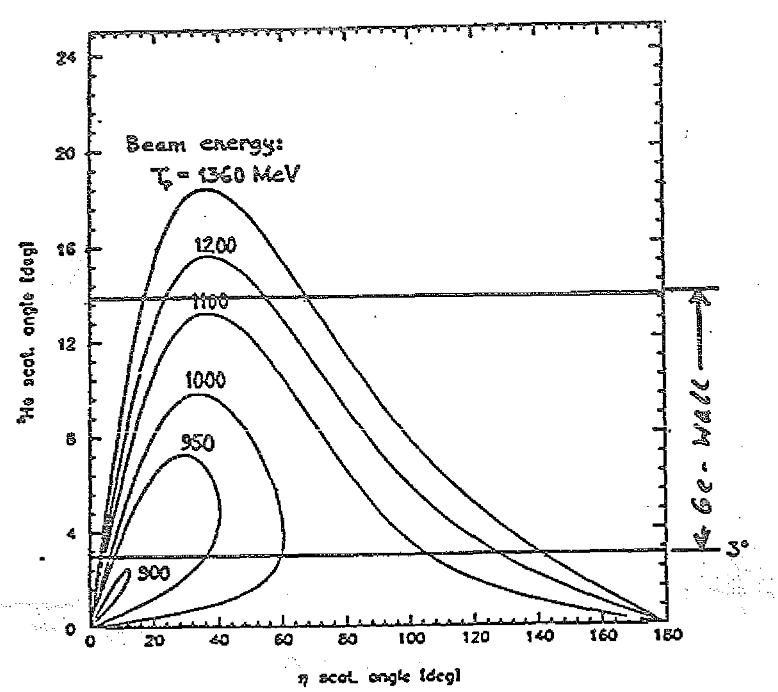

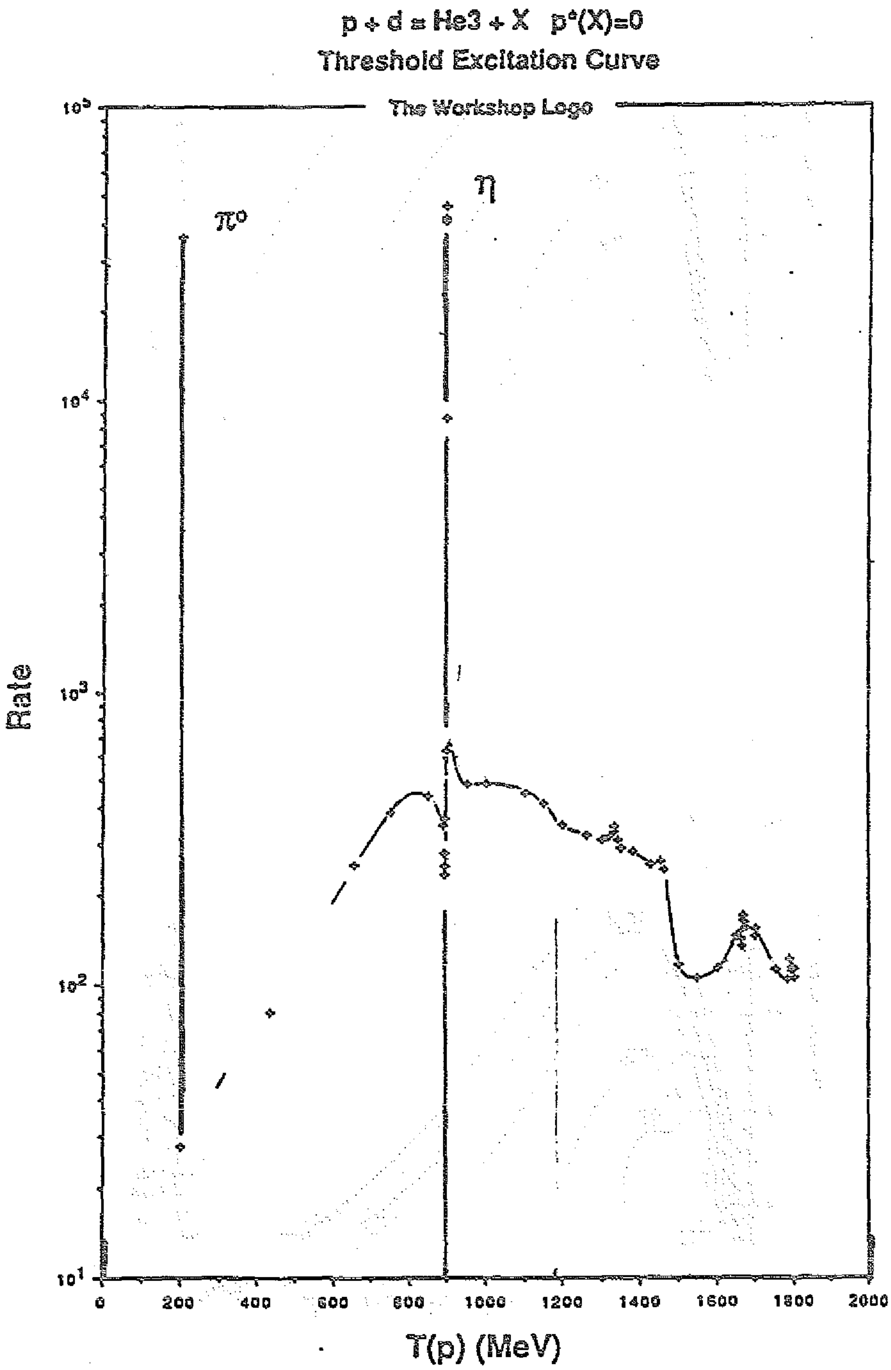

Fig.1. The threshold excitation curve. We have derived the two data points at the π^0 threshold from the 1986 Saclay raw data. The other points are from the 1987 data. The event rate corresponds to an integration over a c.m. momentum space as sketched in Fig.3.

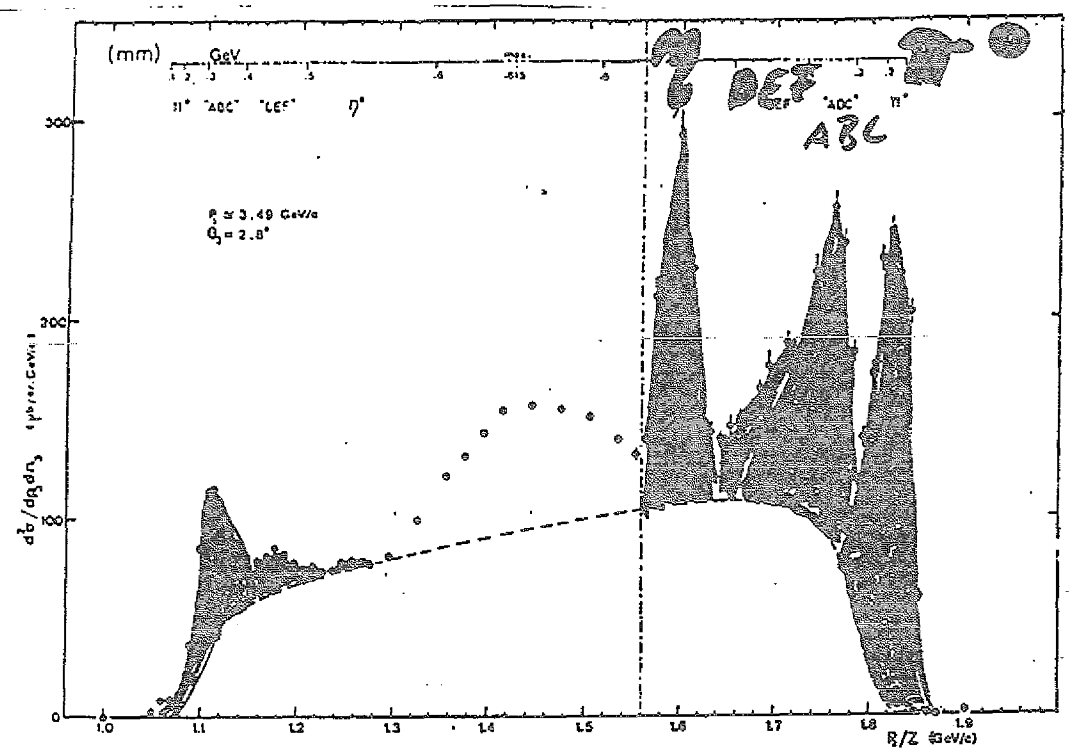

Fig. 1. Laboratory momentum spectrum for recoil He^3 from the reaction $d+p \rightarrow He^3 + (mm)^0$ at $P_{Lab} = 3.50$ GeV/c, $\theta_{Lab} = 2.8$ deg.

$d + p \rightarrow {}^3He + mm$

$P_i = 3.5$ GeV/c

$\theta_{LAB} = 2.8°$

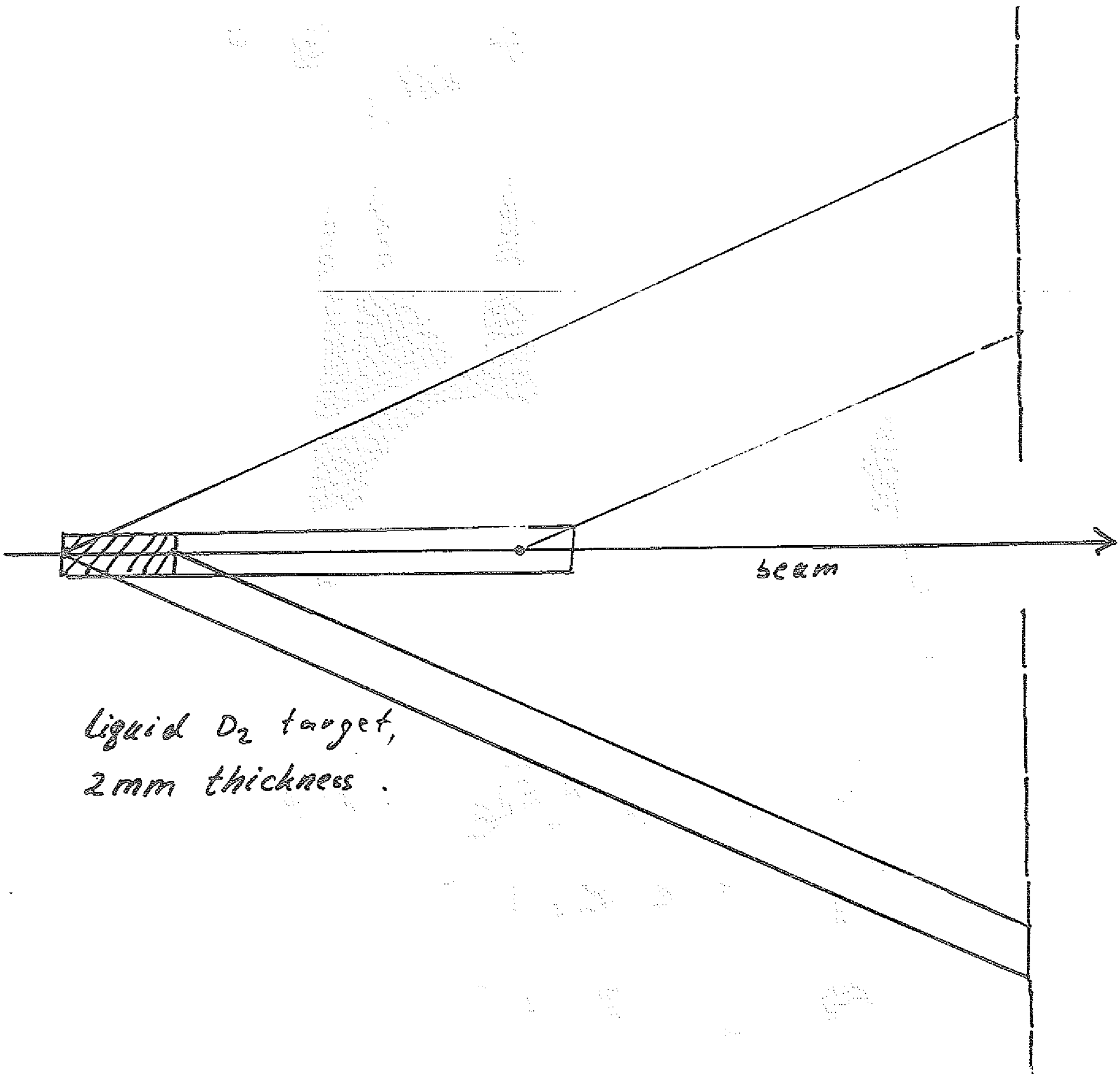

Liquid D_2 target,
2mm thickness.

Prototyp LH_2 target with very thin windows

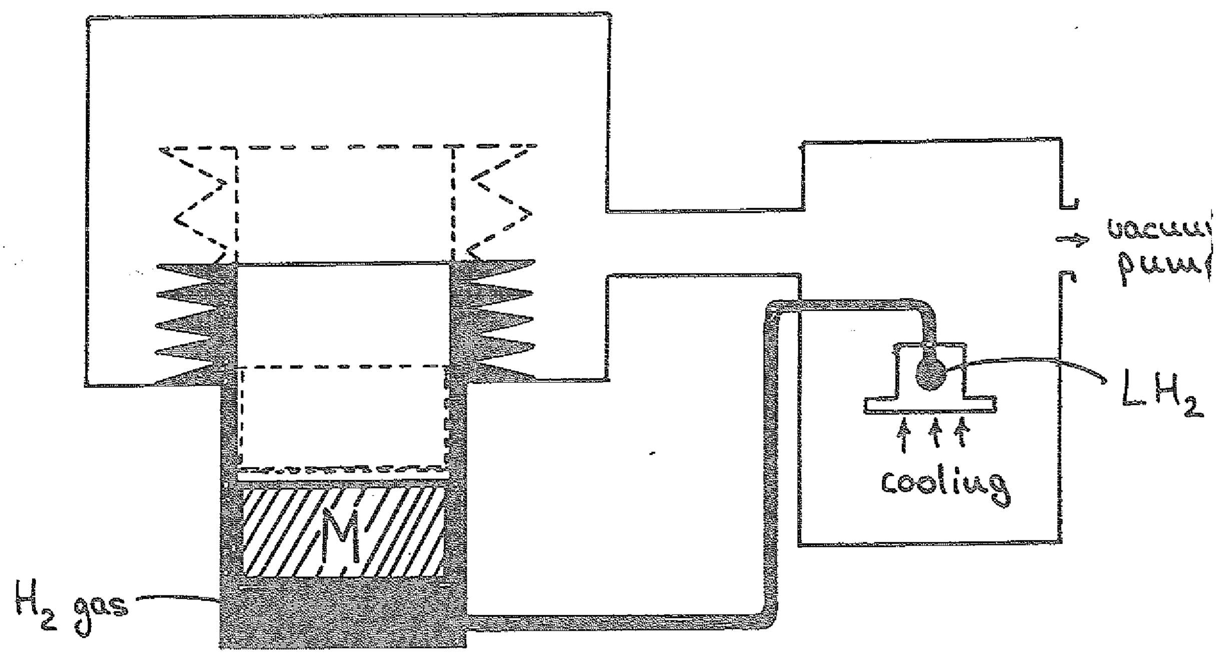

$$\Delta p = \frac{g \cdot M}{A} = \text{const}$$

all working conditions!

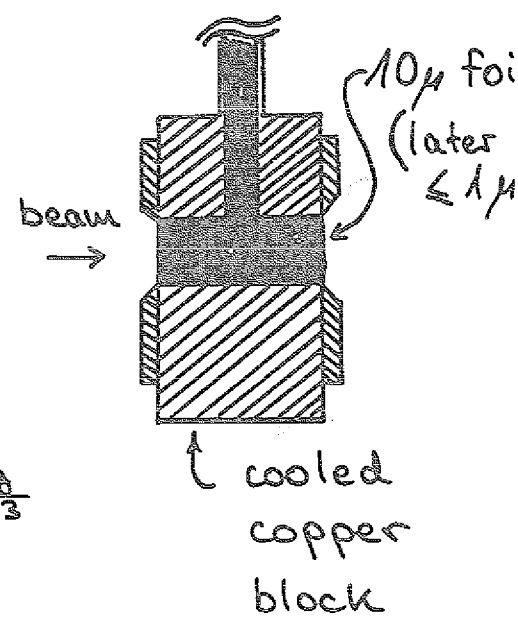

H_2 liquid-gas equilibrium

K	atm	g
15,86	0,2	74,6 $\frac{mg}{cm^3}$

Counting rate estimated

$$I = \frac{N \cdot A}{\sigma \cdot d \cdot L} \quad (\text{part.}/s)$$

I = beam
N = counting rate — $5000 \cdot 32$
A = mass number — 2
σ = cross section — 80 mb el. scattering
d = thickness — 324 mg/cm^2 = 2 mm
L = Avogadro's number

$I = 1.2 \cdot 10^3$ part./s

$$\frac{\sigma_{el}}{N_{el}} = \frac{\sigma_\eta}{N_\eta} \qquad \sigma_\eta \approx 0.4\ \mu b$$

$$N_\eta = \sigma_\eta \cdot \frac{N_{el}}{\sigma_{el}} \approx \underline{\underline{0.8/s = 2880/h.}}$$

Measurable quantities:

σ_{tot} absolute

$\frac{d\sigma}{d\Omega}$

A_y with polarized beam

DISCUSSION

H. MACHNER, in reply to a question stated that the electronics intended for the experiment can handle $\sim 5 \times 10^5$ counts/s.

E. RODERBURG: Will the Ge Wall to be used in this experiment provide the only trigger for outgoing particle detection? K. KILIAN: ^3He, one of the two outgoing particles, is an excellent trigger by itself because of the large amount of ionization it causes. H. MACHNER noted that this will therefore be a low–background experiment.

K. KILIAN noted that the Ge Wall is a 4π detector, so that one gets a complete angular distribution in addition to a full energy spectrum. Hence there is no need to reset the angle or the momentum acceptance. Such complete acceptance has been accomplished so far only in very few experiments at GeV energies.

H. MACHNER expressed the need for a Monte Carlo calculation for the experiment. He also said that there was potential interest in this experiment at Orsay and that efforts are under way to get people at Saclay interested, where the experiment could best be done.

Finally he pointed out that the experiment would be a test of recoil–free kinematics as applied to a particle interaction. If successful at that level, the experiment could also be used to produce η–mesic nuclei.

The meeting closed with an announcement that B.J. Lieb would give a seminar the following day on the results so far for searches for η–mesic nuclei at BNL and at LAMPF.

SUMMARY

The presentations and discussions at the collaboration meeting gave a clear picture of the motivation for the planned experiment and of the apparatus and methods to be used for its realization. Technical and other problems were discussed in detail and possible solutions were considered. It was agreed that the Saclay experiment proposed to test the detector and data handling systems would be a highly desireable step in the preparations for COSY 10.

A short follow–up meeting of the collaboration is tentatively planned to take place at the time of the annual COSY Users (CANU) Meeting at the Bad Honnef Physikzentrum, 16–17 December 1991.

LIST OF PARTICIPANTS

<u>IKP, KFA</u>
A. Djaloeis
D. Filges
V. Jaeckle
K. Kilian
H. Machner
R.–D. Neef
D. Protic
J. Rama Rao[1)]
G. Riepe
E. Roderburg
P. v. Rossen
P. Turek
K. Watzlawik

<u>ZEL, KFA</u>
H. Kopp
K. Zwoll

<u>TU Dresden</u>
R. Krause
W. Meiling
J. Pöthig
R. Schwierz

<u>Institute of Nuclear Physics, Cracow</u>
A. Budzanowski

<u>Jagellonian University, Cracow</u>
L. Jarczyk
A. Kozela
J. Smyrski
A. Stzralkowski

<u>NIKHEF Amsterdam</u>
J. Konijn

<u>George Mason University, Fairfax</u>
B.J. Lieb

<u>Florida State University, Tallahassee</u>
H.S. Plendl

[1)] On leave from Banaras Hindu University, Varanasi

THE COSY 10 COLLABORATION
(as of June 1991)

P. Cloth, A. Djaloeis, D. Filges, D. Gotta, K. Kilian, H. Machner (spokesperson), H.P. Morsch, D. Protic, G. Riepe, E. Roderburg, P. von Rossen, P. Turek, K.H. Watzlawik
Institut für Kernphysik, Forschungszentrum Jülich, Germany

L. Jarczyk, A. Kozela, J. Smyrski, A. Strzalkowski
Institute of Physics, Jagellonian University, Cracow, Poland

A. Budzanowski, D. Dabrowski, I. Skwirczynska
Institute of Nuclear Physics, Cracow, Poland

H.S. Plendl
Florida State University, Tallahassee, Florida, USA

J. Konijn
NIKEF K, Amsterdam, Netherlands

B.J. Lieb
George Mason University, Fairfax, Virginia, USA

K. Zwoll, W. Even, J. Holzer, H. Kopp
Zentralinstitut für Elektronik, Forschungszentrum Jülich, Germany

W. Meiling and R. Krause
Sektion Physik, T.U. Dresden, Germany

J. Rama Rao
Banaras Hindu University, Varanasi, India

FORSCHUNGSZENTRUM JÜLICH GmbH

KFA

Jül-2500
July 1991
ISSN 0366-0885